Coordinating Radiometals of Copper, Gallium, Indium, Yttrium, and Zirconium for PET and SPECT Imaging of Disease

Thaddeus J. Wadas,*,† Edward H. Wong,‡,§ Gary R. Weisman,‡,§ and Carolyn J. Anderson*,†

Mallinckrodt Institute of Radiology, Washington University School of Medicine, 510 S. Kingshighway Blvd., Campus Box 8225 St. Louis, Missouri 63110, and Department of Chemistry, University of New Hampshire, Durham, New Hampshire 03824-3598

Received September 29, 2009

Contents

1. Introduction 2858
2. The Coordination Chemistry of Cu, Ga, Y, In, and Zr 2860
   2.1. General Considerations 2860
   2.2. Aqueous Copper Coordination Chemistry 2862
   2.3. Copper(II) Complexes of Selected Chelators 2863
      2.3.1. Acyclic Tetradentate Chelators 2863
      2.3.2. Acyclic Hexadentate Chelators 2864
      2.3.3. Macrocyclic Chelators 2865
   2.4. Aqueous Gallium(III) Coordination Chemistry 2869
      2.4.1. Tetradentate Ligands 2869
      2.4.2. Hexadentate Ligands 2870
   2.5. Aqueous Indium(III) Coordination Chemistry 2872
      2.5.1. Tetradentate Chelators 2872
      2.5.2. Hexa- to Octadentate Chelators 2873
   2.6. Aqueous Yttrium(III) Coordination Chemistry 2875
   2.7. Aqueous Zirconium(IV) Coordination Chemistry 2877
   2.8. Summary 2877
3. Radioisotope Production 2878
   3.1. Production of Copper Radiometals 2878
   3.2. Production of Gallium Radiometals 2879
   3.3. Production of Indium Radiometals 2879
   3.4. Production of Yttrium Radiometals 2880
   3.5. Production of Zirconium Radiometals 2881
4. Applications of Zr, Y, Ga, In, and Cu Radiopharmaceuticals 2881
   4.1. Oncology 2881
      4.1.1. Integrin Imaging 2881
      4.1.2. Somatostatin Receptor Imaging 2883
      4.1.3. HER-2/neu Receptor Imaging 2886
      4.1.4. Gastrin Releasing Peptide Receptor Imaging 2887
      4.1.5. Epidermal Growth Factor Receptor Imaging 2888
      4.1.6. Vascular Endothelial Growth Factor Receptor Imaging 2888
      4.1.7. Melanoma Imaging 2889
   4.2. Imaging Gene Expression 2890
   4.3. Imaging Inflammation and Infection 2891
   4.4. Imaging Hypoxia and Perfusion 2892
5. Conclusion 2893
6. Glossary 2893
7. Acknowledgments 2893
8. References 2893

* Corresponding authors: Carolyn J. Anderson, phone 314.362.8427, fax 314.362.9940, e-mail andersoncj@wustl.edu; Thaddeus J. Wadas, phone 314.362.8441, fax 314.362.9940, e-mail wadast@wustl.edu.
† Washington University School of Medicine.
‡ University of New Hampshire.
§ Contact information: Edward H. Wong, phone 603-862-1788, fax 603-862-4278, e-mail ehw@cisunix.unh.edu; Gary R. Weisman, phone 603-862-2304, fax 603-862-4278, e-mail gary.weisman@unh.edu.

1. Introduction

Molecular imaging is the visualization, characterization, and measurement of biological processes at the molecular and cellular levels in humans and other living systems. Molecular imaging agents are probes used to visualize, characterize, and measure biological processes in living systems. These two definitions were put forth by the Society of Nuclear Medicine (SNM) in 2007 as a way to capture the interdisciplinary nature of this relatively new field. The emergence of molecular imaging as a scientific discipline is a result of advances in chemistry, biology, physics, and engineering, and the application of imaging probes and technologies has reshaped the philosophy of drug discovery in the pharmaceutical sciences by providing more cost-effective ways to evaluate the efficacy of a drug candidate and allow pharmaceutical companies to reduce the time it takes to introduce new therapeutics to the marketplace. Finally, the impact of molecular imaging on clinical medicine has been extensive since it allows a physician to diagnose a patient's illness, prescribe treatment, and monitor the efficacy of that treatment noninvasively.

Single-photon emission computed tomography (SPECT) and positron emission tomography (PET) were the first molecular imaging modalities used clinically. SPECT requires the use of a contrast agent labeled with a γ-emitting radionuclide, which should have an ideal γ energy of 100−250 keV. These γ rays are recorded by the detectors of a dedicated γ camera or SPECT instrument and after signal processing can be converted into an image identifying the localization of the radiotracer. PET requires the injected radiopharmaceutical to be labeled with a positron-emitting radionuclide. As the radionuclide decays, it ejects a positron from its nucleus, which travels a short distance before being annihilated with an electron to release two 511 keV γ rays 180° apart that are detected by the PET scanner (Figure 1). After sufficient acquisition time, the data are reconstructed using computer-based algorithms to yield images of the radiotracer's location within the organism. Compared with SPECT, PET has greater advantages with respect to sensitivity and resolution and has been gaining in clinical popularity, with the number of PET-based studies expected to reach 3.2 million by 2010.[1] While SPECT and PET technologies have

10.1021/cr900325h © 2010 American Chemical Society
Published on Web 04/23/2010

Thaddeus J. Wadas was born in Nanticoke, PA, in 1974. He received his B.S. degree in Biology from King's College, Wilkes-Barre, PA, in 1996 and, while working in the environmental science industry, completed his second major in Chemistry in 1998. After completing his second major, he pursued graduate studies at the University of Rochester, Rochester, NY, where he received his M.S. and Ph.D. degrees in Chemistry under the supervision of Richard Eisenberg. His Ph.D. work focused on the synthesis and characterization of luminescent Pt(II) acetylide complexes for photoinduced charge transfer and light-to-chemical energy conversion. On completion of his Ph.D., he moved to the Washington University School of Medicine in St. Louis, MO, to pursue postdoctoral studies with Carolyn Anderson and develop targeted radiopharmaceuticals for diagnostic imaging and radiotherapy. In 2005, he was the recipient of a National Institutes of Health National Research Service Award (NRSA) Fellowship to study bone metastasis imaging with copper-64-labeled peptides, and in 2009 he was promoted to the position of Instructor at the School of Medicine. His current research interests include the application of combinatorial display methods to radiopharmaceutical development and understanding the respective roles gadolinium-based contrast agents and renal insufficiency play in the development of nephrogenic systemic fibrosis.

Edward H. Wong was born in Wuhan, China, in 1946 but was raised in Hong Kong where he discovered the joy of mixing chemicals at St. Louis High School. He then majored in chemistry at the University of California at Berkeley and obtained his Ph.D. doing boron hydride synthesis with William N. Lipscomb at Harvard University in 1974. After a postdoctoral stint with M. Frederick Hawthorne at the University of California, Los Angeles, he began his academic career at Fordham University in 1976 before moving to the University of New Hampshire in 1978. He has performed research in main group boron and phosphorus chemistry as well as metal−phosphine coordination chemistry. In recent years, with his colleague Gary Weisman he has focused on the coordination chemistry of cross-bridged tetraamine macrocycles. Together they have also explored applications of these chelators in copper-based radiopharmaceuticals with Carolyn Anderson and her research group.

Gary R. Weisman was born in Mason, Ohio, in 1949, receiving his primary and secondary education in the public school system there. He was interested in chemistry from a young age, working with his cousin Thomas J. Richardson in their substantial home laboratories. He earned his B.S. in Chemistry with Distinction at the University of Kentucky in 1971, carrying out research with Robert D. Guthrie. At the University of Wisconsin—Madison, he worked on conformational analysis of hydrazines and their radical cations under the mentorship of Stephen F. Nelsen, earning the Ph.D. in Organic Chemistry in 1976. After a postdoctoral stint with Donald J. Cram at the University of California, Los Angeles, in 1976−1977, he started his independent academic career at the University of New Hampshire, where he has enjoyed both teaching and research. He was Gloria G. and Robert E. Lyle Professor at UNH from 2005 to 2009 and has been the recipient of Outstanding Teaching awards in 1995 and 2009. He has been a visiting professor at the University of Wisconsin (1986), University of Bristol (1987, 1998), University of Melbourne (2005), and Australian National University (2005). He was a Wilsmore Fellow at the University of Melbourne in 2002. His research interests are in both physical organic and synthetic organic chemistry, with special emphasis on stereochemical aspects. His recent research has centered on the chemistry of polyaza molecules, ligand design and synthesis, and biomedical applications of coordination complexes. He has enjoyed a productive collaboration with Edward H. Wong for almost two decades and more recently with Carolyn J. Anderson.

been around for decades, their use remained limited because of the limited availability of relevant isotopes, which had to be produced in nuclear reactors or particle accelerators. However, the introduction of the small biomedical cyclotron, the self-contained radionuclide generator, and the dedicated small animal or clinical SPECT and PET scanners to hospitals and research facilities has increased the demand for SPECT and PET isotopes.

Traditional PET isotopes such as ^{18}F, ^{15}O, ^{13}N, and ^{11}C have been developed for incorporation into small molecules, but due to their often lengthy radiosyntheses, short half-lives, and rapid clearance, only early time points were available for imaging, leaving the investigation of biological processes, which occur over the duration of hours or days, difficult to explore. With the continuing development of biological targeting agents such as proteins, peptides, antibodies and nanoparticles, which demonstrate a range of biological half-lives, a need arose to produce new radionuclides with half-lives complementary to their biological properties. As a result, the production and radiochemistry of radiometals such as Zr, Y, In, Ga, and Cu have been investigated as radionuclide labels for biomolecules since they have the potential to combine their favorable decay characteristics with the biological characteristics of the targeting molecule to become a useful radiopharmaceutical (Tables 1 and 2).[2]

The number of papers published describing the production or use of these radiometals continues to expand rapidly, and in recognition of this fact, the authors have attempted to present a comprehensive review of this literature as it relates to the production, ligand development, and radiopharmaceutical applications of radiometals (excluding ^{99m}Tc) since 1999. While numerous reviews have appeared describing

Carolyn Anderson was born in Superior, WI, in 1962, and remained there throughout her school years. In 1985, she graduated Summa Cum Laude with a B.S. in Chemistry from the University of Wisconsin—Superior. In 1984, she received a fellowship to attend the Summer School in Nuclear Chemistry at San Jose State University, and this is where her interest in nuclear and radiochemistry began. She pursued her Ph.D. in Inorganic Chemistry with Prof. Gregory R. Choppin at Florida State University, studying the electrochemistry and spectroscopy of uranium complexes in room-temperature molten salts. On completion of her Ph.D. in 1990, she moved to Washington University School of Medicine (WUSM) in St. Louis, MO, to carry out postdoctoral research with Prof. Michael J. Welch in the development of radiopharmaceuticals for PET imaging. In 1993, she was promoted to Assistant Professor of Radiology, and she is currently Professor in the departments of Radiology, Biochemistry & Molecular Biophysics, and Chemistry. Her research interests include the development of radiometal-labeled tumor receptor-based radiopharmaceuticals for PET imaging and targeted radiotherapy of cancer and cancer metastasis. She greatly enjoys the productive collaboration with Edward Wong and Gary Weisman on the development of novel chelation systems for attaching metal radionuclides to biomolecules for nuclear medicine imaging applications.

certain aspects of the production, coordination chemistry, or application of these radiometals,[2−18] very few exhaustive reviews have been published.[10,12] Additionally, this review has been written to be used as an individual resource or as a companion resource to the review written by Anderson and Welch in 1999.[12] Together, they provide a literature survey spanning 50 years of scientific discovery. To accomplish this goal, this review has been organized into three sections: the first section discusses the coordination chemistry of the metal ions Zr, Y, In, Ga, and Cu and their chelators in the context of radiopharmaceutical development; the second section describes the methods used to produce Zr, Y, In, Ga, and Cu radioisotopes; and the final section describes the application of these radiometals in diagnostic imaging and radiotherapy.

2. The Coordination Chemistry of Cu, Ga, Y, In, and Zr

2.1. General Considerations

The development of metal-based radiopharmaceuticals represents a dynamic and rapidly growing research area that requires an intimate knowledge of metal coordination chemistry and ligand design. This section of the review covers general considerations regarding the parameters that are important in developing stable, kinetically inert radiometal complexes that can be incorporated into radiopharmaceuticals. Additionally, the aqueous coordination chemistry of these metals and their coordination complexes that are most relevant to radiopharmaceutical development are discussed below.

Relevant properties in aqueous solution of the five metal cations covered in this review are presented in Table 3. The acidic cations Ga(III), In(III), and especially Zr(IV) present precipitation problems at neutral pH in the absence of suitable complex formation. In terms of plausible aqueous redox processes relevant to radiopharmaceutical applications, only Cu(II) and its complexes are susceptible to reduction chemistry, although the possibility of an ascorbic acid reduction of a ^{89}Zr(IV) complex has been postulated.[19] Based on Pearson's hard−soft acid−base theory, the tetravalent Zr(IV) is an extremely hard acidic cation, followed by Y(III), Ga(III), and In(III). The Cu(II) cation is considered a borderline acid.

Table 1. γ- and β-Emitting Radiometals

Isotope	$t_{1/2}$ (h)	production methods	decay mode	E_γ (keV)	E_β (keV)	ref
^{67}Cu	62.01	accelerator ^{67}Zn(n,p)	β^- (100%)	91, 93, 185	577, 484, 395	578
^{67}Ga	78.26	cyclotron	EC (100%)	91, 93, 185, 296, 388		578
^{90}Y	64.06	^{90}Sr/^{90}Y generator	β^- (72%)		2288	578
^{111}In	67.9	cyclotron, ^{111}Cd(p,n)^{111}n	EC (100%)	245, 172		578

Table 2. Positron-Emitting Radiometals

isotope	$t_{1/2}$ (h)	methods of production	decay mode	E_{β^+} (keV)	ref
^{60}Cu	0.4	cyclotron, ^{60}Ni(p,n)^{60}Cu	β^+ (93%) EC (7%)	3920, 3000 2000	578
^{61}Cu	3.3	cyclotron, ^{61}Ni(p,n)^{61}Cu	β^+ (62%) EC (38%)	1220, 1150 940, 560	578
^{62}Cu	0.16	^{62}Zn/^{62}Cu generator	β^+ (98%) EC (2%)	2910	578
^{64}Cu	12.7	cyclotron, ^{64}Ni(p,n)^{64}Cu	β^+ 19(%) EC (41%) β^- (40%)	656	578
^{66}Ga	9.5	cyclotron, ^{63}Cu(α,nγ)^{66}Ga	β^+ (56%) EC (44%)	4150, 935	578
^{68}Ga	1.1	^{68}Ge/^{68}Ga generator	β^+ (90%) EC (10%)	 1880, 770	578
^{86}Y	14.7	cyclotron, ^{86}Sr(p,n)^{86}Y	β^+ (33%) EC (66%)	2335, 2019 1603, 1248 1043	578
^{89}Zr	78.5	^{89}Y(p,n)^{89}Zr	β^+ (22.7%) EC (77%)	897 909, 1675, 1713, 1744	208, 578

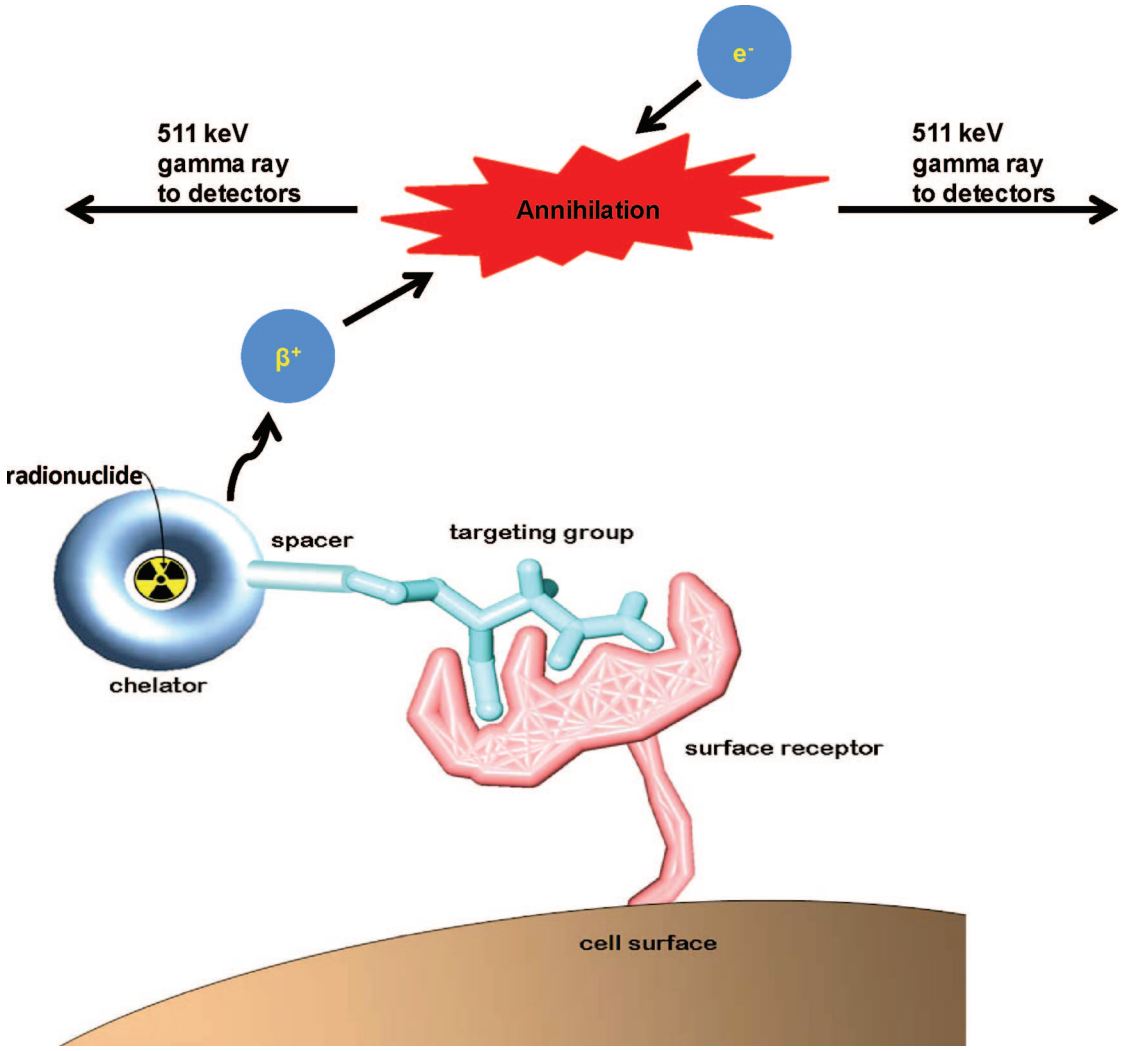

Figure 1. Cartoon depicting the fundamental principle of positron emission tomography (PET). As the targeting group interacts with the cell surface receptor, the positron-emitting radiometal decays by ejecting β^+ particles from its nucleus. After traveling a short distance in the electron-rich tissue, the positron recombines with an electron in a process called annihilation. During annihilation, the mass of the positron and electron are converted into two high-energy photons (511 keV γ rays), which are released approximately 180° apart to ensure that energy and momentum are conserved. Although attenuation is possible, these two γ rays are usually energetic enough to escape the organism and be collected by the detectors of a PET scanner.

Since the preponderance of radiometal complexes of note feature at least tetradentate ligands, we have restricted our discussion here to ligands with four or more donor sites coordinating the cation of interest. Rather than exhaustive coverage of all chelators of potential interest, we will discuss only selected representatives of the most-frequently reported ligands, especially those with more complete data of relevance. For the chosen representative chelators of each cation, we have listed available pertinent data on their denticity, coordination geometry, and thermodynamic stability. Where X-ray structural data are available, geometrical data on the coordination mode can provide useful insight into the "goodness of fit" for a specific cation−chelator pairing, the caveat being that actual solution structures or indeed number of species may be distinct from solid-state observations. For the four diamagnetic cations, solution NMR spectroscopic studies can be used to supplement X-ray data. Despite the difficulty of comparing stability constants of complex formation between ligands of different basicity and denticity, the listed log K_{ML}'s provide a convenient gauge of their relative affinities for a specific metal.

Table 3. Properties of Relevant Metal Cations

cation/electron configuration	ionic radius[a] (CN)	pK_a[b]	$k_{exchange}$,[c] s^{-1}	E_{red},[d] V, (acid)	hardness classification (I_A)[e]
Cu(II)/[Ar]3d^9	57 (4) 65 (5) 73 (6)	7.53	2×10^8	+0.34 (Cu^0) +0.16 (Cu^I)	borderline (2.68)
Ga(III)/[Ar]3d^{10}	47 (4) 55 (5) 62 (6)	2.6	7.6×10^2	−0.56 (Ga^0) −0.65 (Ga^{II})	hard (7.07)
In(III)/[Kr]4d^{10}	62 (4) 80 (6) 92 (8)	4.0	4.0×10^4	−0.34 (In^0) −0.49 (In^{II})	hard (6.30)
Y(III)/[Kr]	90 (6) 102 (8) 108 (9)	7.7	1.3×10^7	−2.37 (Y^0)	hard (10.64)
Zr(IV)/[Kr]	59 (4) 72 (6) 84 (8) 89 (9)	0.22		−1.54 (Zr^0)	hard

[a] Picometers.[579] [b] As hydrated cation.[580] [c] In H_2O.[581] [d] Versus NHE; ref 582, Table 6.2, p 267; ref 583, Appendix E. [e] $I_A = E_A/C_A$; refs 584 and 585; ref 586, Table 2.3.

For *in vivo* applications, kinetic inertness of metal−chelator complexes or conjugates can be more relevant than thermodynamic stability.[12,20,21] In general, acyclic chelator com-

plexes are less kinetically inert than macrocyclic complexes of comparable stability.[22−26] By the same token, acyclic chelators typically have faster metal-binding kinetics compared with their macrocyclic analogues, which can be a significant advantage for shorter-lived radiometals.[27−30] There have been efforts to enhance the binding rate of macrocycles by incorporation of an acyclic polydentate pendant arm.[31]

A variety of *in vitro* assays of metal−chelator complex integrity can be found in the literature.[32−35] A popular assay of aqueous kinetic inertness is acid decomplexation. This has some relevance in biological environments that are relatively acidic such as in hypoxic tissues and certain cell vesicles. However, the extremely high acidities, for example, 1−5 M HCl, often required to decompose relatively inert complexes clearly have no parallel to any *in vivo* conditions. Nor can such data be relied upon, without considerations of other factors, as the sole predictor of biological behavior.[36] Typically, the decomplexation of Cu(II) complexes is readily monitored through their electronic spectra. Demetalation of the diamagnetic Ga(III), In(III), Y(III), and Zr(IV) complexes can usually be followed by proton and ^{13}C NMR spectroscopy in acidified D_2O solutions. Where feasible, ^{71}Ga, ^{115}In, and ^{89}Y NMR studies can also be undertaken.[37−39] Although detailed mechanistic investigations are sometimes reported, more commonly only pseudo-first-order half-lives are reported, which should only be used to rank inertness qualitatively. Nonetheless, such data remain useful as a preliminary indicator of the *in vivo* viability of specific metal-based radiopharmaceuticals.

Competition or challenge assays of complexes of interest with excess biometals and biochelators are relevant since their typical concentrations are orders of magnitude higher than the radiolabeled complex's, requiring high chelator selectivity for the radiometal. For example, copper homeostasis is tightly regulated in biology,[40] and as a result, a variety of copper-binding biomolecules are present in extracellular (serum albumin, ceruloplasmin, transcuprin, etc.) and intracellular (transporters, chaperones, metallothioneins, superoxide dismutase, cytochrome *c* oxidase, etc.) environments.[41−43] A viable Cu(II) chelator should therefore be both thermodynamically stable and kinetically inert to transchelation challenges by these species. Highly charged cations like Y(III) and Zr(IV) may also have high affinity for bone tissues, while the avid Ga(III) binding of transferrin is well-established.[44−46] Serum stability studies using radiometal-labeled chelator complexes or their bioconjugates are routinely used in inertness assays. These are readily monitored by radio-TLC, HPLC, and LC-MS techniques.[47−49] *In vitro* uptake studies using specific cell lines have also been carried out in many assays. While simulating extracellular environments to an extent, these studies cannot always accurately forecast *in vivo* behavior. Ultimately, studies of animal biodistribution and bioclearance using radiometal-labeled complexes or bioconjugates need to be carried out to obtain realistic data on their *in vivo* performance.

The following discussion of pertinent acyclic and macrocyclic ligands and their specific metal coordination chemistry is organized according to their denticity. Most of these ligands have been designed to provide a minimum of four donor atoms, usually also incorporating anionic sites for charge balance (See Figures 2 and 3). While all are given numerical "**L(number)**" designations, many have been labeled additionally with their respective acronyms. Published X-ray crystal structures of Cu, In, Ga, Y, and Zr coordination complexes involving these ligands are also provided where appropriate. They were prepared from published CIF files using CrystalMaker 8.2 for Mac (CrystalMaker Software Ltd., Centre for Innovation & Enterprise, Oxford University Begbroke Science Park, Sandy Lane, Yarnton, Oxfordshire, OX5 1PF, UK; http://www.crystalmaker.com). Each atomic sphere is scaled to 0.4 times the covalent atomic radius, using the recently updated radii of Alvarez and co-workers.[50] In addition to the labeled and uniquely colored metal atoms, common elements are color coded as follows: C = gray, Cl = green, F = light green, N = blue, O = red, P = orange, and S = yellow. Hydrogen atoms have been omitted from the structures for clarity.

2.2. Aqueous Copper Coordination Chemistry

While +1 and +3 oxidation states are both accessible for copper in the presence of suitable donors, 3d^9 Cu(II) remains the predominant state for radiocopper chemistry in protic media. The aqueous cupric ion was long believed to have a tetragonally distorted hexa-aqua structure until a 2001 report suggested only five-coordination.[51] Its water-exchange rate has been found to be very rapid compared with most common first-row transition metal cations and as a result it has relatively facile substitution chemistry despite having some crystal-field stabilization. This is usually ascribed to the Jahn−Teller distortion that elongates one or more of its coordinated ligands. Classified as a cation of borderline hardness, the high affinity of Cu(II) for borderline nitrogen donors is well-established. With a relatively small ionic radius of between 57 and 73 pm for coordination numbers 4−6, it is particularly suitable for the formation of five-membered chelate rings; indeed the chelate effect is epitomized in its ethylenediamine family of complexes.[52] The popular use of polyazamacrocycles, especially cyclen and cyclam, for strong binding of Cu(II) is a consequence of the added advantage of the macrocyclic effect,[53] as borne out by their extensive coordination literature.[54−57]

The importance of *in vivo* redox activation of metallodrugs incorporating Pt(IV), Ru(III), and Co(III) has received increasing attention.[58−61] The role of bioreduction in copper radiopharmaceutical efficacy has been intensively studied in their thiosemicarbazone complexes, especially Cu-ATSM (**L9**).[62−64] Convincing evidence for the formation and selective retention/decomplexation of Cu(I)-intermediates from Cu(II) precursors in hypoxic tissues has been presented.[65,66] Whether Cu(II)/Cu(I) bioreduction is also a viable pathway for irreversible *in vivo* radiocopper loss from other chelator complexes and their bioconjugates is an intriguing possibility. There is some compelling evidence for the deteriorated *in vivo* performance of related Cu(II) complexes differing only in their reduction propensities. Specifically, the "long arm" dicarboxyethyl pendant-armed Cu(II) complex of cross-bridged cyclam has an E_{red} almost 400 mV higher (or more positive) than that its carboxymethyl-armed analogue, Cu-CB-TE2A (**L57**).[67] The former has been found to exhibit significantly inferior bioclearance behavior despite very similar coordination geometry and acid-inertness. More structure−activity studies, including the consequence of protonation on reduction feasibility, are warranted. Most polyazamacrocyclic complexes of Cu(II), however, have rather negative reduction potentials that are well below the estimated −0.40 V (NHE) threshold for typical bioreductants. It should be further noted that an appropriate *in vivo* donor able to alter the first or, perhaps even second coordination

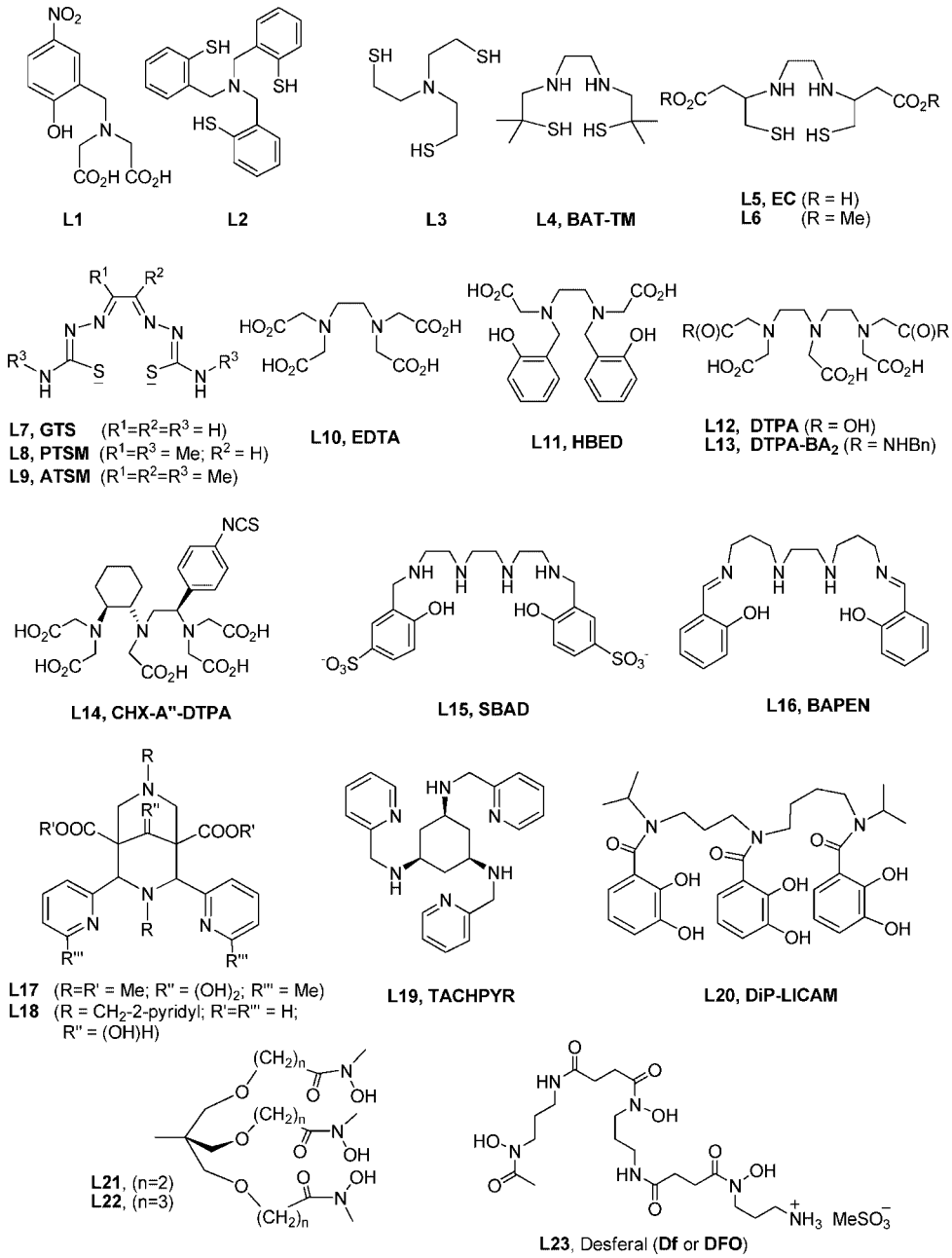

Figure 2. Selected acyclic chelators.

sphere around a metal cation can dramatically facilitate its redox processes. The relevance of this tuning of redox-active metal lability during biological iron transfer has been substantiated.[68,69] Whether such ternary interactions can play a role in the reductive demetalation of thermodynamically stable Cu(II) complexes *in vivo* has not been explored.

2.3. Copper(II) Complexes of Selected Chelators

The plasticity of the Cu(II) coordination geometry can be gleaned from a literature survey of 89 of its complexes with cyclen and cyclam derivatives.[70] Coordination numbers (CN) ranging from 4 to 6 were found with geometries approximating square planar, square pyramidal, trigonal bipyramidal, and octahedral. Tetradentate chelators are usually designed to cater to Cu(II)'s strong affinity for ligands favoring a square-planar geometry. Common donor sets include two amino or imino nitrogens combined with two charge-neutralizing anionic amido, oxo, or thiolato sites. These include numerous Schiff base or amino acid derived chelators. Full envelopment of Cu(II) in its maximum six-coordinate mode is much sought after. As a result, hexadentate chelators have become the most investigated in radiocopper chemistry. Popular scaffolds include triaza- or tetraazamacrocycles, especially TACN (**L26**), cyclen (**L38**), and cyclam (**L48**). Methodologies for selective attachment of appropriate pendant arms to their secondary amine nitrogen sites as well as to the carbon backbone have been developed.[71−79] Resulting donor sets usually incorporate anionic carboxylate or thiolate sites to provide a medley of charge-neutralizing N_3O_3, N_3S_3, or N_4O_2 coordination spheres. Data for selected Cu(II)−chelator complexes are listed in Table 4.

2.3.1. Acyclic Tetradentate Chelators

A dimethyl ester of *N*,*N*′-ethylenediamine-di-L-cysteinato, EC (**L5**), was reacted with Cu(II), and the resulting complex

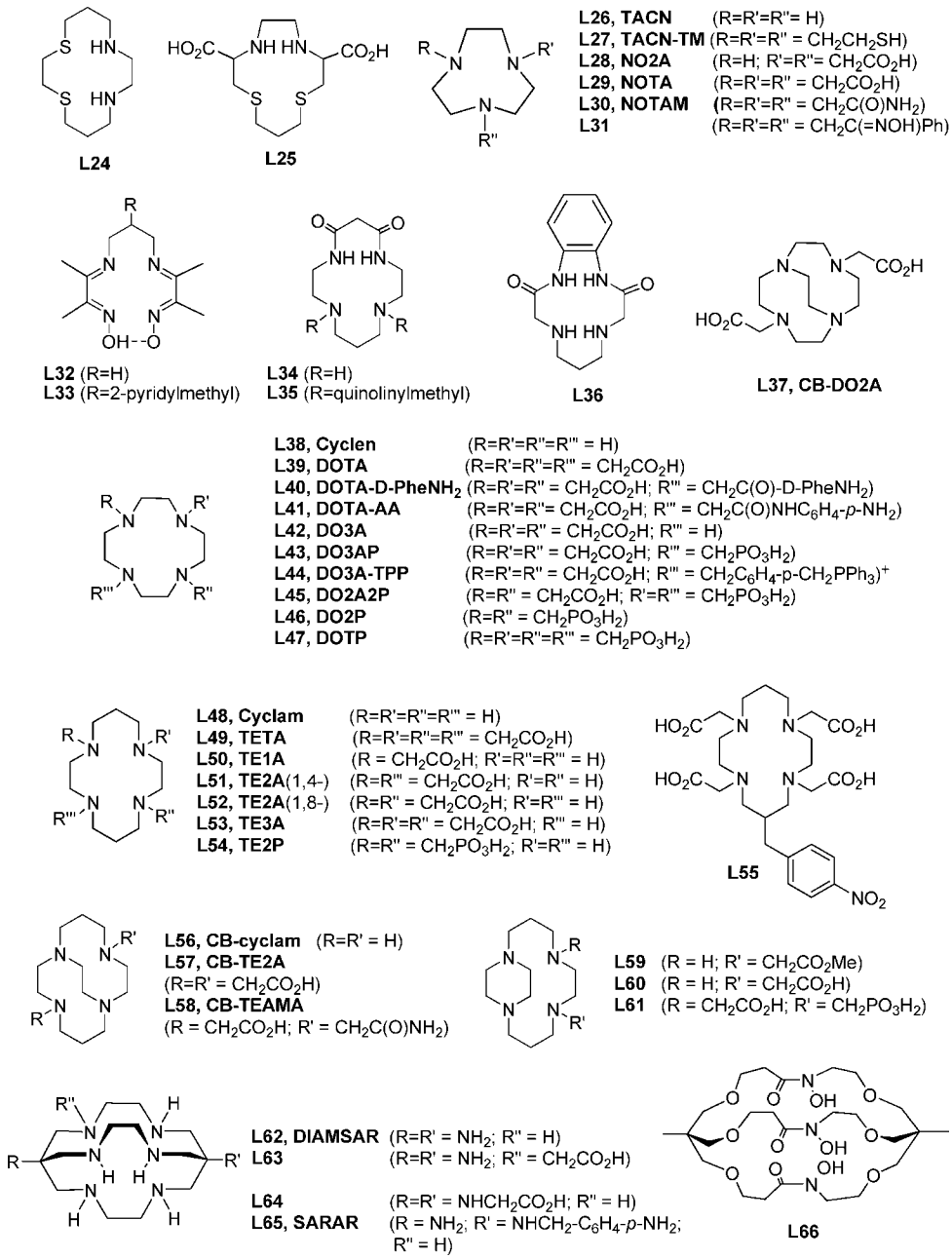

Figure 3. Selected macrocyclic chelators.

was structurally characterized and found to be substantially twisted (21°) from a square-planar geometry (Figure 4).[80]

Bis(thiosemicarbazonato) complexes of cold and radio-Cu(II) have been intensely investigated for hypoxia imaging (*vide infra*).[62,63,81] A series of X-ray structures of these complexes have been determined, and near square-planar geometries were typically observed (e.g., Cu-GTS (Cu-**L7**) and Cu-ATSM (Cu-**L9**) in Figures 5 and 6). Alkylation at the backbone C atoms was found to increase the backbone C−C bond length and allow the metal to fit better into the ligand cavity with shorter Cu−S bonds.[82] Their Cu(II)/Cu(I) reduction potentials have been shown to have significant bearing on their *in vivo* biological behavior.[62,63,66]

2.3.2. Acyclic Hexadentate Chelators

The Cu(II)-EDTA (**L10**) structure has been reported to be a tetragonally distorted N_2O_4 octahedron along one O−Cu−O axis (Figure 7).[83] A DTPA (**L12**) analogue also features a hexadentate chelator but with an N_3O_3 coordination environment (Figure 8).[84]

Rigid bispidine (3,7-diazabicyclo[3.3.1]nonane) derivatives with two appended pyridyl functions have been shown to be tetradentate in five-coordinate Cu(II) complexes (Cu-**L17**, Figure 9).[85] Variations with four pyridyl as well as two noncoordinating carboxylate groups for charge neutralization are hexadentate chelators, which were found to bind Cu(II) rapidly. An X-ray structure revealed a distorted octahedral N_6 coordination mode (Cu-**L18**, Figure 10). This chelator was conjugated to bombesin, radiolabeled with ^{64}Cu, and studied in rats.[86]

Hexadentate ligands based on the 1,3,5-triaminocyclohexane backbone appended with three methylpyridines (TACHPYR, **L19**) have been investigated as radiocopper chelators.[87,88] These form tetragonally distorted octahedral Cu(II) complexes (Figure 11).

Table 4. Data on Selected Cu(II)−Chelator Complexes

chelator	donor set (total CN)	cation coordination geometry	log K_{ML}[a]	E_{red} or E_p[b]	acid inertness, $t_{1/2}$ (conditions)	ref
L6	N_2S_2 (4)	distorted square planar				80
L9, ATSM	N_2S_2 (4)	distorted square planar		−0.40 (q-rev)		81, 82
L10, EDTA	N_2O_4 (6)		18.8, 19.2			587, 588
L12, DTPA	N_3O_3 (6)		21.4			589
L17	N_6 (6)	distorted octahedron	16.3	0.08 (q-rev)		590
L19, TACHPYR	N_6 (6)	distorted octahedron				88
L29, NOTA	N_3O_3 (6)	distorted trigonal prism	19.8, 21.6	∼−0.70 (irrev)	<3 min (5 M HCl, 30°)	586, 591, 592
L38, cyclen	N_4 (5)	square pyramid	24.6		<3 min (5 M HCl, 30°)	112, 593
L34, **L36**	N_4 (5)	distorted square pyramid	8.3	∼−1.60[b] (irrev)		99, 100
L39, DOTA	N_4O_2 (6)	distorted octahedron	22.2, 22.7	∼−0.74 (irrev)	<3 min (5 M HCl, 90°)[112]	145, 594, 595
L46, DO2P	N_4O_2 (6?)		28.7			103
L48, cyclam	N_4 (5−6)	square pyramid, tetragonally elongated octahedral	27.2	∼−0.48 (irrev)	3.8 min (5 M HCl, 90°)[112]	593
L49, TETA	N_4O_2 (6)	distorted octahedron	21.1, 21.9	∼−0.98 (irrev)	<3 min (5 M HCl, 90°)[112]	145, 594, 595
L54, TE2P	N_4O_2 (6)	tetragonally distorted octahedron	26.5	∼−0.45 (irrev)	1.7 h (1 M HCl, 60°)	114
L56, CB-cyclam	N_4 (5)	distorted square pyramid	27.1	−0.32 (q-rev)	11.8 min (1 M HCl, 90°)	111, 112, 596
L37, CB-DO2A	N_4O_2	distorted octahedron		∼−0.72 (irrev)	4.0 h (1 M HCl, 30°)	21, 112
L57, CB-TE2A	N_4O_2 (6)	distorted octahedron		−0.88 (q-rev)	154 h (5 M HCl, 90°)	111, 112
L62, DIAMSAR	N_6 (6)	distorted octahedron or trigonal prism		∼−0.90 (irrev)[13]	40 h (5 M HCl, 90°)[13]	118

[a] K_{ML} = [ML]/[M][L]. [b] E_{red} = reduction potential and E_p = peak potential only, both vs NHE; (q-rev) = quasi-reversible; (irrev) = irreversible reduction.

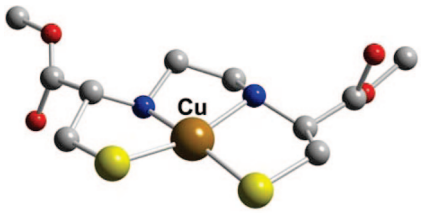

Figure 4. Cu-**L6**.

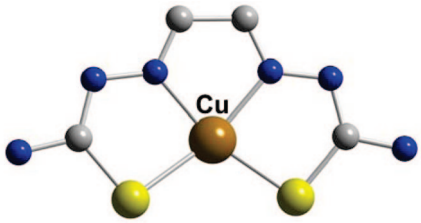

Figure 5. Cu-GTS (**L7**).

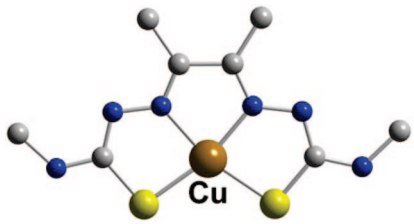

Figure 6. Cu-ATSM (**L9**).

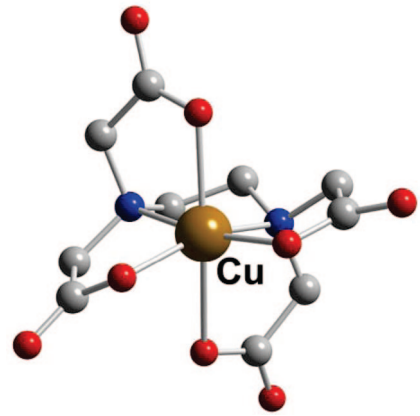

Figure 7. Cu-EDTA (**L10**).

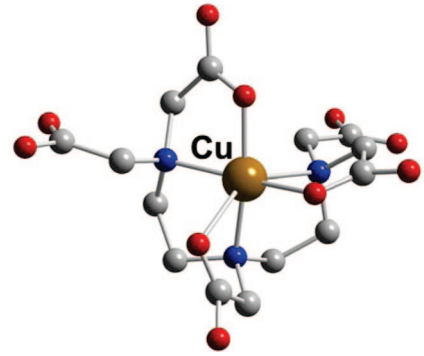

Figure 8. Cu-DTPA (**L12**).

2.3.3. Macrocyclic Chelators

The 14-membered N_2S_2 macrocycle **L24** was found to form the most inert Cu(II) complex compared with other ring sizes.[89] New N_2S_2 macrocycles with two appended carboxymethyl arms (**L25**) have been synthesized and complexed with both Cu(II) and ^{64}Cu(II).[90] Molecular modeling suggested that only the 13-membered macrocycle can form a six-coordinate complex while the 14-membered analogue can only coordinate with its O_2S_2 donors.

Derivatives of TACN with either two (NO2A, **L28**) or three (NOTA, **L29**) carboxymethyl pendant arms both complex Cu(II) with good affinity. Their structures (Figures 12 and 13) reflect the ability of the cation to adopt either 5- or 6-coordination modes. The former has an N_3O_2 square-pyramidal geometry with one N axial.[91] The latter N_3O_3 donor set forms a distorted trigonal prismatic geometry.[92] A TACN derivative with three oxime arms (**L31**) yielded a 5-coordinate Cu(II) complex with one oxime arm loosely coordinated (- - -) but held by a strong hydrogen bond to a coordinated oxime (Figure 14).[93]

Monocationic diimine dioxime (**L32**) complexes of Cu(II) were labeled with ^{64}Cu, and their biodistributions were studied.[94−96] The X-ray structure of a Cu(II) complex of a pyridyl-tethered derivative revealed a tetradentate ligand

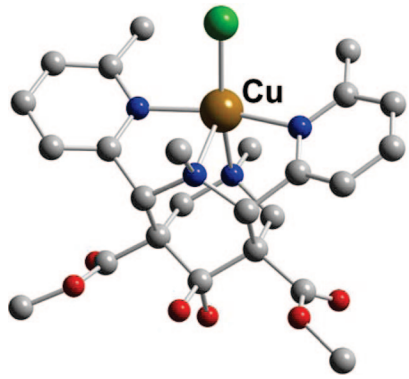

Figure 9. Cu-**L17**.

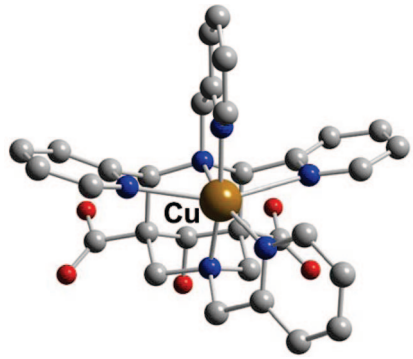

Figure 10. Cu-**L18**.

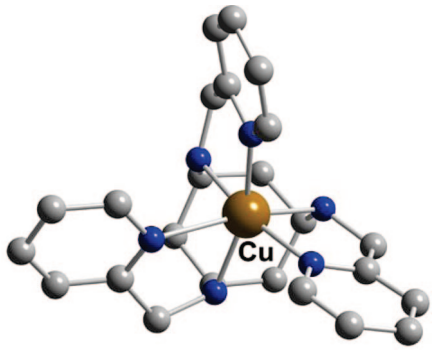

Figure 11. Cu-TACHPYR (**L19**).

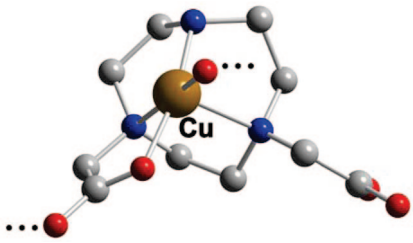

Figure 12. Cu-NO2A (**L28**).

(**L33**) forming the base of a square pyramid with an axial water but no pyridyl coordination (Figure 15).[97] Propylenediamine dioxime ligands have also been examined for their Cu(II) complexation in order to model radiopharmaceuticals.[98] The cation was again found to adopt a square-pyramidal coordination geometry featuring an apical water.

Dioxotetraazamacrocyclic Cu(II) complexes have been investigated for their radiocopper chelation potential.[99] Of the chelators with varying ring sizes studied, dioxocyclam (**L34**) was shown to form the most stable complex. A methylquinoline pendant-armed dioxocyclam (**L35**) was

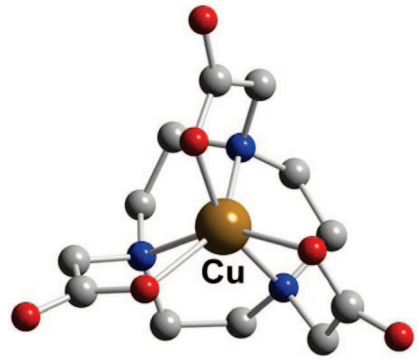

Figure 13. Cu-NOTA (**L29**).

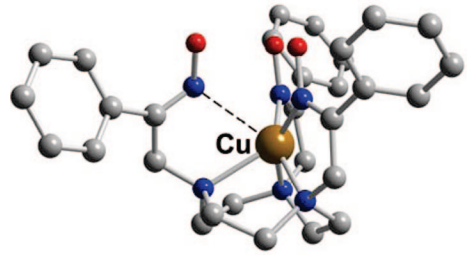

Figure 14. Cu-**L31**.

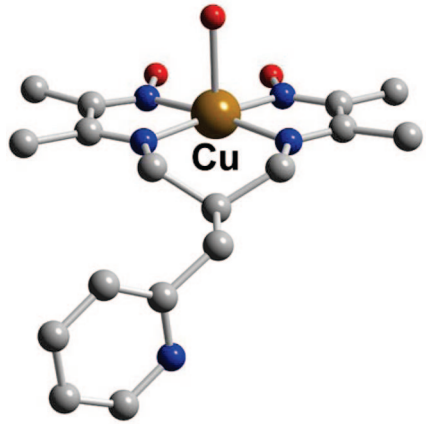

Figure 15. Cu-**L33**.

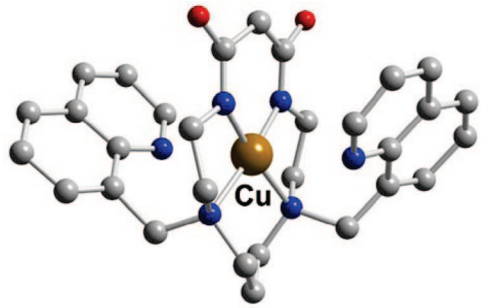

Figure 16. Cu-**L35**.

found to doubly deprotonate at its amide N's upon Cu(II) binding. Its structure has a distorted square-planar coordination geometry (Figure 16).[82] Recently, a benzo-annelated dioxohomocyclen (**L36**) was synthesized, and its Cu(II) complexation and ^{64}Cu radiolabeling were investigated.[100] A four-coordinate distorted square-planar structure was found. This complex has an extremely low reduction potential but can be reversibly oxidized.

Carboxymethyl pendant-armed derivatives of cyclen including DOTA (**L39**) and DO3A (**L42**) have been investi-

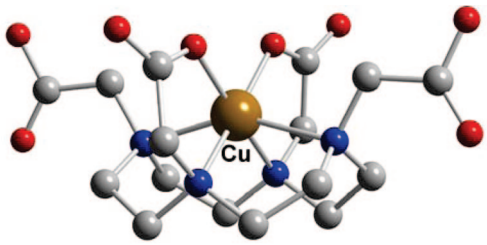

Figure 17. Cu-DOTA (**L39**).

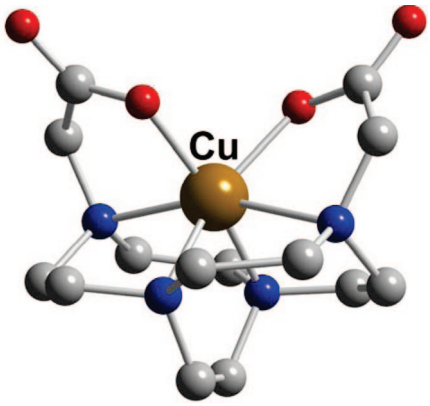

Figure 18. Cu-CB-DO2A (**L37**).

gated for their Cu(II) binding. An X-ray structure of Cu-DOTA (Cu-**L39**) shows the expected pseudo-octahedral geometry with all cyclen N's and two carboxymethyl arms from nonadjacent N's coordinating *cis* to each other (Figure 17).[101] An analogous geometry was found for the Cu-DO3A (**L42**) structure.[102] The dicarboxymethyl armed cross-bridged cyclen (CB-DO2A, **L37**) was shown to envelop the Cu(II) in a very distorted octahedral geometry with the carboxylate donor sites *cis* to each other (Figure 18).[21] It was pointed out that the metal center is significantly distended from the chelator cavity, which may account for its significantly lower inertness compared with its cyclam analogue Cu-CB-TE2A (Cu-**L57**) (*vide infra*).

Cyclen derivatives appended with methanephosphonate pendant arms such as DO2P (**L46**) and DOTP (**L47**) have been synthesized and chelated to Cu(II) and ^{64}Cu.[103] Mixed phosphonate- and acetate-armed cyclen (e.g., DO2A2P, **L45**) has also been studied with the highest log K_{ML} found for Cu-DO2P (Cu-**L46**).[104]

Due to the good cation/cyclam match, numerous Cu(II) complexes of cyclam and its derivatives with at least one carboxymethyl pendant arm on N have been prepared and studied. As expected, the singly armed chelator C-hexamethyl-TE1A (Me_6-**L50**) yielded a square-pyramidal Cu(II) structure (Figure 19).[105] Several structures of the doubly armed ligand complexes have been determined. The first features carboxylates on adjacent ring N's (1,4-TE2A, **L51**, Figure 20)[106] while the latter on nonadjacent N's (1,8-TE2A, **L52**, Figure 21).[107] Two diprotonated Cu-TETA (**L49**) structures were shown to have their axial elongations either along the acetate O's or across two cyclam ring N's (Figure 22).[108] A C-functionalized TETA Cu(II) complex, Cu-**L55**, also has a pseudo-octahedral metal coordination mode (Figure 23).[109]

Two cross-bridged cyclam chelators, one with two carboxymethyl arms (CB-TE2A, **L57**), the other with one carboxymethyl and one acetamide arm (CB-TEAMA, **L58**) have been prepared to compare the *in vivo* behavior of their

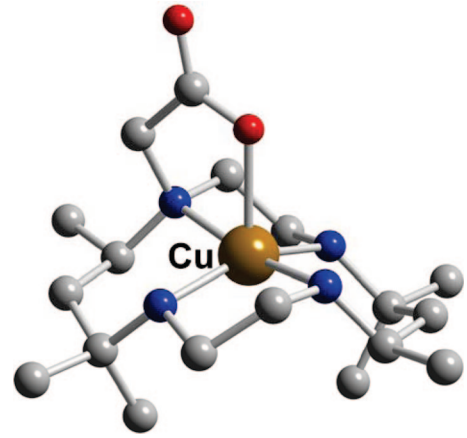

Figure 19. Cu-TE1A (**L50**).

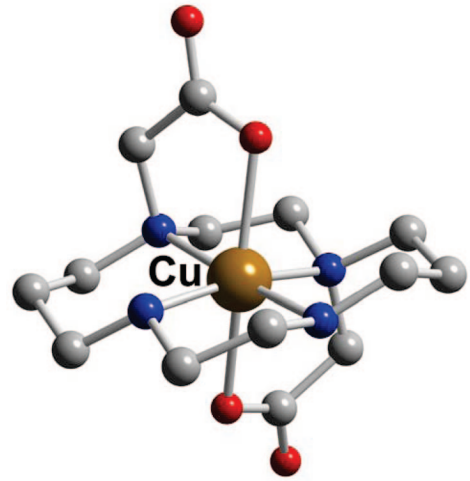

Figure 20. Cu-**L51**.

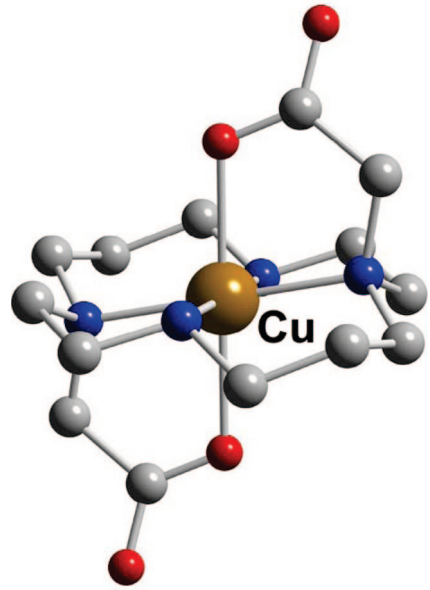

Figure 21. Cu-**L52**.

^{64}Cu complexes.[110] The former structure revealed full envelopment of the Cu(II) in a pseudo-octahedral geometry with elongation along one N−Cu−O axis (Figure 24).[111] While the latter has a very similar geometry, a weaker amide O-coordination is observed (Figure 25).[110] The Cu-CB-TE2A complex has been shown to have remarkable kinetic inertness toward acid decomplexation, with a half-life of almost a week

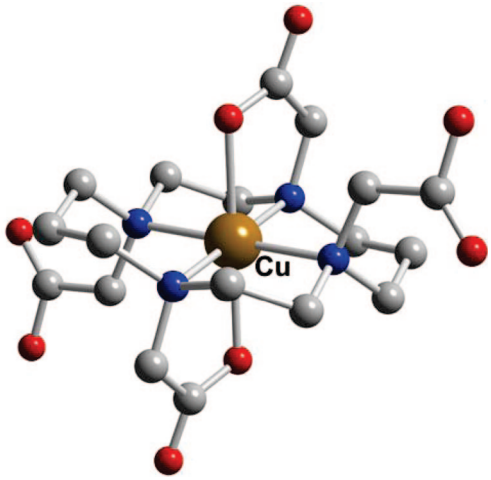

Figure 22. Cu-H_2TETA (**L49**).

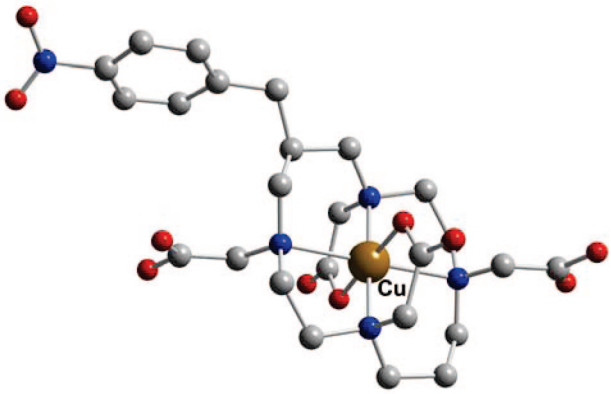

Figure 23. Cu-**L55**.

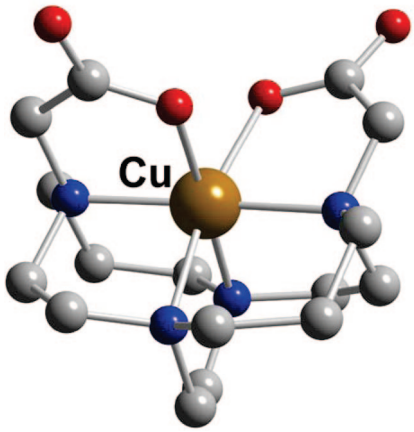

Figure 24. Cu-CB-TE2A (**L57**).

in 5 M HCl, even at 90°.[112] A derivative of this chelator with a C-functionalized *p*-isothiocyanatobenzyl group has been prepared and successfully conjugated to biotin.[113]

The diphosphonate pendant-armed cyclam TE2P (**L54**) has been reported to form a very stable Cu(II) complex with a tetragonally distorted octahedral geometry (Figure 26).[114] This complex also has a respectable acid inertness compared with typical cyclam copper complexes.

Pendant-armed derivatives of adjacent or side-bridged cyclam (**L58**, **L59**) have been prepared and complexed with Cu(II).[108] These chelators strongly favor square-planar coordination of the cation by the macrocycle with axial coordination by a pendant arm to give square-pyramidal

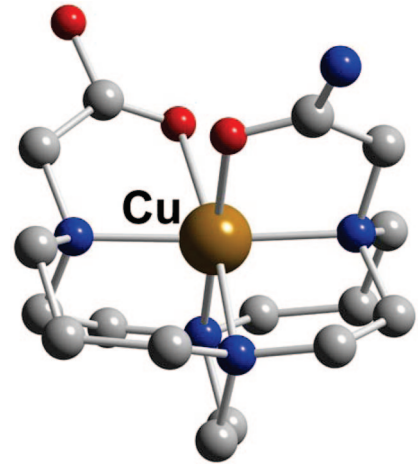

Figure 25. Cu-CB-TEAMA (**L58**).

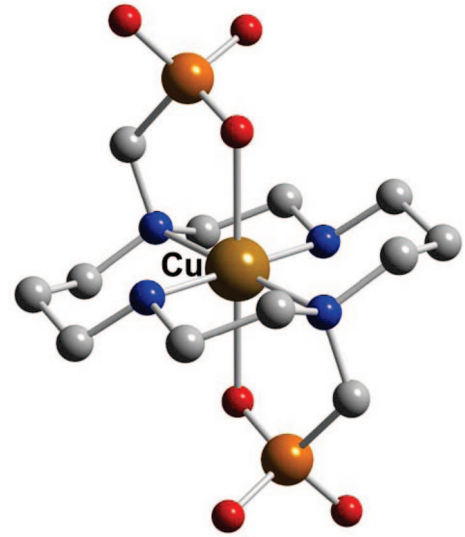

Figure 26. Cu-TE2P (**L54**).

geometries. A recent novel side-bridged cyclam with one acetate and one phosphonate pendant arm (**L60**) has been synthesized, labeled with ^{64}Cu, and studied *in vivo*. It was reasoned that unlike CB-TE2A, this bifunctional chelator (BFC) will form a charge-neutral Cu(II) complex despite conjugation of one acetate arm.[115]

The venerable hexaamine cryptand, sarcophagine, is well-known for its strong binding of Cu(II) and inertness of its complexes.[116−118] Its derivatives DIAMSAR (**L62**) and SARAR (**L65**) have been investigated as ligands for copper radiopharmaceuticals by several research groups.[119−124] Diprotonated DIAMSAR (**L62**) was found to have a Cu(II) coordination mode halfway toward trigonal prismatic but with two elongated *trans* Cu−N bonds (Figure 27).[118] A related carboxymethyl pendant armed complex (Cu-**L63**) is closer to an octahedral coordination mode again with two long *trans* bonds (Figure 28),[125] while a doubly carboxymethylated DIAMSAR Cu(II) complex (Cu-**L64**) has two elongated *cis* bonds (Figure 29).[126] Recently, the Cu(II) complex of a glutaric acid DIAMSAR derivative suitable for peptide conjugation was synthesized. Its coordination geometry is again distorted octahedral with axial Jahn−Teller elongations.[124]

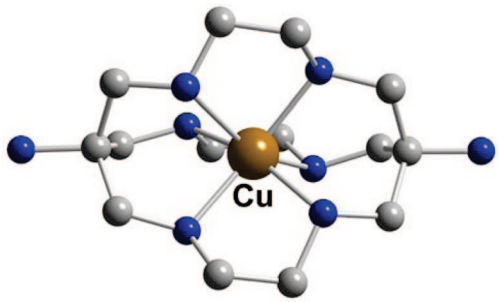

Figure 27. Cu-**L62**.

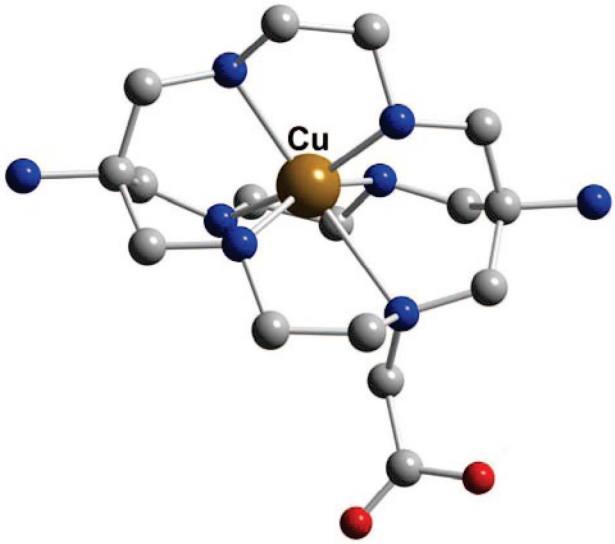

Figure 28. Cu-**L63**.

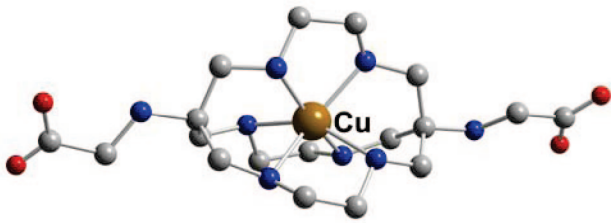

Figure 29. Cu-**L64**.

2.4. Aqueous Gallium(III) Coordination Chemistry

The prevalent gallium oxidation state in aqueous solution is +3. This small and highly charged cation of ionic radius 47−62 pm (CN 4−6) is quite acidic with a pK_a of 2.6 in its hydrated form. As a result, it has low solubility in normal pH media in the absence of suitable donors. Due to its strong affinity for hydroxide, at very high pH, it also has a propensity to demetalate from its complexes and form the gallate anion $Ga(OH)_4^-$. Among the four water-soluble metal cations discussed in this review, aqueous Ga(III) has the most sluggish water exchange rate due to its small size and high charge.

As a classic hard acidic cation, Ga(III) is strongly bound to ligands featuring multiple anionic oxygen donor sites, although it has also been shown to have good affinity for thiolates. Typically chelators have been developed to sequester Ga(III) up to its maximum coordination number of 6 in a pseudo-octahedral geometry. A comprehensive review of six-coordinate Ga(III) complexes has appeared recently.[127]

It is well-known that the biological iron transporter transferrin has a strong affinity for Ga(III) (Table 5).[46,128]

Table 5. Data for Selected Ga(III)−Chelator Complexes

chelator	donor set (total CN)	cation coordination geometry	log K_{ML}[a]	ref
L1	NO_3 (6)	distorted octahedron	19.1 (*p*-NO_2), 25.2 (*p*-OMe)	129
L2	NS_3 (4)	distorted tetrahedron	20.5	130
L4, BAT-TM	N_2S_2 (5)	distorted square pyramid		132
transferrin	NO_5 (6)		20.3, 19.8	46, 128
L5, EC	$N_2O_2S_2$ (6)	distorted octahedron	31.5	133, 586
L10, EDTA	N_2O_4 (6)	distorted octahedron	21.0, 22.0	588, 593
L11, HBED	N_2O_4 (6)		37.7, 38.5	135, 172
L12, DTPA	N_3O_3 (6?)		25.5	593
L15, SBAD	N_4O_2 (6)	distorted octahedron	28.3	139
L16, BAPEN	N_4O_2 (6)	distorted octahedron		143, 144
L29, NOTA	N_3O_3 (6)	distorted octahedron	31.0	145, 597
L27, TACN-TM	N_3S_3 (6)	distorted octahedron	34.2	145
L39, DOTA	N_4O_2 (6)	distorted octahedron	21.3	145
L49, TETA	N_4O_2 (6)	distorted octahedron	19.7	145
L37, CB-DO2A	N_4O_2 (6)	distorted octahedron		162
L57, CB-TE2A	N_4O_2 (6)	distorted octahedron		163
L20, DiP-LICAM	O_6 (6)		38.6	187
L66	O_6 (6)		27.5	
L21			25.6	598
L22			27.3	
L23, DFO	O_6 (6)		28.6	599

[a] K_{ML} = [ML]/[M][L].

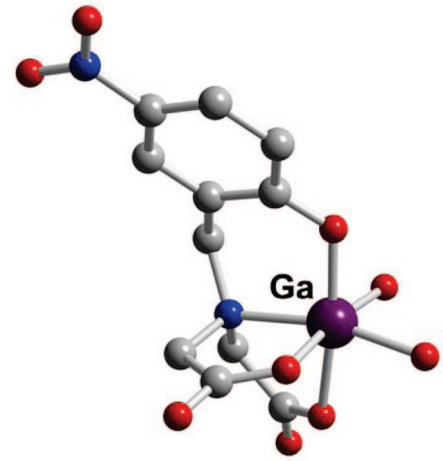

Figure 30. Ga-**L1**.

Radiogallium chelator complexes must therefore be sufficiently inert to transchelation by this biomolecule to have efficacy for *in vivo* applications. Data for selected Ga(III)–chelator complexes are presented in Table 5.

2.4.1. Tetradentate Ligands

Tetradentate *o*-hydroxybenzyl derivatives of iminodiacetic acid (**L1**) were designed to provide an NO_3 donor set, which completes the distorted octahedral coordination around the Ga(III) center together with two *cis*-coordinated waters (Figure 30).[129] In accordance with substituent effects, the *p*-OMe derivative has the highest stability constant, while *p*-NO_2 has the lowest.

The tripodal NS_3 chelator tris(2-mercaptobenzyl)amine (**L2**) formed a stable four-coordinate Ga(III) complex with a distorted tetrahedral structure (Figure 31).[130] Under similar preparative conditions, the analogous In(III) complex was found to be five-coordinate with additional solvent binding.

A bis(aminothiolate) N_2S_2 chelator yielded a distorted square-pyramidal GaCl complex with one S donor in the axial site.[131] A similar structure was determined for the related GaCl−BAT-TM (GaCl−**L4**) except that chloride is

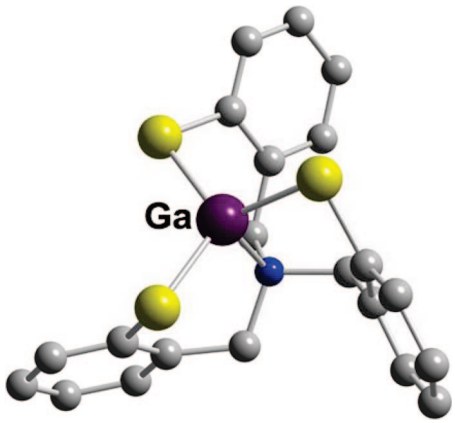

Figure 31. Ga-**L2**.

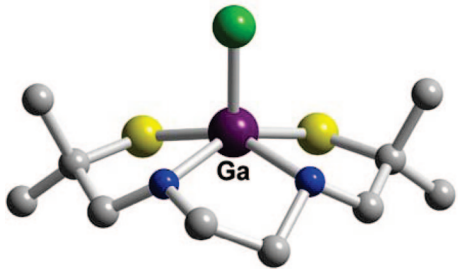

Figure 32. Ga-BAT-TM (**L4**).

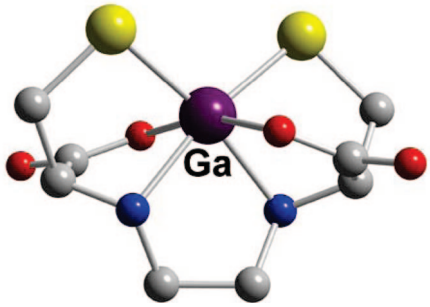

Figure 33. Ga-EC (**L5**).

the axial ligand (Figure 32).[132] In aqueous acetonitrile solution, however, NMR spectra revealed the presence of two different N_2S_2-coordinated species.

2.4.2. Hexadentate Ligands

An acyclic hexadentate chelator *N*,*N*′-ethylene-di-L-cysteine (EC, **L5**) with $N_2O_2S_2$ donor sites has been found to form a very stable complex with Ga(III) (Table 5).[133] This structure is a distorted octahedron with the two carboxylate O's in *trans* arrangement (Figure 33). Additionally, the [Ga-EDTA, **L10**]$^-$ structure has been reported in which the acyclic chelator is fully hexadentate in a distorted octahedral coordination sphere (Figure 34).[134]

The aminophenolate chelator *N*,*N*′-bis(2-hydroxybenzyl)-ethylenediamine-*N*,*N*′-diacetic acid (HBED, **L11**) has an N_2O_4 donor set, and its Ga(III) complex has a very high stability constant (Table 5).[135] As a consequence, it has generated considerable interest as a bifunctional chelator. The derivative *N*,*N*′-bis[2-hydroxy-5-carboxyethyl)-benzyl]ethylene diamine-*N*,*N*′-diacetic acid (HBED-CC)[136] and its tetrafluorophenyl ester derivative have been described to promote facile coupling to both scFV and anti-Ep-CAM diabodies.[137] Using this BFC these biomolecules could be labeled with ^{68}Ga to give specific activities of 142 GBq/

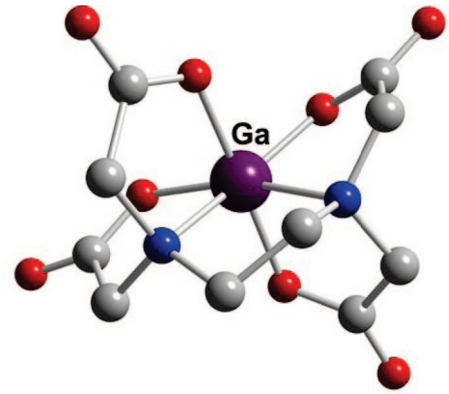

Figure 34. Ga-EDTA (**L10**).

Table 6. Data for Selected In(III)−Chelator Complexes

chelator	donor set (total CN)	cation coordination geometry	log K_{ML}[a]	ref
L2	NS_3 (5)	~trigonal bipyramid	21.2	130, 173
L3	NS_3 (5)	~trigonal bipyramid		
L4, BAT-TM	N_2S_2 (5)	square pyramid		132
transferrin	NO_5 (6)	distorted octahedron(?)	18.7	128
L5, EC	$N_2O_2S_2$ (6)	distorted octahedron	33.0	133
L11, HBED	N_2O_4 (6)		27.9, 27.8	138, 172
L10, EDTA	N_2O_4 (7)	~pentagonal bipyramid	24.9	593
			25.1, 25.3	588, 600
L12, DTPA	N_3O_4 (7)	~pentagonal bipyramid	29.5, 29.0	587, 588, 600
	N_3O_5 (8)	~square antiprism	29.0	
L15, SBAD	N_4O_2		24.5	139
L29, NOTA	N_3O_3 (6)	distorted octahedron	26.2	37, 147
L27, TACN-TM	N_3S_3 (6)	distorted octahedron	36.1	145
L39, DOTA	N_4O_2 (8?)		23.9	186
L49, TETA	N_4O_2		21.89	186
L57, CB-TE2A	N_4O_2 (6)	distorted octahedron		155
L23, DFO	O_6		21.4	599
L20, DiP-LICAM	O_6		39.2	187

[a] K_{ML} = [ML]/[M][L].

μmol. Interestingly, a potentially octadentate DTPA (**L12**) derivative gave a less stable complex likely due to its structural constraints.[138] Linear tetraamines end-capped with phenols, like SBAD (**L15**), have been synthesized, and their Ga(III) complexations have been investigated.[139] These were all found to favor Ga(III) over In(III) binding.

Although numerous complexes of both cold and radio-Ga(III) with DTPA (**L12**) and its derivatives have been prepared and studied, surprisingly no X-ray structure of the parent complex has yet been published. It is noteworthy that both EDTA (**L10**) and DTPA (**L12**) bind In(III) more avidly than Ga(III) (Tables 5 and 6). Recently, a variant of DTPA (**L12**) incorporating the *trans*-1,2-diaminocyclohexane backbone, CHX-A″-DTPA (**L14**),[140] has been bioconjugated and studied as a chelator for ^{68}Ga, ^{86}Y, and ^{111}In in melanoma imaging.[141]

A family of hexadentate bis(salicylaldimine) chelators, BAPEN (**L16**), have been developed as carriers for ^{68}Ga radiopharmaceuticals.[142−144] These all feature a set of N_4O_2 donors enveloping the Ga(III) in a pseudo-octahedral coordination sphere. The structure of one of these is shown (Figure 35).

The tris-acetate pendant armed 1,4,7-triazacyclononane (TACN) derivative, NOTA (**L29**), and its relatives have been found to form highly stable Ga(III) complexes.[145] An X-ray structure of Ga-NOTA (Ga-**L29**) confirmed the distorted octahedral N_3O_3 envelopment of the cation (Figure 36).[37,146] Remarkably, Ga-NOTA (Ga-**L29**) showed such high acid

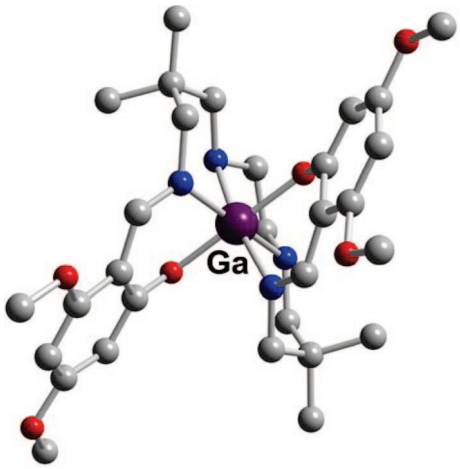

Figure 35. Representation Ga-BAPEN (**L16**) structure.

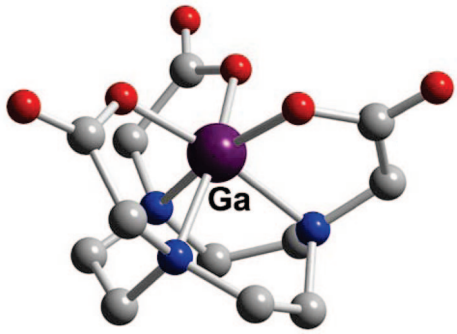

Figure 36. Ga-NOTA (**L29**).

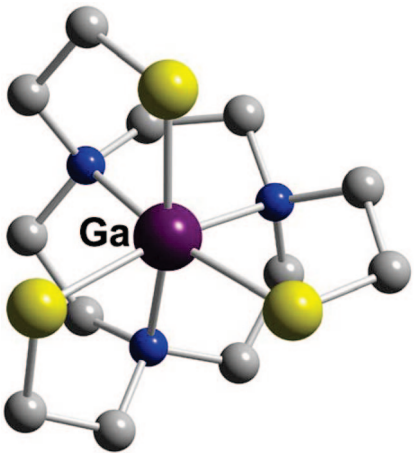

Figure 37. Ga-TACN-TM (**L27**).

inertness that it survived 5 M HNO_3 for over 6 months.[37] This is in stark contrast to In-NOTA (In-**L29**), which demetalated irreversibly within minutes at pD < 0. The tris(2-mercaptoethyl) pendant-armed TACN chelator, TACN-TM (**L27**), also formed a distorted octahedral structure with Ga(III), again with impressive stability (Figure 37).[146] The superb stability of Ga(III)-NOTA (Ga-**L29**) (log $K = 30.1$; pM = 26.4)[147] underscores the use of this agent in radiopharmaceutical chemistry. This exceptional stability is believed to arise from the effective encapsulation of the gallium ion, which has an ionic radius of 0.76 Å within the macrocyclic cavity. Additional protection is afforded by the pendant carboxymethyl arms that help to protect the Ga ion from nucleophilic attack, which would cause complex instability and transchelation *in vitro* or *in vivo*. Since its synthesis, several NOTA (**L29**) analogues have been prepared with modified pendant groups for coupling to biological molecules, to influence the charge on the complexes once complexation has occurred or to facilitate coupling during peptide synthesis.[148−154]

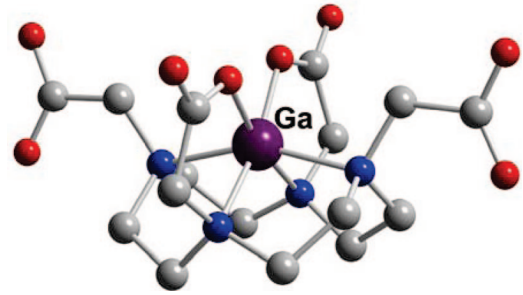

Figure 38. Ga-DOTA (**L39**).

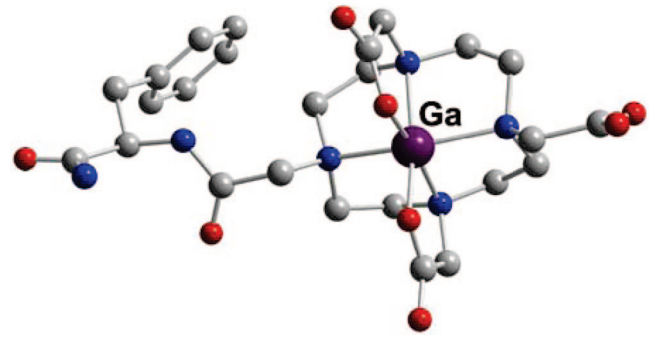

Figure 39. Ga-DOTA-D-PheNH$_2$ (**L40**).

Since the potentially octadentate DOTA (**L39**) can more than saturate Ga(III)'s usual six-coordination sphere, both its mono- and diprotonated structures feature a similar distorted octahedral coordination composed of two *cis*-carboxylates and four macrocyclic N's (Figure 38).[155,156] It is advantageous that a free carboxymethyl arm can be available for conjugation to targeting moieties. A variety of such complexes have appeared in the literature. The Ga-DOTA-D-PheNH$_2$ (Ga-**L40**) coordination mode is again pseudo-octahedral with *cis*-carboxylate coordination, while the remaining acetate and amide arms are unbound (Figure 39).[157] It was therefore postulated that the better kidney clearance of the radiolabeled DOTA^0-D-Phe^1-Tyr^3-octreotide, ^{67}Ga-DOTA(**L39**)-TOC, compared with its ^{90}Y-labeled analogue was due to their different coordination modes. Whereas the former has uncoordinated amide and carboxylate arms, the latter is likely fully octa-coordinated. When DOTA (**L39**) was linked to a mitochondrion-targeting triphenylphosphonium moiety to give DO3A-TPP (**L44**), its Ga(III) complex again retained the six-coordinate pseudo-octahedral geometry (Figure 40).[158] Unfortunately, DOTA (**L39**) has many potential drawbacks as a BFC for gallium radiometals, which include an overly large cavity size that can lead to lower thermodynamic stability as well as nonselectivity as a metal chelator.[159] Additionally, the complexation kinetics are slower, and as a result the complexation reactions often require elevated temperatures and longer reaction times, which are counterproductive given the short half-life of the ^{68}Ga radionuclide. The thermodynamic stability of Ga(III)-DOTA (Ga-**L39**) is approximately 10 orders of magnitude lower than that of Ga(III)-NOTA (Ga-**L29**), with a log K of 21.3 and a pM of 15.2.[160] Given the low pM values, it is interesting that radiogallium DOTA (**L39**) complexes have

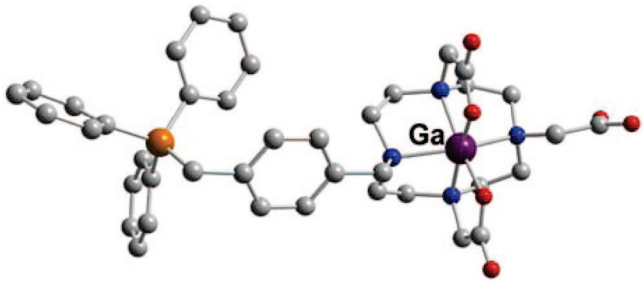

Figure 40. Ga-DO3A-TPP (**L44**).

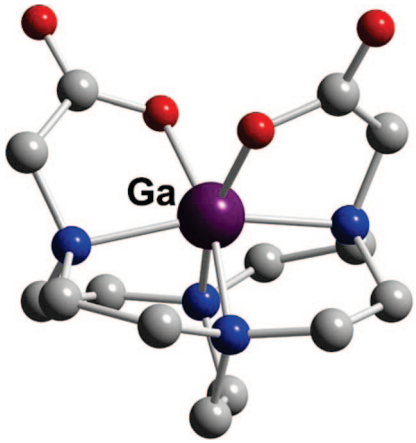

Figure 41. Ga-CB-DO2A (**L37**).

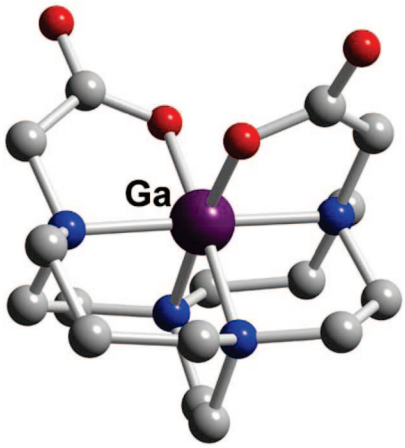

Figure 42. Ga-CB-TE2A (**L57**).

shown *in vivo* stability in agents such as $^{67/68}$Ga-DOTA(**L39**)-TOC. However, there are reports that radiogallium DOTA(**L39**)-RGD peptides have demonstrated compromised stability *in vivo*, with the radiogallium demonstrating binding to plasma proteins.[161]

Related to Ga-DOTA (Ga-**L39**) is the complex Ga-TETA (Ga-**L49**), but no structural data has been reported for it. Further, Ga-TETA (Ga-**L49**) has a lower stability constant than the former complex (log K = 19.7; pM = 14.1).[160] It should be noted that TETA (**L49**), unlike DOTA (**L39**), does not have a favorable *fac*-coordinating conformation.

Both dicarboxymethyl pendant-armed cross-bridged cyclen (CB-DO2A, **L37**) and cross-bridged cyclam (CB-TE2A, **L57**) gallium complexes have been synthesized and structurally characterized.[162,163] As expected, distortions from an octahedral geometry are much more pronounced in the former (Figures 41 and 42). Of these two, only Ga-CB-TE2A

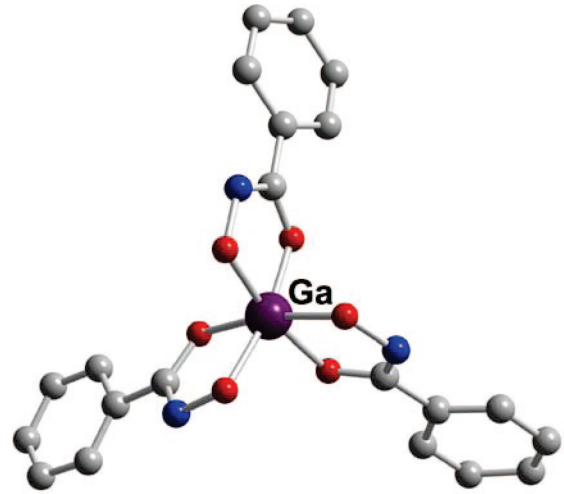

Figure 43. Ga-tris(benzohydroxamate).

(Ga-**L57**) showed impressive acid inertness. A sample of it in 5 M DCl at 90° was less than 20% demetalated even after 6 months.

The high thermodynamic stability of Ga(III) complexes of preorganized O_6 trihydroxamate chelators, especially desferal or deferrioxamine-B, DFO (**L23**) (log K = 28.6), has spurred much activity toward their biological and radiopharmaceutical applications.[164−169] Early solution NMR spectroscopic studies had revealed the presence of two major isomeric forms of Ga-DFO (Ga-**L23**).[170] An X-ray structure that can model Ga-DFO (Ga-**L23**) has been obtained in a Ga-tris(benzohydroxamate) complex, which has a *fac*-octahedral coordination sphere (Figure 43).[171] The stability constants of Ga(III) complexes of a tris(hydroxamate) cryptate, **L66**, as well as two acyclic analogues, **L21** and **L22**, were compared and the cryptate complex was found to be the most stable of the three (log K's = 27.5, 25.6, and 27.3, respectively).[172] An enterobactin model DiP-LICAM (**L20**) has been reported to bind ^{67}Ga(III) with a very high stability constant (log K = 38.6; Table 5).[185]

2.5. Aqueous Indium(III) Coordination Chemistry

Like gallium, the only stable aqueous indium oxidation state is +3. The significantly larger size of In(III) at 62−92 pm for CN 4−8, however, results in its attainment of coordination numbers of 7 and even 8 in its complexes. While still a hard acid, its higher pK_a of 4.0 and faster water exchange rate also reflect its distinction from Ga(III). A slightly enhanced affinity for softer donor types compared with Ga(III) can be noted in In(III) coordination chemistry. For example, acyclic N_4O_2 aminophenols as well as the biological iron transporter transferrin bind Ga(III) more avidly than In(III). By contrast, the tripodal NS_3 chelators, EDTA (**L10**), DTPA (**L12**), and DOTA (**L39**) all complex In(III) more securely, as well as with higher denticity, than Ga(III). Such differences in fundamental coordination preferences can have significant consequences in their biological behavior.[157] Data for selected complexes are listed in Table 6.

2.5.1. Tetradentate Chelators

A variety of acyclic tetradentate chelators featuring mixed amine and thiolate donor sets have been synthesized for In(III) complexation. The InCl-*bis*(aminothiolate), InCl-BAT-

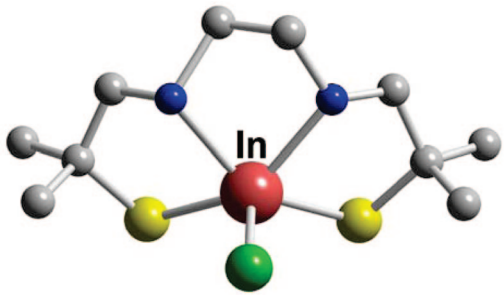

Figure 44. InCl-BAT-TM (**L4**).

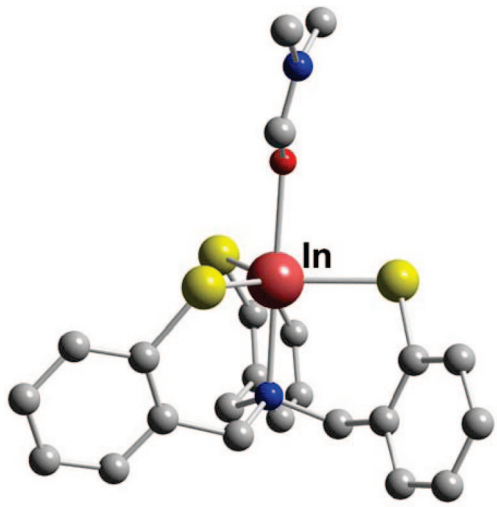

Figure 45. In-**L2**·DMF.

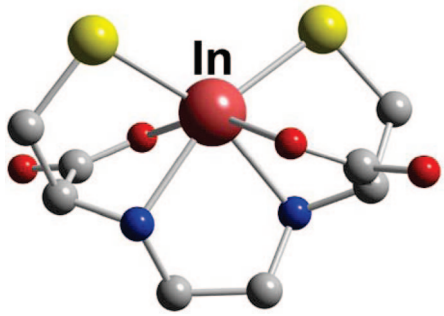

Figure 46. In-EC (**L5**).

TM (**L4**), structure is five-coordinate and near square pyramidal with an axial chloride (Figure 44).[132] While the complex was found to be stable in aqueous acetonitrile at pD 4.6, NMR spectra revealed the presence of two isomeric solution species. Tripodal NS_3 chelators such as *tris*(2-mercaptobenzyl)amine (**L2**) favor a trigonal bipyramidal coordination including an axial solvent dimethylformamide (DMF) at the metal center (Figure 45).[130] This can be contrasted with the ready isolation of a 4-coordinate Ga(III) analogue.[130] Both the synthesis and structural determination of a related *tris*(mercaptoethyl)amine (**L3**) complex of In(III) have also been reported.[173]

2.5.2. Hexa- to Octadentate Chelators

A hexadentate chelator boasting $N_2O_2S_2$ donors, *N*,*N*′-ethylene-di-L-cysteine (EC, **L5**), was found to form a distorted octahedral complex of In(III) with both carboxylate donors at axial sites (Figure 46).[133] This has an impressively high stability constant and was not demetalated by transferrin. The related *N*,*N*′-bis(2-hydroxybenzyl)ethylene-diamine-

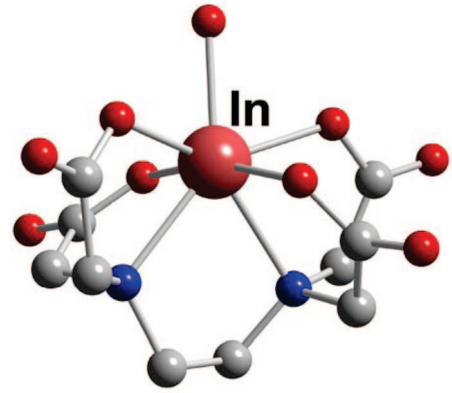

Figure 47. In-EDTA (**L9**).

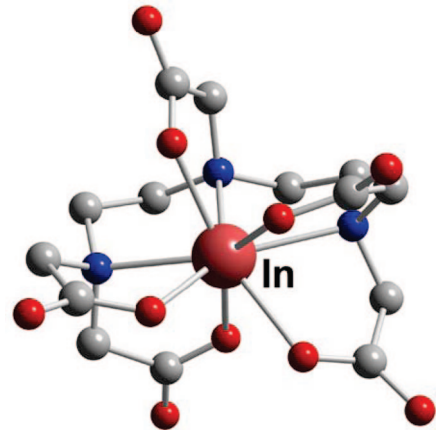

Figure 48. In-DTPA (**L12**).

N,*N*′-diacetic acid (HBED, **L11**) has also been found to bind In(III) strongly, though still with much lower affinity when compared with Ga(III) (Tables 5 and 6).[138]

Popular acyclic chelators EDTA (**L10**) and DTPA (**L12**) form very thermodynamically stable complexes with indium (Table 6). The seven-coordinate In-EDTA (In-**L10**) structure features a hexadentate chelator and approximates a pentagonal bipyramidal geometry with a single water at an equatorial position (Figure 47).[174] In-DTPA (In-**L12**) structures feature both seven- and full eight-coordination by the chelator in distorted pentagonal-bipyramidal and square-antiprismatic geometries, respectively; the latter is shown in Figure 48.[175,176] A $^{13}C\{^1H\}$NMR spectroscopic study of Na_2[In-DTPA] [Na_2(In-**L12**)] in D_2O confirmed retention of its square antiprismatic geometry in neutral aqueous solution.[176] The *N*,*N*″-bis(benzylcarbamoyl-methyl) derivative of DTPA (**L12**), DTPA-BA_2 (**L13**), was first designed as a model for a doubly bioconjugated chelator.[177] An X-ray structure of its In(III) complex also features an eight-coordinated cation in a distorted square antiprismatic envelopment (Figure 49).[178] Unlike In-DTPA (In-**L12**), however, its solution NMR spectrum revealed the presence of at least three isomeric species. It was proposed that the two amide carbonyls are no longer coordinated in solution, thus rendering this complex more hydrophilic in its HPLC retention behavior compared with its Y(III) analogue. A DTPA derivative with a *trans*-1,2-diaminocyclohexane backbone, CHX-A″-DTPA (**L14**), has been conjugated to a targeting peptide and found to be a viable ligand for ^{68}Ga, ^{86}Y, and ^{111}In radiometals for melanoma imaging.[141]

Linear N_4O_2 aminophenols such as SBAD (**L15**) have been prepared, and their complexations with Ga(III) and In(III)

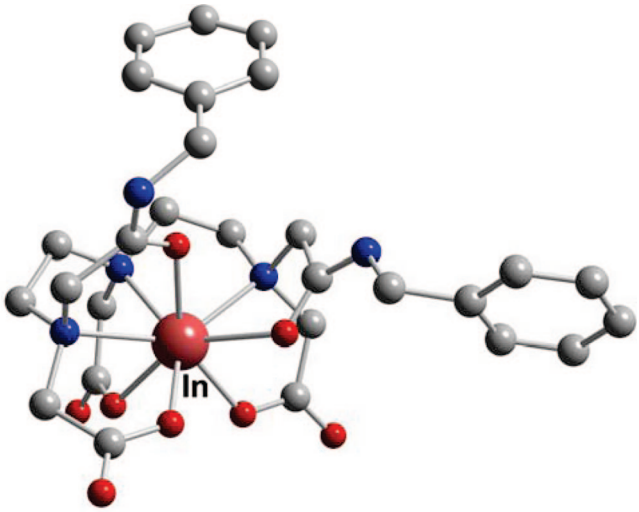

Figure 49. In-DTPA-BA_2 (**L13**).

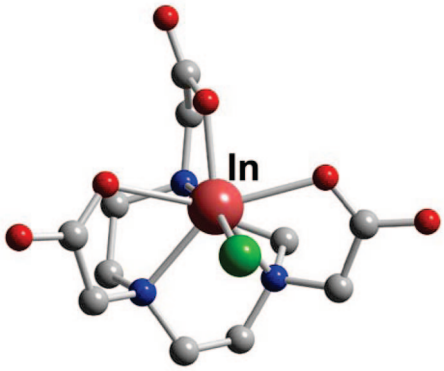

Figure 50. InCl-HNOTA (**L29**).

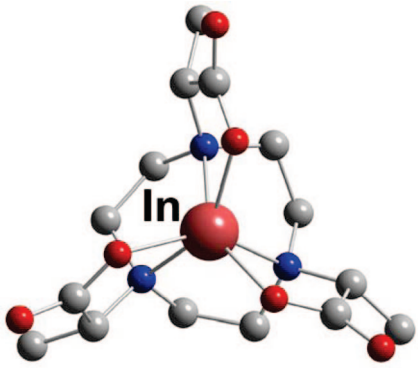

Figure 51. In-TACN (**L26**)-tris(2′-methylcarboxylmethyl).

have been studied.[139] These consistently bind the former cation more tenaciously. Additionally, several In(III) complexes of pendant-armed triazacyclononane (TACN, **L26**) derivatives have had their solid-state structures determined. An InCl-NOTA (InCl-**L29**) complex protonated at one carboxylate arm was found to have a near pentagonal-bipyramidal geometry with the chelator hexadentate (Figure 50).[37,179] In aqueous solution, however, NMR spectral data suggested a time-averaged six-coordinate C_3-symmetric species instead. At pD < 0, this complex decomposed irreversibly. The related In-(*R*,*R*,*R*)-1,4,7-tris(2′-methylcarboxymethyl)-triazacyclononane structure has a distorted trigonal prismatic coordination sphere (Figure 51).[180] A tris(phenylphosphinate)-armed derivative of TACN (**L26**),[181]

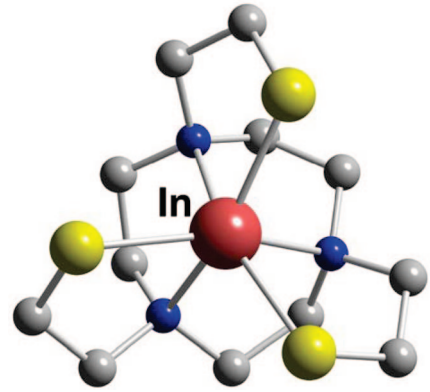

Figure 52. In-TACN-TM (**L27**).

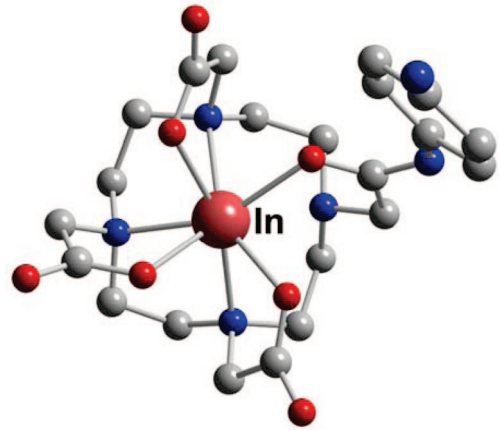

Figure 53. In-DOTA-AA (**L41**).

as well as the tris(mercaptoethyl)-armed derivative TACN-TM (**L27**) can both bind In(III) in a similar mode (Figure 52).[182]

The valuable octadentate chelator DOTA (**L39**) has also been shown to form a robust complex with In(III) (Table 6).[183] Surprisingly, no X-ray structural data are yet available for the parent In-DOTA (In-**L39**) complex. There are, however, several reported structures of its amide-armed derivatives. The In(III) complex of the *p*-aminoanilide, DOTA-AA (**L41**), was found to have a twisted (∼28°) square-antiprismatic geometry (Figure 53).[184] Inside the chelator cavity, the cation is approximately 1.2 and 1.3 Å from the O_4 and N_4 coordination planes, respectively. This indicates that its fit may not be as ideal as that for the larger Y(III) cation (*vide infra*). With one fewer carboxymethyl pendant arm than DOTA (**L39**), the chelator DO3A (**L42**) has also been complexed to In(III) and its structure adopts the expected seven-coordinate geometry.[185] Biodistribution studies using DOTA (**L39**) conjugated to D-Phe[1]-Tyr[3]-octreotide, DOTATOC (**L39**-TOC), and labeled with ^{67}Ga, ^{111}In, and ^{90}Y revealed that the Ga-DOTATOC (Ga-**L39**-TOC) had the best tumor uptake and kidney clearance.[157] It was postulated that this may be the result of a hexacoordinate Ga(III) compared with the higher coordination requirements for the In(III) and Y(III) analogues. Another seven-coordinate In(III) geometry, described as monocapped trigonal prismatic, was found for In-DO3A-TPP (**L44**), which features DOTA (**L39**) linked to a triphenylphosphonium moiety to target mitochondria (Figure 54).[158] Proton NMR data supported retention of this heptadentate chelation mode in aqueous solution.

A tris(carboxymethyl)-armed cyclam chelator, TE3A (**L53**), has also been found to complex In(III) in a hepta-

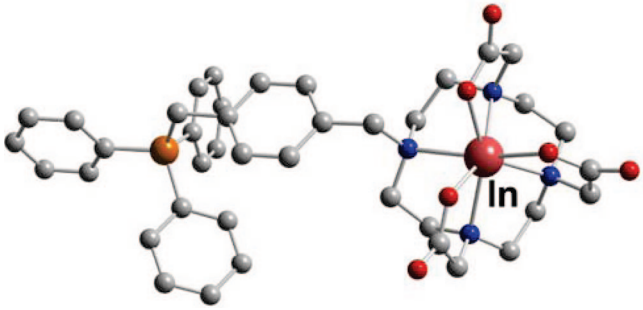

Figure 54. In-DOTA-TPP (**L44**).

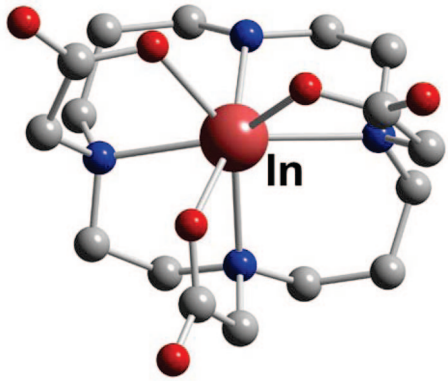

Figure 55. In-TE3A (**L53**).

dentate monocapped trigonal-prismatic geometry (Figure 55).[185] No structure of In-TETA (In-**L49**) has been reported though its stability constant has been determined to be 2 orders of magnitude lower than that of In-DOTA (In-**L39**) due to a poorer cation−chelator match.[186]

An early report of ^{111}In-labeling of tricatecholamide analogues of enterobactin (DiP-LICAM (**L20**)) yielded impressive stability constants (Table 6). However biodistribution studies were not performed.[187]

2.6. Aqueous Yttrium(III) Coordination Chemistry

Aqueous yttrium chemistry is often discussed together with that of the lanthanides because of their common tricationic state and similar ionic radii. Yttrium(III), 90−108 pm (CN 6−9), is significantly larger than the other four metal cations discussed in this review and can readily reach coordination numbers of 8 and 9 in its complexes. With a closed-shell electron configuration, it is also considered a harder acidic cation than Ga(III) or In(III). This can be seen in its higher Drago−Wayland parameter I_A, which is an indicator of the relative significance of the electrostatic versus covalent component of its coordination interaction.[579,580] Data for selected complexes are presented in Table 7.

Both EDTA (**L10**) and DTPA (**L12**) have been shown to form reasonably stable complexes with Y(III). Several solid-state structures of these have been determined, and two

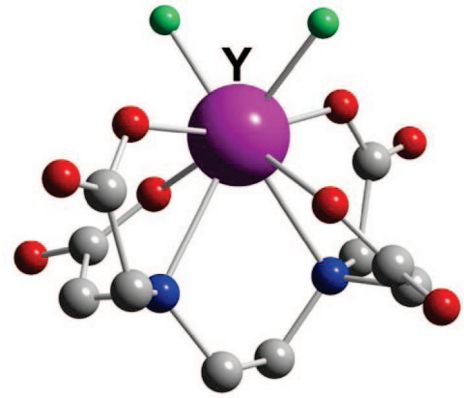

Figure 56. YF_2-EDTA (**L10**).

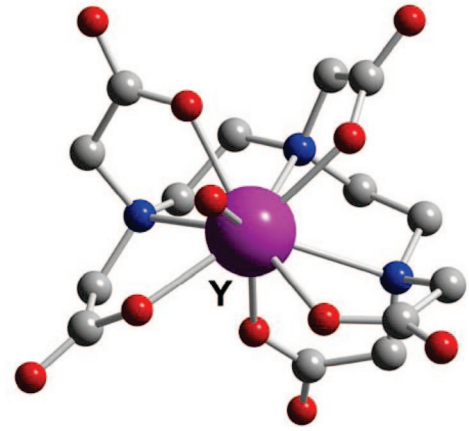

Figure 57. Y-DTPA (**L12**)·H_2O.

selected examples are shown in Figures 56 and 57. The YF_2-EDTA (YF_2-**L10**) structure approximates a dodecahedron with a hexadentate EDTA (**L10**),[188] while Y-DTPA (Y-**L12**) is nine-coordinate with a monocapped antiprismatic geometry including an octadentate DTPA (**L12**) and one coordinated water.[189] Two related structures are of Y-DTPA-BA_2 (**L13**), a *N*,*N*″-bis(benzylcarbamoylmethyl) derivative of DTPA (**L12**), which served as a model for a dual biomolecule-labeled chelator.[177,178] In each case, the nine-coordinate Y(III) adopts a distorted tricapped trigonal prismatic geometry featuring an octadentate chelator plus a coordinated solvent (methanol) molecule (Figure 58). In D_2O solution, however, NMR spectroscopy revealed the presence of at least three isomers up to 85 °C. It was suggested that these accessible structural variations may account for the relatively low inertness of typical Y-DTPA (Y-**L12**) complexes.

The structure of a Y(III) triflate complex of a *tris*(carbamoylmethyl) derivative of TACN (**L26**), NOTAM (**L30**), has been reported.[190] This nine-coordinate geometry can be viewed as a capped square antiprism, although alternative

Table 7. Data for Selected Y(III)−Chelator Complexes

chelator	donor set (total CN)	cation coordination geometry	log K_{ML}[a]	ref
L10, EDTA	N_2O_4 (8)	distorted dodecahedron	18.1, 18.5	593, 601
L12, DTPA	N_3O_5 (8)	monocapped square antiprism	21.2, 22.0, 22.5	587, 601, 602
L30, NOTAM	N_3O_3 (9)	monocapped square antiprism		190
L39, DOTA	N_4O_4 (8)	square antiprism	24.3, 24.4, 24.9	37, 601, 602
L49, TETA	N_4O_2 (8?)	distorted dodecahedron (?)	14.8	195

[a] K_{ML} = [ML]/[M][L].

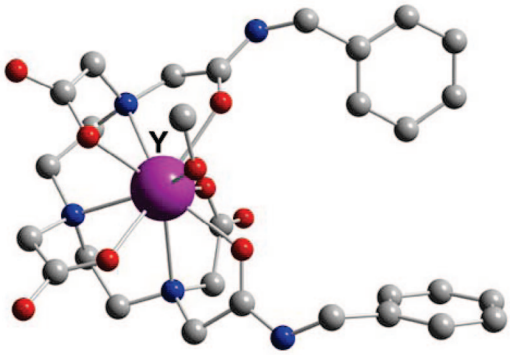

Figure 58. Y-DTPA-BA_2 (**L13**)·CH_3OH.

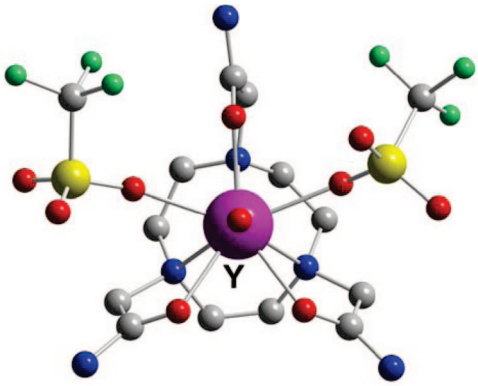

Figure 59. Y(triflate)$_2$-NOTAM (**L30**).

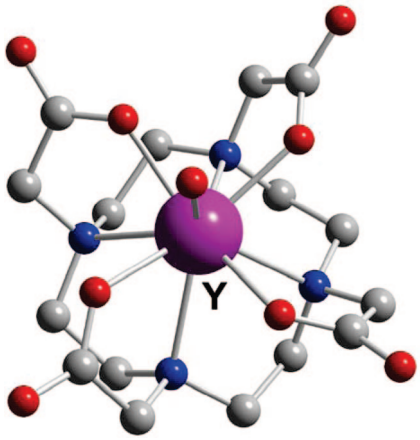

Figure 60. [Y-DOTA (**L39**)]$^-$·H_2O.

descriptions are also viable (Figure 59). NMR spectroscopic studies showed that this complex is fluxional in acetonitrile solution.

A number of yttrium(III) complexes of DOTA (**L39**) and its derivatives have been prepared. An X-ray structure of [Y-DOTA]$^-$ (Y-**L39**$^-$) is shown in Figure 60.[177,191] The nine-coordinate Y(III) center has a monohydrate capped square-antiprismatic (SA) coordination sphere (often referred to as the "*M*" isomeric geometry) featuring an octadentate DOTA (**L39**) with the cation held significantly closer to the O_4 plane than the N_4 plane (0.72 versus 1.62 Å, respectively). A related structure of a DOTA (**L39**) derivative with one carboxymethyl arm conjugated to phenylalanine, Y-DOTA-D-PheNH_2 (Y-**L40**), has also appeared (Figure 61). This adopts instead a twisted square-antiprismatic (TSA) geometry (or "*m*" isomer) with four macrocyclic amine nitrogens, three carboxylate oxygens, and an amide oxygen coordinating.[157] As

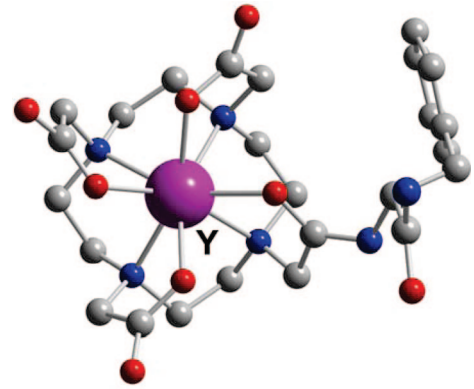

Figure 61. Y-DOTA-D-Phe-NH_2 (**L40**).

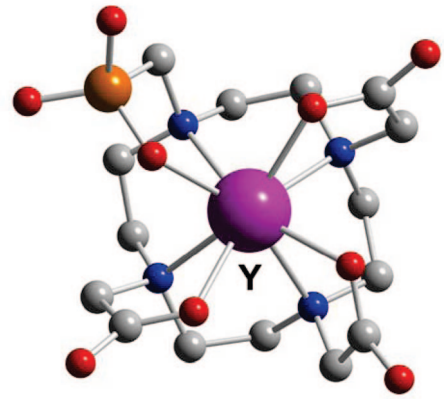

Figure 62. Y-DO3AP (**L42**).

mentioned in the gallium section, octreotide-conjugated ^{90}Y-DOTATOC (^{90}Y-**L39**-TOC) was found to have inferior biological behavior compared with its ^{67}Ga analogue, possibly as a result of the higher coordination requirement of Y(III). According to solution NMR spectroscopic data, a similar complex with a DOTA (**L39**) *p*-aminoanilide was found to retain the chelator's full N_4O_4 coordination mode.[47] The consequence of substituting a carboxylate pendant arm with a phosphonate in a DOTA (**L39**) derivative, DO3AP (**L43**), can be seen in its yttrium complex geometry (Figure 62). A twisted square antiprismatic configuration (TSA, twist angle ~25°) can be noted, while the cation remains closer to the O_4 plane (1.04 Å) than the N_4 plane (1.52 Å).[192]

A very interesting crystal structure of the yttrium(III) complex of a chiral DOTA (**L39**) derivative bound to the antibody 2D12.5 Fab has been reported,[193] but no direct complex−protein interactions were found. Likely as a result of the symmetrical nature of this type of complex, only modest differences in binding affinities were found for enantiomers of opposite helicity. Additionally, C-functionalized DOTA (**L39**) chelators have recently been investigated as BFCs for yttrium-86.[194] The (*S*)-*p*-aminobenzyl derivative's Y(III) complex was successfully separated into SA (major *M*) and TSA (minor *m*) isomeric forms, which were assigned by solution 2-D NMR as well as CD spectroscopy.

The cyclam analog, TETA (**L49**), has been reported to bind Y(III), though with far less affinity than either DOTA (**L39**) or even the acyclic DTPA (**L12**) indicating a poorer cation/chelator match (Table 7).[195] Both the labeling efficiency and acid inertness of ^{90}Y-TETA (^{90}Y-**L49**) (half-life at pH 3.6 of 5 min) have been found to be inferior to that of its DOTA (**L39**) analogue (no decomplexation after 3 months).[196] Although no Y-TETA (Y-**L49**) structure has

been reported to date, it is likely to resemble that of Tb-TETA (Tb-**L49**) and Eu-**L49**. Both of these were described as having a highly distorted octadentate dodecahedral geometry with the metal cation significantly distended from the cyclam cavity.[197,198]

Although often used as a surrogate for Y(III) in ^{90}Y-radiopharmaceutical studies, In(III) can exhibit appreciably different coordination chemistry due to its smaller ionic radius and typical coordination numbers of less than 8. Acyclic aminopolycarboxylates like EDTA (**L10**) and DTPA (**L12**) form far more stable complexes with In(III) than with Y(III). By contrast, the octadentate DOTA (**L39**) binds Y(III) with more avidity. While Y-DOTA-D-PheNH$_2$ (Y-**L40**) adopts the twisted square-antiprismatic (TSA) solid-state geometry, In-DOTA-D-Phe-NH$_2$ (In-**L40**) has the square-antiprismatic (SA) configuration.[157,199] These complexes also have distinct NMR spectral behavior in solution with only the indium complex showing fluxional behavior. Another Y-DOTA (Y-**L39**) derivative with a single amide pendant arm, Y-DOTA-AA (Y-**L41**), was observed to retain a rigidly octadentate chelator coordination sphere in solution at ambient temperature, while its In(III) analogue again exhibited dynamic behavior suggestive of an uncoordinated amide pendant arm.[184] Consistent with the observation, this and related indium DOTA (**L39**) complexes were found to be more hydrophilic in their RP-HPLC retention data.[184,200] Similar discrepancies were also noted for the corresponding DTPA-RGD (**L12**-RGD) and DTPA-BA$_2$ (**L13**) complexes of these cations.[178,201] Although potentially significant, no general conclusions about the relevance of these differences to the *in vivo* properties of these species can yet be made. Finally, the antibody 2D12.5 was reported to bind Y-DOTA (**L39**) with much higher affinity than In-DOTA (In-**L39**).[193]

2.7. Aqueous Zirconium(IV) Coordination Chemistry

With its high charge and small radius (59−89 pm for CN 4−9), hydrated Zr(IV) likely exists only at high dilution in very acidic solutions. Multiple monomeric as well as polynuclear oxo/hydroxy species are believed to be present before onset of precipitation as the pH is raised.[202,203]

As a consequence of its extreme hardness, a strong preference of Zr(IV) for polyanionic hard donor chelators can be expected. This predilection can be seen in the very impressive stability constants of its EDTA (**L10**) and DTPA (**L12**) complexes (Table 8). A total coordination number of 8 is typical in their X-ray structures (Figures 63 and 64). The Zr-EDTA (Zr-**L10**) geometry approximates a dodecahedron including a hexadentate chelator,[204] while DTPA (**L12**) is fully octadentate in its Zr(IV) envelopment.[205] The use of ibritumomab tiuxetan, a MX-DTPA (**MX-L12**)-conjugated monoclonal antibody, to chelate ^{89}Zr has been reported. No solid-state structure of Zr-DOTA (Zr-**L39**) has yet been reported. Although its D$_2$O solution ^{13}C{^{1}H} NMR spectral data were consistent with a time-averaged symmetric C_4 species implying full N$_4$O$_4$ chelator coordination, its proton NMR spectrum actually revealed a lower symmetry species in equilibration with a second minor isomer.[177]

Table 8. Data for Selected Zr(IV)−Chelator Complexes

chelator	donor set (total CN)	cation coordination geometry	log K_{ML}[a]	ref
L10, EDTA	N$_2$O$_4$ (8)	~dodecahedron	27.7, 29.4	589, 600
L12, DTPA	N$_3$O$_5$ (8)	~dodecahedron	35.8, 36.9	587, 600
L39, DOTA	N$_4$O$_4$ (8?)	square antiprism (?)		177

[a] K_{ML} = [ML]/[M][L].

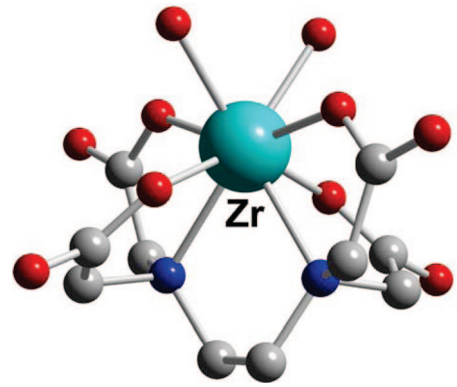

Figure 63. Zr-EDTA (**L10**).

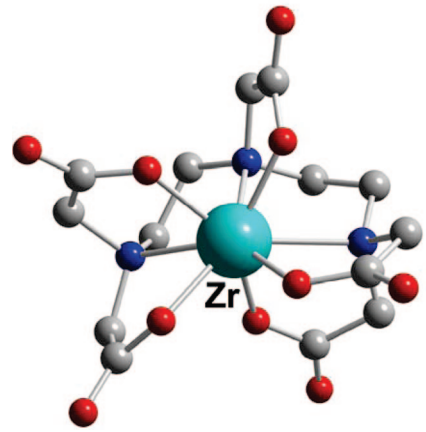

Figure 64. Zr-DTPA (**L12**).

The hydroxamate-based iron chelator Desferal, DFO (**L23**), and its derivatives have been frequently used to bind Zr(IV),[19,44,206−210] yet no structural characterization or stability constant data of resulting complexes are available. With the current interest in zirconium-based radiopharmaceuticals, future investigations of other hard metal cation-binding chelators likely to have high affinity for Zr(IV) such as catecholates and catecholamides should be timely. The family of tripodal hydroxypyridinone (HOPO) chelators developed recently for lanthanide complexation toward MRI applications also merits attention.[211]

2.8. Summary

Viable chelators for Cu(II) range from tetradentate N$_2$O$_2$, N$_2$S$_2$, and N$_4$ ligands favoring square-planar coordination to fully encapsulating N$_3$O$_3$, N$_4$O$_2$, and N$_6$ hexadentate ligands giving distorted octahedral binding modes. Especially high thermodynamic stabilities as well as acid inertness are realized using polyazamacrocycles and cryptands, often appended with ionizable carboxylate or phosphonate arms. Highly stable Ga(III) complexes have been attained with hexadentate chelators featuring N$_2$O$_2$S$_2$, N$_2$O$_4$, N$_3$O$_3$, N$_3$S$_3$, N$_4$O$_2$, and O$_6$ donor sets, usually in a pseudo-octahedral coordination geometry. Selected macrocyclic N$_3$O$_3$ and N$_4$O$_2$ chelator complexes also have remarkable inertness in strong acids. Although it is possible for the larger In(III) cation to adopt higher coordination numbers of 7 and 8, its most robust complexes are formed by hexadentate chelators similar to those for Ga(III) containing N$_2$O$_2$S$_2$, N$_2$O$_4$, N$_3$O$_3$, N$_3$S$_3$, N$_4$O$_2$, and O$_6$ donor motifs. Due to the higher coordination number

requirement of Y(III), the octadentate lanthanide chelator DOTA (**L39**) provides an almost ideal fit with associated high affinity. Only limited thermodynamic, kinetic, and structural data are available for Zr(IV)−chelator complexes in comparison to the other four metals discussed in this review. These indicate a strong preference for octadentate chelators with hard anionic oxygen donors. Finally, as demonstrated from the examples contained in this section, the affinity between metal and chelator plays an integral role in the development of useful radiopharmaceuticals.

3. Radioisotope Production

The availability of radiometals that are carrier-free and radionuclidically pure is essential to the development of effective radiopharmaceuticals for diagnostic imaging and radiotherapy. While the production of Zr, Y, In, Ga, and Cu radiometals requires a thorough understanding of the nuclear reactions and decay schemes available, their processing methods rely upon an intimate knowledge of their aqueous solution chemistry. The next section describes these methods.

3.1. Production of Copper Radiometals

The production of copper radiometals has been an area of intense research since they offer a variety of half-lives and decay energies that are applicable to diagnostic imaging and radiotherapeutic applications. Additionally, depending upon the application, copper radionuclides can be utilized by facilities with limited resources.

Copper-62 ($t_{1/2}$ = 0.16 h, β^+ 98%, $E_{\beta^+,max}$ 2.19 MeV; EC 2%) can be produced in a small cyclotron[212] and is the only generator-produced copper radionuclide, resulting from the decay of its parent, ^{62}Zn. Zinc-62 is produced by irradiation of an enriched Cu target with protons according to the nuclear reactions ^{63}Cu(p,n)^{62}Zn or ^{65}Cu(p,4n)^{62}Zn.[213] Numerous ^{62}Zn/^{62}Cu generator configurations were produced before 1999, using a glycine solution or other aqueous and organic mixtures to elute the ^{62}Cu in a form suitable for radiopharmaceutical preparation.[214,215] Haynes and co-workers developed a method for the direct labeling of PTSM (**L8**) to produce a patient-ready dose using a generator system designed to simultaneously deliver the ^{62}Cu eluate, NaOAc buffer, and PTSM (**L8**) ligand solution into a dedicated syringe.[216] While the life span of a ^{62}Cu generator is only 24 h, a clinically useful dose can be prepared every 30 min, which can be economical for hospitals that do not have the resources for an onsite cyclotron. Additional improvements in generator preparation by Fukumura et al. have increased the probability of ^{62}Cu use in the clinic.[217]

Copper-60 ($t_{1/2}$ = 0.4 h, β^+ 93%, $E_{\beta^+,max}$ 3.9 and 3.0 MeV, EC 7%, $E_{\gamma,max}$ 2.0 MeV) is another potentially useful copper radionuclide since high-quality images can be obtained due to the high percentage of positron decay, despite its high β^+ energy and prompt γ emission.[218] Additionally, ^{61}Cu ($t_{1/2}$ = 3.3 h, β^+ 62%, $E_{\beta^+,max}$ 1.2 and 1.15 MeV, EC 38%, $E_{\gamma,max}$ 940 and 960 MeV) also has potential applications in medical imaging since its half-life is suitable for biological applications that occur between 1 and 4 h after injection.[218] Both isotopes can be produced using targetry systems, which were designed for the production of ^{64}Cu. Copper-60 can be prepared by the ^{60}Ni(p,n,)^{60}Cu reaction, while ^{61}Cu can be prepared by the ^{61}Ni(p,n)^{61}Cu or ^{61}Ni(d,n)^{61}Cu nuclear reactions[219] on a biomedical cyclotron using 14.7 MeV protons or 8.1 MeV deuterons, respectively, and using natural or enriched nickel targets. Approximately 16.7 GBq of ^{60}Cu and up to 3.7 GBq of ^{61}Cu can be produced after the isotopic products are separated from the target material by ion exchange chromatography. However, the need for enriched target materials, which increases production costs, presents a significant limitation to the cost-effective production of these two radiometals and has prompted investigators to develop other production methods using the nuclear reactions ^{59}Co(^{3}He,2n)^{60}Cu and ^{59}Co(^{3}He,n)^{61}Cu, which can be carried out on Co foil using beam energies of 70 MeV.[220−222]

Copper-67 ($t_{1/2}$ = 62.01 h, β^- 100%, $E_{\beta^-,max}$, 0.577 MeV, $E_{\gamma,max}$ 0.185 MeV) decays by β^- emission. These particles have sufficient energy to penetrate small tumors, and the medium range half-life of ^{67}Cu makes it an attractive radiometal for radioimmunotherapy with intact antibodies. It can be produced on a cyclotron or high-energy accelerator using the nuclear reactions ^{65}Zn(p,2p)^{67}Cu and ^{68}Zn(p,2p)^{67}Cu or ^{65}Zn(n,p)^{67}Cu, respectively.[223] While several different Zn target materials are used, ^{68}Zn targets are preferred since their irradiation leads to substantial increases in ^{67}Cu yields.[224,225] However production yields are relatively low, since numerous contaminants such as ^{62}Zn, ^{67}Ga, ^{65}Zn, ^{55}Co, ^{58}Co, and ^{57}Ni have to be removed by numerous ion-exchange chromatography steps. Despite the availability of these purification methods, high specific activity ^{67}Cu is still difficult to obtain because of the ubiquity of natural copper and zinc in the environment.[224,226] The need for the high-energy cyclotron or accelerator, which drives up the cost, has also prevented mass production of this radiometal. Accordingly, interest in the applications of this radiometal remains limited.[227−235]

The production and preparation of ^{64}Cu ($t_{1/2}$ =12.7 h, β^+ 19% $E_{\beta^+,max}$, 0.656 MeV, EC 41%, β^- 40%) has been extensively reviewed and discussed.[236−238] Briefly, ^{64}Cu can be prepared in a nuclear reactor by several reactions including ^{63}Cu(n,γ)^{64}Cu, though the product cannot be isolated in a carrier-free state. A second method, which can lead to carrier-free ^{64}Cu, involves bombarding the target in a reactor with fast neutrons according to the nuclear reaction ^{64}Zn(n,p)^{64}Cu. Two other methods involve the nuclear reaction ^{64}Ni(p,n)^{64}Cu and ^{64}Ni(d,2n)^{64}Cu,[239,240] which can be carried out on a biomedical cyclotron to yield carrier-free ^{64}Cu, but an enriched nickel target must be irradiated to increase the yield of ^{64}Cu,[241,242] and this has spurred the development of ^{64}NiO targets to enhance ^{64}Ni recovery.[243] Recently, Obata and colleagues described the production of ^{64}Cu using 12 MeV proton irradiation via ^{64}Ni(p,n)^{64}Cu.[244] Automated processing and purification of the ^{64}Cu by AG1-X8 anion exchange chromatography allowed for the recycling of the ^{64}Ni target material and the generation of up to 185 GBq of ^{64}Cu depending upon target thickness.

Avila-Rodriquez et al. were able to simultaneously produce ^{64}Cu and ^{61}Co with an 11.4 MeV proton beam on a biomedical cyclotron using the ^{64}Ni(p,n)^{64}Cu reaction.[245] A single chromatography step using an anion exchange column separated the chloride salts of Ni, Cu, and Co, providing carrier-free ^{64}Cu with higher specific activities than previously reported.[237,244,246]

While Van So et al. attempted to produce ^{64}Cu from a ^{68}Zn target,[247] others have explored making ^{64}Cu with ^{64}Zn targets using the nuclear reaction ^{64}Zn(d,2p)^{64}Cu, but the production of other radionuclide contaminants has remained problematic.[248−250] Recently, Kozempel and colleagues reported the production of no-carrier-added (NCA) ^{64}Cu using the ^{64}Zn(d,2pn)^{64}Cu reaction with a 19.5 MeV deuteron

beam.[251] After irradiation, the radioactive target material is subjected to dual ion exchange chromatography using a strong cation exchange resin to remove any Ga-based radioimpurities and a strong anion exchange column to retain the ^{64}Cu and ^{64}Zn target material, while allowing other impurities such as ^{24}Na and ^{58}Co to flow through the column. The ^{64}Cu is then eluted in 2 M HCl, while the Zn fraction is eluted in neutral water. Additionally, Hassanein and co-workers separated ^{64}Cu from the zinc target using a gel matrix consisting of 6-tungstocerate(IV), which is highly insoluble in water and has a mean particle size of 230−464 μm.[252] The matrix's affinity for metal ions such as Zn(II) and Cu(II) is dependent on the hydrogen ion concentration in the column with the distribution of both cations decreasing with decreasing pH. In dilute acid, the Cu ions have an increased affinity toward the matrix compared with Zn ions, which can be washed from the column using 1 mM HCl, while the ^{64}Cu can be eluted in a carrier-free state using 1 M HCl.[252]

3.2. Production of Gallium Radiometals

Three gallium radioisotopes have suitable properties to be used in radiopharmaceutical applications. ^{67}Ga is used in SPECT and gamma scintigraphy, while ^{66}Ga and ^{68}Ga are used in the development of PET radiopharmaceuticals. This next section will discuss the production and purification of these three radioisotopes.

Gallium-67 ($t_{1/2}$ = 78.3 h, γ 93.3 keV, 37%; γ 184.6 keV, 20.4%; γ 300.2 keV, 16.6%) is produced using a cyclotron by bombarding a zinc or copper target with protons using the ^{67}Zn(p,xn)^{67}Ga reaction,[253,254] deuterons by the ^{67}Zn(d,2n)^{67}Ga reaction,[255] or α particles by the ^{64}Zn(^{4}He,n)^{67}Ga or ^{65}Cu(^{4}He,2n)^{67}Ga reactions.[254,256] Additionally, it can be produced using a tandem ^{Nat}Ge−^{Nat}Zn target, where separation of the ^{67}Ga from the target material is accomplished by acid dissociation followed by resin-based chromatography on an organic polymer to achieve high radionuclidic purity.[256] In some cases, however, iron contamination can be problematic, but the use of a reducing agent such as $TiCl_3$ can resolve this issue.[257] Recently, ^{67}Ga was produced from the irradiation of a target consisting of natural cobalt foil with 52 MeV $^{11}B^{4+}$ and 73 MeV $^{12}C^{6+}$ ions through one of the following reactions: ^{59}Co(^{11}B,3n)^{67}Ge or ^{59}Co(^{12}C, 4n)^{67}As.[258] The ^{67}Ge and ^{67}As products are short-lived radionuclides that decay to ^{67}Ga after a short "cooling" time. Separation of the target material is achieved by liquid−liquid extraction using concentrated acid and trioctylamine (TOA), which is then back-extracted using a basic solution of DTPA or EDTA. Alternatively, ^{67}Ga has been purified from cobalt target materials using alginate biopolymers,[259] which are naturally occurring polymers extracted from microalgae, shrimp, crab, and fungi that are known to bind strongly to metal ions.[260] Upon addition of the radioactive target material, nearly 90% of the ^{67}Ga is retained in the biopolymeric matrix, while the cobalt target material is removed from the column using an aqueous solution of $NaNO_2$. After all of the target material is removed, elution of the no-carrier-added ^{67}Ga occurs using 0.1 M HCl, which is suitable for radiopharmaceutical applications. In many medical centers that have PET scanners, the use of ^{67}Ga has been replaced by [^{18}F]FDG-PET.[261]

Gallium-68 ($t_{1/2}$ = 67.71 min, β^+ 89%, $E_{\beta^+,max}$, 1.9 MeV, EC 11%, $E_{\gamma,max}$ 4.0 MeV) is an important positron-emitting radiometal that is produced by electron capture decay of its parent radionuclide ^{68}Ge ($t_{1/2}$ = 270.95 days),[159] and it can be produced from a compact generator system that contains the parent radionuclide. The ^{68}Ge/^{68}Ga generator system provides a continuous source of Ga-based PET radiopharmaceuticals for approximately 1 year; it has been extensively reviewed,[262−264] and numerous commercial systems are available. Cyclotron Co. (Obninsk, Russia) has recently produced a popular TiO_2-based generator system, which can contain 370−18500 MBq of ^{68}Ge.[159] This system is eluted with 0.1 M HCl to provide the user with ionic $^{68}GaCl_3$; however, there are drawbacks, including ^{68}Ge breakthrough, large eluate volume, high HCl concentration, and the presence of metallic impurities such as Zn^{2+}, Ti^{4+}, and Fe^{3+}, which can lead to difficulties in synthesizing the ^{68}Ga radiopharmaceutical. To circumvent these difficulties, research groups have explored purification protocols using anion and cation exchange microchromatography[264,265] and fractionation,[266] while additional work has sought to develop facile synthetic routes to radiopharmaceuticals that complement this generator system including infrared (IR)- and microwave-supported syntheses.[265,267]

Gallium-66 ($t_{1/2}$ = 9.49 h, β^+ 56.5%, E_{β^+max}, 4.15 MeV; EC 43.5%, $E_{\gamma,max}$ 4.0 MeV) is another radiometal that is relevant in nuclear medicine and molecular imaging applications. As a positron emitter, it can be used in PET imaging, and its longer half-life allows for data collection at later time points, which is not possible with the positron-emitting isotope ^{68}Ga. Gallium-66 can be produced and purified using methods similar to those that have been described for ^{67}Ga[258] (*vide supra*). An alternative method for ^{66}Ga production has been accomplished using the ^{66}Zn(p,n)^{66}Ga nuclear reaction on a small biomedical cyclotron.[268] This publication also compared purification of the ^{66}Ga by cation exchange chromatography with the traditional purification method involving diisopropyl ether extraction using 20% $TiCl_3$ in 3% HCl. The authors report that using cation exchange chromatography to purify the ^{66}Ga has several advantages. First, 200 mCi of ^{66}Ga can be prepared and purified in this manner. Second, it can be automated, and the processing time was more than twice as fast compared with the diisopropyl ether extraction protocol. However, a potential limitation lies in the high concentration of metal impurities in the cation exchange column, which will need to be reduced if this process is to be used to regularly prepare ^{66}Ga radiopharmaceuticals. Additionally, although the longer half-life of ^{66}Ga compared with ^{68}Ga provides more flexibility with respect to the types of biomolecules to be investigated and the amount of time required for radiochemistry, the very high energy of the positron (4.15 MeV), as well as a high-energy γ emission (4.0 MeV), provide a prohibitively high absorbed dose to the subject being imaged, as well as to the personnel working with this radiometal. These intrinsic physical properties of this radiometal have severely limited its practical use.

3.3. Production of Indium Radiometals

The production, purification, and application of indium radiometals are active areas of research in the nuclear medicine, radiochemistry, and molecular imaging communities. While numerous reports exist that involve the use of ^{110}In,[269,270] ^{110m}In,[271] and ^{114m}In,[272] this review will focus on the production, purification, and radiopharmaceutical applications of ^{111}In, since it is the most widely used and extensively studied indium radiometal.

Indium-111 ($t_{1/2}$ = 2.8 d; γ 171 keV; γ 245 keV (EC 100%)) is produced commercially by irradiating a natural cadmium target with energetic protons according to the reaction ^{111}Cd(p,n)^{111}In or ^{112}Cd(p,2n)^{111}In, and both remain the most widely used production methods of ^{111}In.[273] Indium-111 can be separated from the cadmium target by ion exchange or solvent extraction, with both techniques providing similar yields.[270] Alternatively, ^{111}In can also be produced in an accelerator by irradiating a rhodium target with ^{12}C ion beam[274] or irradiating silver targets with 55 MeV ^{11}B ions by the ^{107,109}Ag(^{11}B,3pxn)^{111}In nuclear reaction.[275] In this process, the ^{111}In is separated from the target material by first dissolving it with HNO_3, Aliquat-336 (a phase transfer catalyst), and 0.001 M HCl, which are used to separate the silver target and the radiometal. A second extraction step involving 1 M HCl and 0.1 M trioctylamine (TOA) separates the ^{111}In, which remains in the organic phase while impurities such as $^{116/117}$Te and $^{116/116m/117}$Sb remain in the aqueous phase. A final extraction using a basic solution of 0.1 M EDTA isolates the ^{111}In in a carrier-free state.

3.4. Production of Yttrium Radiometals

The most abundant source of yttrium (Y) is found in the naturally occurring isotope ^{89}Y. Additionally, there are numerous radioisotopes of Y that are synthetically produced during the nuclear fission process and have half-lives that range from nanoseconds to months. For example, ^{88}Y ($t_{1/2}$ = 106.62 days) is produced by irradiating a strontium target with 16 MeV protons or a rubidium carbonate target with 7.3 MeV deuterons, 19 MeV ^{3}H ions, and 12.4 MeV ^{4}He ions.[276] This radiometal has been used in place of ^{90}Y for determining biodistribution of radioyttrium compounds,[277] is often considered invaluable as an active component of the ^{88}Y−Be photoneutron source,[278] and is important in the characterization of electrical materials. Additionally, ^{87}Y, which serves as the parent radionuclide in a ^{87}Y/^{87m}Sr generator, can be prepared by irradiating a rubidium target with α particles or by irradiating an enriched ^{87}Sr target with protons.[279,280] Because a discussion of the production and purification of all of the Y radiometals is beyond the scope of this text, the remainder of this section will be devoted to the production and purification of the most medically relevant yttrium radiometals, ^{90}Y and ^{86}Y.

Yttrium-90 ($t_{1/2}$ = 64.1 h, β^- 100%, $E_{\beta^-,max}$ = 2.3 MeV) is currently used as a therapeutic radionuclide in nuclear medicine because it has a half-life of 64.1 h and emits β^- radiation ($E_{\beta^-,max}$ = 2.28 MeV) with no accompanying γ rays, reducing the received radiation dose to both patients and hospital staff.[281] Yttrium-90 can be produced by (n,γ) reactions on yttrium metal or yttrium oxide, but the resulting product is obtained with a low specific activity.[281] Additionally, it can be produced by the ^{90}Zr(n,p)^{90}Y reaction in a nuclear reactor.[281] Following irradiation of the Zr starting material, it is extracted with HNO_3 and mandelic acid leaving a solution containing the ^{90}Y product and the ^{90}Sr parent, which can be separated from the ^{90}Y product by its retention on a DOWEX cation exchange column. The radiochemical yield of this method is 90% ± 8%.

Since large quantities are needed for nuclear medicine applications, the majority of the ^{90}Y obtained by hospitals is from facilities that manage nuclear materials produced within fission reactors. In this fissile material, ^{90}Y is associated with its parent ^{90}Sr ($t_{1/2}$ = 29 years), which must be separated in sufficient purity to meet hospital quality control standards. This has previously been accomplished with the use of coprecipitation[282] or solid-supported solvent-extraction chromatography.[283]

Recently, Happell et al. used nuclear track microfilters (NTMF) as supported liquid membranes by impregnating them with 1:1 bis-(2-ethylhexyl)-phosphate (HDEHP) and tributylphosphate (TBP).[284] ^{90}Y separation from its parent ^{90}Sr is achieved by its selective transport through the pores of the impregnated NTMF. While initial ^{90}Y recovery was good, the system lacked long-term stability, and ^{90}Sr breakthrough was problematic.

Although ^{90}Y is becoming more commonly used as a radiotherapeutic, not every hospital has access to ^{90}Y on a routine basis. However, since ^{90}Y and ^{90}Sr have such distinctly different half-lives, they represent a daughter/parent radionuclide combination that is ideal for incorporation into a generator system. Numerous generator systems have been developed where the ^{90}Sr is adsorbed onto a solid support and the ^{90}Y is eluted using lactate,[285] methanol and acetate,[286] oxalate,[287] citrate,[288] or EDTA.[289,290] Recently, Chakravarty et al. developed the Kamadhenu generator.[291] This ^{90}Y generator uses a dual electrochemical separation technique to separate ^{90}Y from the ^{90}Sr parent in very high radionuclidic purity by performing both electrolytic steps potentiostatically, and the constant voltage minimizes the level of ^{90}Sr contamination to 30 kBq per 37 GBq ^{90}Y, which is well below 74 kBq, the upper limit of exposure defined by international regulatory agencies. This method offers several advantages over conventional column-based generator systems. First, this generator can constantly be supplied by a ^{90}Sr feed solution, and there is an insignificant loss of ^{90}Sr except by natural decay. There is minimal radioactive and nonradioactive waste production, and minimal amounts of chemicals are used in the entire process. Finally, the ^{90}Y is obtained in acetate buffer making it suitable for labeling biological molecules without further modifications.

Yttrium-86 ($t_{1/2}$ = 14.7 h, β^+ 34%, E_{β^+max} = 1.2 MeV) has gained attention as a new imaging surrogate for ^{90}Y and as a positron-emitting radioisotope for diagnostic PET imaging because of its favorable half-life and decay characteristics. This increased demand for ^{86}Y has led to an intense research effort to develop efficient and high-yielding production methods. Several methods for the production and purification of ^{86}Y have been investigated that involve irradiation of germanium targets with accelerator-produced heavy ion particles such as 15 MeV $^{16}O^{6+}$,[292] but most ^{86}Y production protocols have used $SrCO_3$ or SrO as the target material and protons with energies from 8−15 MeV. Separation of the ^{86}Y has been accomplished using coprecipitation and ion exchange chromatography,[293] ion exchange chromatography,[294,295] a Sr-selective resin,[296,297] and electrolysis, which separated the ^{86}Y from the $SrCO_3$ target material resulting in high yields of no-carrier added ^{86}Y in only 2 h.[298]

Yoo et al. published a report that described the production of ^{86}Y using either an enriched $SrCO_3$ or a SrO target on a small biomedical cyclotron via the ^{86}Sr(p,n)^{86}Y nuclear reaction.[299] The authors demonstrated that the use of SrO coated onto a platinum disk target and two electrolytic steps allowed for a more efficient preparation of ^{86}Y with 99% of the available ^{86}Y being recovered. Specific activities with this method were observed to be as high as 282 GBq/μmol, and since no coprecipitates are formed or exchange resins are used in the purification process, the introduction of carrier

species is greatly reduced. Furthermore, electrolysis requires fewer steps, is easier to handle, can be adapted for automation and can produce no-carrier-added (NCA) ^{86}Y sufficient for biological studies in less than three hours. Recently, further modifications to the electrolytic procedures have been published that have optimized the electrochemical separation of ^{86}Y, resulting in reliable yields of 91% in only 60 min.[300]

3.5. Production of Zirconium Radiometals

Several isotopes of Zr can be produced on a cyclotron using a variety of nuclear reactions with particle energies between 5 and 85 MeV, and include ^{86}Zr ($t_{1/2}$ =17 h, γ 100%, E_γ = 241 keV), ^{88}Zr ($t_{1/2}$ = 85 d, γ 100%, E_γ = 390 keV), and ^{89}Zr ($t_{1/2}$ = 78.4 h, β^+ 22.8%, $E_{\beta^+\max}$ = 901 keV, EC 77%, E_γ = 909 keV).[301] However, for radiopharmaceutical development and radioimmunotherapy applications, ^{89}Zr has received considerable attention owing to its favorable decay characteristics and longer half-life, which make it useful in the labeling of antibodies for PET imaging at relatively long time points. A caveat to ^{89}Zr is the high abundance of the 909 keV gamma photons, which contribute greatly to the absorbed dose of ^{89}Zr radiopharmaceuticals, especially in slower clearing agents such as mAbs.

Zirconium-89 was first produced by Link et al. in 1986 by a (p,n) reaction by bombarding ^{89}Y on Y foil with 13 MeV protons.[302] After irradiation, ^{89}Zr was purified by a double extraction protocol. The target was first mixed with 4,4,4-trifluoro-1-(2-thienyl)-1,3-butanedione (TTA) in xylene to remove the Zr(IV) from the foil followed by a second extraction step involving HNO_3/HF to return the Zr(IV) to the aqueous phase. Anion exchange using 1 M HCl/0.01 M oxalate completes the purification procedure to afford ^{89}Zr in an 80% yield and with a purity of 99.99%. A similar method reported by Dejesus et al. yielded similar results.[303]

A third method of production involves the irradiation of ^{89}Y pellets, prepared from high purity powder, with 16 MeV deuterons (^{89}Y(d,2n)^{89}Zr reaction).[304] Unlike the previous two methods, which relied upon solvent−solvent extraction as a means to purify the ^{89}Zr, this method relied solely upon the differences in the distribution coefficients of these two elements on an anion exchange resin at different HCl concentrations. The authors reported that the overall radionuclidic yield was 80%. The purification protocol is simpler than the procedures proposed by Link, but the precipitation of YCl_3 before and after anion-exchange chromatography has been problematic.[305]

Finally, using a Philips AVF cyclotron, Meijs and coworkers were able to produce ^{89}Zr using the (p,n) reaction, 14 MeV protons, and ^{89}Y (300 μmol), which was sputtered onto a natural copper target that was cooled by water during bombardment.[306] These simple modifications led to the production of 8140 MBq of ^{89}Zr after 2 h. After oxidation of the ^{89}Zr to the M^{4+} oxidation state using H_2O_2, it was separated from other metal impurities such as ^{89}Y, ^{88}Y, ^{65}Zn, ^{48}V, and ^{56}Co using an anion exchange column chemically modified with hydroxamate groups. Hydroxamate was chosen because of its ability to form complexes with ^{89}Zr under highly acidic conditions, which allows the ^{89}Zr to be retained in the column while the other metal impurities are removed with highly concentrated HCl. The purified ^{89}Zr can then be eluted in 95% yield using 1 M oxalic acid, which is removed by sublimation under vacuum. However, newly established purification and labeling protocols have improved the separation efficiency of the hydroxamate column and rendered this sublimation step obsolete.[19]

4. Applications of Zr, Y, Ga, In, and Cu Radiopharmaceuticals

As new production and processing methods of Cu, Ga, In, Y, and Zr radiometals become available, their use in radiopharmaceutical development has allowed researchers and physicians to utilize the variable half-lives and emission energies to explore a variety of research problems including imaging multidrug resistance[143,307,308] and treating refractory arthritis and synovitis.[309,310] However, a thorough discussion of every application is beyond the scope of this text. To make this review more manageable for the reader, only applications involving oncology, gene expression, infection and inflammation, and hypoxia and perfusion will be emphasized. A representative summary of applications can be found in Table 9.

4.1. Oncology

Each year 10.9 million people are diagnosed with cancer worldwide.[311] Cancer is caused by the effects of genetic mutation and environmental stress, either individually or in concert. Additionally, the aggressiveness and responsiveness to therapy displayed by each malignancy varies, and while satisfactory progress continues to be made in the successful diagnosis and treatment of some cancers, the overall success rate remains low. While several of the radiometals such as ^{67}Cu[227−235] and ^{90}Y[312−345] are used in oncology as radiotherapeutics, the remainder of this discussion will focus on the incorporation of In, Cu, Ga, Y, and Zr radiometals into radiopharmaceuticals for the diagnostic imaging of cancer. Moreover, while numerous radiopharmaceuticals have been prepared to detect biomarkers such as the folate receptor,[166,346,347] the neurotensin receptor,[348,349] oxytocin receptor expressing tumors,[350] apoptosis using annexin-5,[351−355] urokinase-type plasminogen activator receptor (uPAR),[356] matrix metalloproteinases (MMPs),[357,358] Met-expression,[359] antigens in head-and-neck cancer,[208,360−362] lymphoma,[363−371] non-Hodgkin's lymphoma,[45] and esophageal and pancreatic cancer,[372,373] the remainder of this discussion will be further confined to several biomarkers that have received the most attention and include the integrin $\alpha_v\beta_3$, the somatostatin receptor, the gastrin-releasing peptide receptor, melanoma and melanocortin-1 receptor, HER-2/neu receptor, VEGF receptor, and EGF receptor.

4.1.1. Integrin Imaging

Integrins are a family of cell surface heterodimeric transmembrane glycoproteins that mediate the attachment of cells to the extracellular matrix.[374,375] They consist of α and β subunits, which are needed for adhesion to the extracellular domain. The cytoplasmic domain of both subunits anchors the cytoskeleton to the plasma membrane and is required to mediate signaling events. While imaging agents that target several different integrins have been reported,[376−378] the most widely investigated in this superfamily of proteins has been the vitronectin receptor, $\alpha_v\beta_3$, since it has been observed to be involved in tumor growth, local invasiveness, and metastatic potential and it is highly expressed on endothelial cells undergoing angiogenesis.[379,380] While several different protein, peptide, and peptidomimetic motifs have been used

Table 9. Biologically Targeted Radiopharmaceuticals Developed with Zr, Y, Ga, In, and Cu Radiometals

metal	bifunctional chelator	targeting molecule	target	preparatory notes[a]
Zr	**L23**, DFO	antibody	HNSCC,[19,208] Met expression,[359] non-Hodgkin's lymphoma,[45] EGFR,[44] VEGF[210]	labeling in oxalate solution requires a strong, indifferent buffer (HEPES (pH 7.2)); tetrafluorophenyl ester modified DFO facilitates coupling to targeting molecule
Y	**L14**, CHX-A″-DTPA	peptide, antibody	SSTR,[433] Lewis Y antigen[603]	acetate buffer (pH 5.5), 25 °C
	L39, DOTA	peptide, ODNs	MC-1R,[500] GRPR,[461] gene expression[194,509]	acetate buffer (pH 5.5−7); reaction temperature 60−90 °C, (peptides) 25−37 °C (antibody); DOTA-NHS facilitates coupling to peptides and antibodies
	L23, DFO	peptide	folate receptor[347]	Tris-buffered saline (pH 7.4), 25 °C; 24 h is suggested
Ga	**L11**, HBED	peptide, antibody	EGFR,[137] MUC1[136]	tetrafluorophenyl ester modified HBED facilitates coupling to targeting molecule; low final pH (4.1−4.5) is necessary for Ga complexation
	L39, DOTA	peptide, ODNs	MC-1R,[502] GRPR,[459,604] K-ras oncogene,[511] EGFR,[479] SSTR[268,439,441−443,605,606]	anion exchange chromatography can be used to concentrate generator eluates;[605] the use of acetate or HEPES buffer is suggested; the final pH of the reaction solution should be 4−5.5; high reaction temperatures required (85−100 °C); microwave heating reduces reaction time
	L29, NOTA	peptide	SSTR,[154] integrin $\alpha_v\beta_3$[395,401]	labeling can occur at 25 °C over a pH range of 3.5−6 in less than 30 min
	L12, DTPA	peptide, ODNs/PNA, peptidomimetic, antibody	GRPR,[456] EGFR,[449,473,474] p21[WAF-1CIP-1510], mRNA,[515] LTB4R,[523,607] SSTR[9]	labeling can occur at 25 °C with reaction times no longer than 60 min; acetate buffers (pH 5.5−6.5) are recommended
In	**L39**, DOTA	peptide, peptidomimetic	GRPR,[457] MC-1R,[496] SSTR,[9,407] integrin $\alpha_v\beta_3$,[383,386] integrin $\alpha_4\beta_1$[378]	final solution pH should be 5.0−7.0; acetate buffer is recommended; reaction conditions are 30−60 min at 65−100 °C
	L12, DTPA	peptide, peptidomimetic	inflammation	acetate buffer (pH 5.5) is recommended; final solution pH is 4.5−5.0
	L14, CHX-A″-DTPA	antibody	hEGFR-2[608]	acetate buffer is recommended; reaction conditions are 30−60 min at 25 °C
Cu	**L39**, DOTA	peptide, antibody, peptidomimetic	integrin $\alpha_v\beta_3$,[397] $\alpha_v\beta_6$,[376] VEGFR (various),[489,490,493] MC-1R,[500,501] EGFR,[480] GRPR,[466,461,464,465] SSTR[7,425,609]	acetate buffer recommended; final solution pH should be 5.5−8.0; reaction temperatures are 25−100 °C depending on conjugate; PD-10 or Waters SepPak light C18 cartridge can be used for antibody or peptide purification, respectively
	L49, TETA	peptide	SSTR[431,610,611]	acetate buffer recommended (pH 5.5−6.5); reaction conditions of 60 min at 25−37 °C are recommended; gentisic acid (1 mg/mL) can be used to counteract radiolysis
	L57, CB-TE2A	peptide, peptidomimetic	integrin $\alpha_v\beta_3$,[399,611] integrin $\alpha_v\beta_6$,[376] MC-1R[504]	acetate buffer (pH 7.5−8.5), 95 °C; 1−2 h is recommended
	L62, DIAMSAR	peptide	$\alpha_v\beta_3$[121,399]	acetate buffer (pH 5.0−8.0) 25 °C; 60 min is recommended
	L29, NOTA	peptide	GRPR[462,467,468,612]	acetate buffer; final pH 6.5; 60 min at 70 °C is recommended

[a] Presented as an initial reference for radiopharmaceutical preparation.

to image this biomarker,[200,381−387] the vast majority of published reports have targeted this receptor using an arginine−glycine−aspartic acid (RGD) peptide motif (Figure 65). For example, Yoshimoto et al. prepared ^{111}In-DOTA (**L39**)-c(RGDfK)[388] and demonstrated that this radiopharmaceutical had rapid tumor uptake and renal clearance in SKOV-3 human ovarian carcinoma cells implanted in female BALB/c nu/nu mice, while van Hagen et al. used ^{111}In-DTPA(**L12**)-c(RGDyK) to investigate the imaging of neoangiogenesis in CA20948 rat pancreatic tumors.[389] Receptor-specific but dose-dependent accumulation of the tracer was observed in these tumors with more accumulation being observed when the mass of the injected radiopharmaceutical was reduced. Additionally, several ^{64}Cu-DOTA(**L39**)-RGD based radiopharmaceuticals have been developed to target $\alpha_v\beta_3$ expression in order to monitor dasatinib therapy[390] and image glioma,[391] inflammation,[392] lung cancer,[393] and teratoma.[394] Additional research has been conducted to improve $\alpha_v\beta_3$ positive tumor targeting using RGD multimers,[395] enhance the biokinetics of RGD-based radiopharmaceuticals using PEG linkers[396] and develop multimodal imaging agents for PET/MR[397] or PET/NIR applications.[398]

Since ^{64}Cu-DOTA (**L39**) complexes were previously shown to be unstable *in vivo*,[21] Wei and colleagues compared the properties of ^{64}Cu-CB-TE2A(**L57**)-c(RGDyK) and ^{64}Cu-DIAMSAR(**L62**)-c(RGDfD) in M21 ($\alpha_v\beta_3$ positive) and

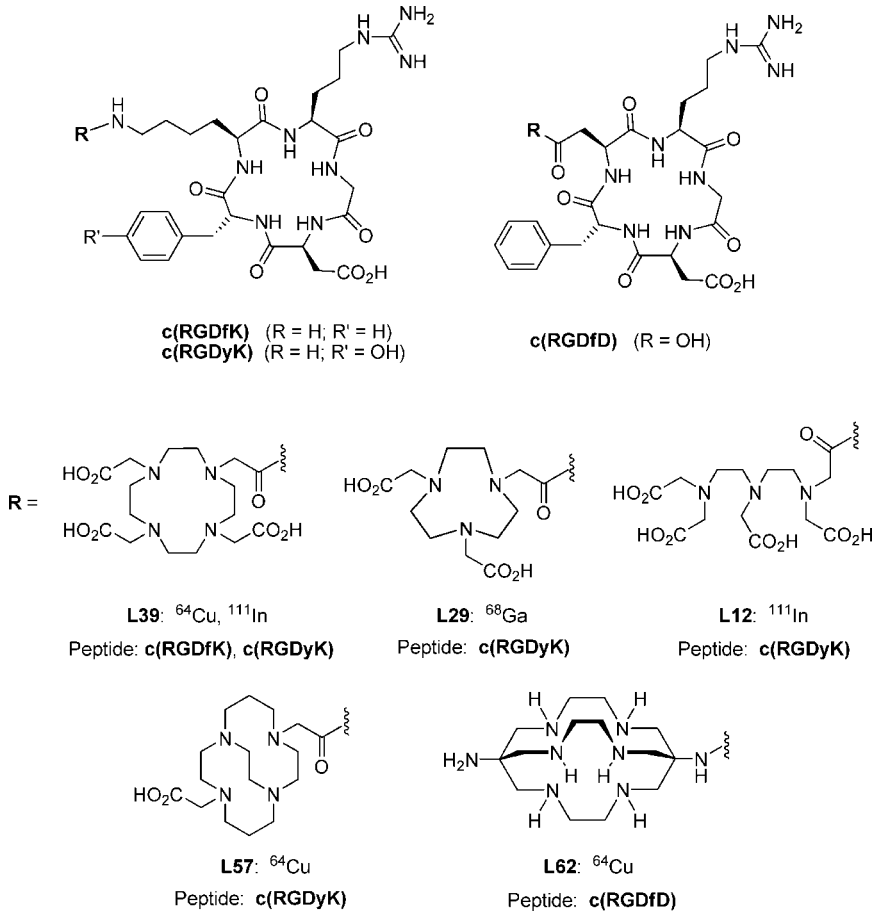

Figure 65. Selected RGD analogues used in $\alpha_v\beta_3$ targeting radiopharmaceuticals.

M21L ($\alpha_v\beta_3$ negative) melanoma bearing mice.[399] These ligands were developed to form more kinetically inert Cu(II) complexes with the hope of preventing Cu transchelation *in vivo*. While both radiopharmaceuticals exhibited similar binding affinities for $\alpha_v\beta_3$ integrin, ^{64}Cu-CB-TE2A(**L57**)-c(RGDyK) demonstrated better tumor targeting at all time points examined and demonstrated more rapid liver and blood clearance resulting in lower liver and blood concentrations at 24 h p.i.

In another interesting application using CB-TE2A(**L57**), Sprague et al. used the radiopharmaceutical ^{64}Cu-CB-TE2A(**L57**)-c(RGDyK) to image osteoclasts, which express high levels of $\alpha_v\beta_3$ integrin and are a component of osteolytic bone metastases.[400] This radiopharmaceutical was observed to have a 30-fold greater affinity for $\alpha_v\beta_3$ than $\alpha_v\beta_5$ and was observed to bind to osteoclasts through $\alpha_v\beta_3$-mediated interactions. Biodistribution and small animal imaging of a pharmacologically induced mouse model of osteolysis demonstrated increased uptake at the mouse calvarium, which was the site of pharmacological induction (Figure 66). This increased uptake could be blocked with a coinjection of c(RGDyK), demonstrating that imaging of $\alpha_v\beta_3$-expressing osteoclasts was possible.

Gallium-based imaging agents have been developed for imaging $\alpha_v\beta_3$. Jeong et al. labeled NOTA(**L29**)-c(RGDyK) with ^{68}Ga.[401] Although some purification was necessary, the purified complex could be obtained with a specific activity of 17.4 GBq/μmol, and biodistribution studies in nude mice bearing human colon cancer (SNUC4) xenografts demonstrated appreciable receptor-mediated tumor uptake. Additionally, small animal PET studies were performed, which demonstrated excellent tumor uptake that was significantly reduced by the coadministration of c(RGDyK); however, quantification of the microPET imaging was not reported. In another report, Li et al. examined the differences between ^{68}Ga-NOTA(**L29**)-(RGD)$_4$, ^{68}Ga-NOTA(**L29**)-(RGD)$_2$, and ^{68}Ga-NOTA(**L29**)-RGD.[402] In all cases, nearly quantitative labeling of these conjugates was achieved, and specific activities of 12−17 MBq/nmol were achievable. The ^{68}Ga-NOTA(**L29**)-(RGD)$_4$ demonstrated the highest receptor affinity and tumor uptake based upon biodistribution and small animal PET studies, but it also demonstrated the highest kidney uptake, which can be problematic since the kidney is a dose-limiting organ. Similarly, a recent study by Liu et al. examined the effects PEG and glycine linkers had on the affinity of RGD dimers for $\alpha_v\beta_3$ positive tumors xenografts.[403]

4.1.2. Somatostatin Receptor Imaging

Somatostatin (SST), which consists of 14 amino acid (aa) and 28 aa peptides, affects several organ systems including the central nervous system, hypothalamopituitary system, gastrointestinal tract, exo- and endocrine pancreas, and immune system.[404] Currently five different somatostatin receptor subtypes have been discovered. While many human tumors express these membrane-bound receptors, the subtype expression pattern is dependent on the origin and type of tumor.[405] This information has led to a continuing flurry of activity, seeking to develop new diagnostic imaging agents for somatostatin receptors and evaluate them in preclinical and clinical settings.

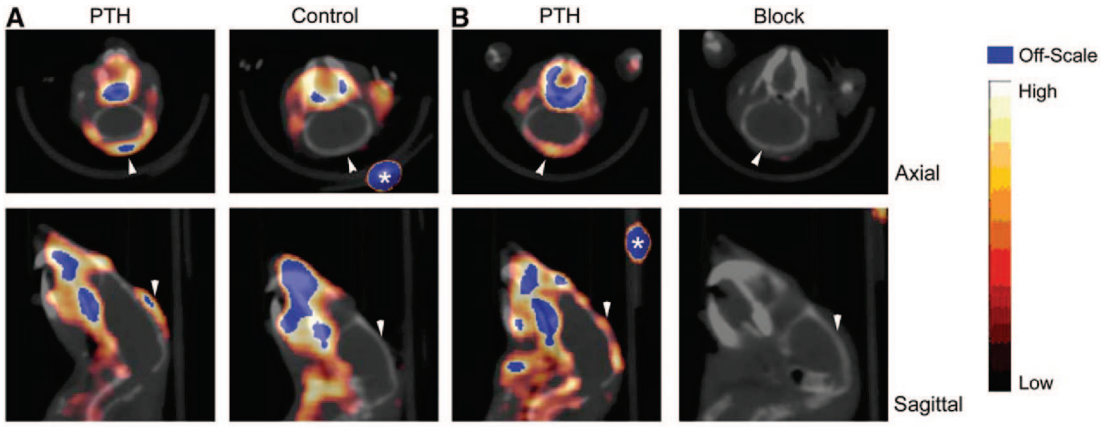

Figure 66. Small-animal PET/CT of PTH-treated mice. (A) Calvarium uptake of ^{64}Cu-CB-TE2A-c(RGDyK) was higher in PTH-treated mice (7.4 MBq [199 mCi],115 ng, SUV 0.53) than in control mice (7.7 MBq [209 mCi], 121 ng, SUV 0.22) (50−60 min summed dynamic image). (B) In PTH-treated mice, uptake was reduced in all tissues, including calvarium, after injection of c(RGDyK) (PTH [left], 159 mCi, 84 ng, SUV 5 0.33; block [right], 164 mCi, 87 ng, SUV 5 0.18; static image obtained 60 min after injection, 10-min scan). Arrowheads indicate calvarium of each animal. Fiducials (∗) are indicated. Reprinted with permission from ref 400. Copyright 2007 Society of Nuclear Medicine.

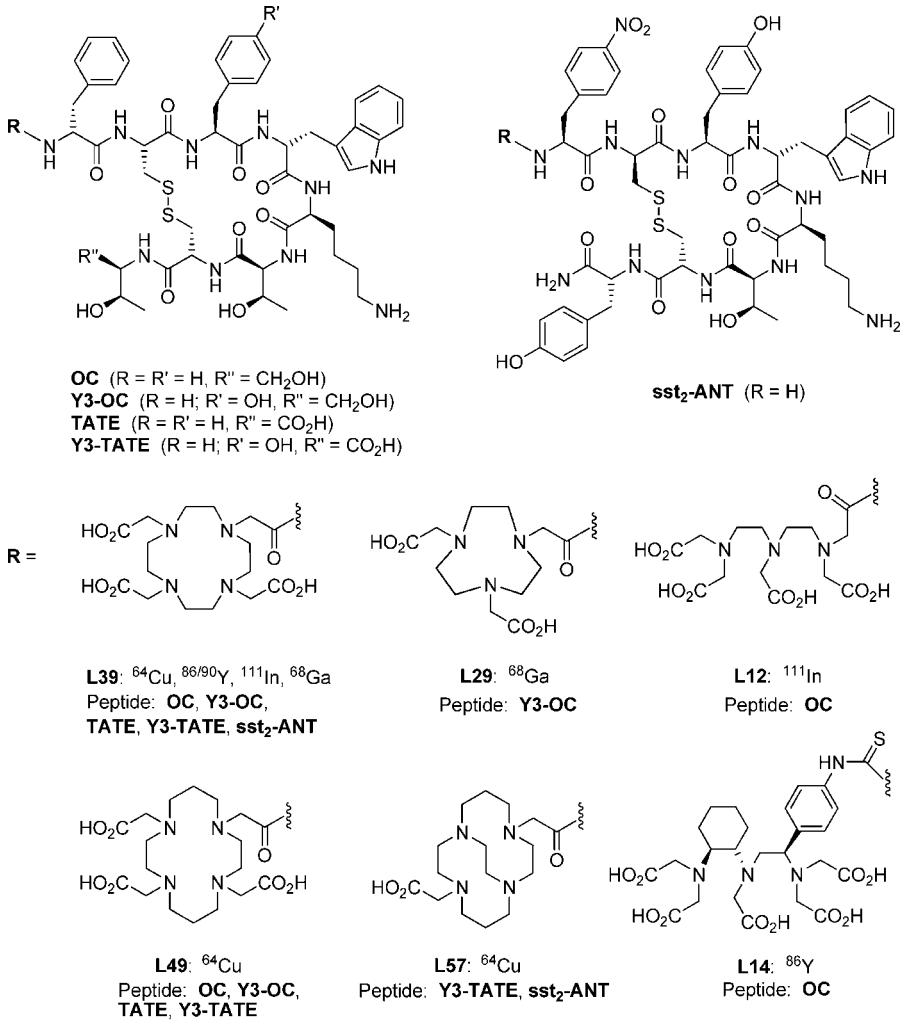

Figure 67. Selected somatostatin analogues used in somatostatin receptor targeting radiopharmaceuticals.

Numerous somatostatin analogues have been prepared, conjugated to various chelators such as DTPA (**L12**) and DOTA (**L39**), labeled with ^{111}In, and evaluated in both the laboratory and the clinic (Figure 67).[9,406−425] de Jong et al. investigated tumor uptake of ^{111}In-DOTA(**L39**)-Y^3-octreotide as a function of injected radiopharmaceutical mass, which is an important factor when seeking to maximize tumor uptake while trying to minimize non-target-organ radiotoxicity.[426] ^{111}In-DOTA(**L39**)-Tyr^3-octreotide was injected into male Lewis rats bearing CA20949 pancreatic carcinoma tumors with the mass of the radiopharmaceutical varying between 0.05−12 μg of peptide. Higher specific uptake was observed only in somatostatin receptor subtype 2 (SSTR(2)) positive organs when the mass of the injected radiopharma-

ceutical was low, illustrating that this parameter is more important in determining radiopharmaceutical uptake in tumor and non-target-organs than its specific activity. Another report by Lewis et al. described the evaluation of the somatostatin analogues ^{64}Cu-TETA(**L49**)-Y^3-OC, ^{64}Cu-TETA(**L49**)-TATE, ^{64}Cu-TETA(**L49**)-OC, and ^{64}Cu-TETA(**L49**)-Y^3-TATE to correlate the *in vivo* changes in biokinetics of these molecules that occurred when a substitution of tyrosine for phenylalanine is induced at position 3 of the peptide sequence and when the C-terminal alcohol is oxidized to a carboxylic acid functional group.[427] The analogue ^{64}Cu-TETA(**L49**)-Y^3-TATE displayed significantly higher affinity for somatostatin receptor positive CA20948 rat pancreatic tumor membranes and demonstrated up to 3.5-fold more tumor retention than the other tracers examined. These findings led to further investigations of this radiopharmaceutical as a diagnostic imaging agent using a non-human primate model[428] and has led to preliminary dosimetry studies in a rat model.[427] However the experimental evidence of copper transchelation *in vivo* has led to the use of other chelators that form more kinetically inert copper complexes.[20] One such chelator currently being investigated is the cross-bridged chelator CB-TE2A (**L57**).[429] To demonstrate its superiority, Sprague et al. prepared the radiopharmaceuticals ^{64}Cu-CB-TE2A(**L57**)-Y^3-TATE and ^{64}Cu-TETA(**L49**)-Y^3-TATE, which differ only in the copper chelator conjugated to the peptide.[430] While both radiotracers had similar binding affinity for SSTR(+) AR42J tumor cell membranes, blood, liver, and nonspecific uptake was lower for the cross-bridged analog. Additionally at 4 h, the non-cross-bridged tracer had 4-fold and 2-fold higher blood and liver uptake, while ^{64}Cu-CB-TE2A(**L57**)-Y^3-TATE demonstrated 4-fold greater tumor uptake at the same time point. These interesting properties led Eiblmaier and colleagues to examine the difference in internalization of these two radiopharmaceuticals in A427-7 cells, which were stably transfected for the SSTR(2) to evaluate their radiotherapeutic and cell killing potential.[431] Cellular internalization and efflux experiments demonstrated that ^{64}Cu-CB-TE2A(**L57**)-Y^3-TATE internalized more rapidly than ^{64}Cu-CB-TETA(**L49**)-Y^3-TATE; however more ^{64}Cu-TETA(**L49**)-Y^3-TATE localized in the nucleus leading the authors to conclude that the difference in kinetic inertness between the two ^{64}Cu complexes led to the higher localization of activity in the nucleus.

In 2004, Milenic et al. reported the development of a DTPA (**L12**) analogue, CHX-A″-DTPA (**L14**), which forms stable complexes with a variety of radiometals and is capable of achieving rapid complex formation at room temperature.[432] In order to evaluate this bifunctional chelator, it was coupled to octreotide (OC), labeled with ^{86}Y, and injected into rats bearing AR42J pancreatic tumors, which overexpress the somatostatin subtype 2 receptor (SSTr2).[433] ^{86}Y- CHX-A″-DTPA(**L14**)-OC demonstrated high tumor uptake along with uptake in the kidneys associated with the renal clearance of the agent. The tumor was easily visualized using small animal PET at 4 h, but effective clearance from the tumor was demonstrated with only 25% of the activity remaining at 24 h compared with the 4 h time point in biodistribution studies.

Several ^{68}Ga-radiopharmaceuticals have also been developed for the somatostatin receptor on neuroendocrine tumors.[434−440] Henze et al. examined the diagnostic utility of ^{68}Ga-DOTA(**L39**)-D-Phe^1-Tyr^3-octreotide in patients with meningiomas.[441] During the study, rapid blood clearance and high uptake in the meningioma lesions of various sizes could be observed, while no tracer accumulation was found in healthy brain tissue allowing for excellent visualization of these lesions. Additionally, Hofmann and co-workers evaluated ^{68}Ga-DOTA(**L39**)-TOC in patients with somatostatin receptor-positive tumors, and compared their results with those obtained with ^{111}In-**DTPA**(**L12**)-octreotide with planar and SPECT imaging.[439] Based upon this study, ^{68}Ga-DOTA(**L39**)-TOC was able to clearly delineate 100% of the lesions predefined with CT or MRI, and an additional 30% more lesions were detected when compared with SPECT using ^{111}In-DOTA(**L39**)-octreotide. Conversely, only 85% of the lesions previously identified using CT or MRI were correctly identified with the γ-emitting radiopharmaceutical demonstrating the utility of ^{68}Ga-DOTA(**L39**)-TOC in PET imaging and preclinical experiments. Kayani et al. demonstrated that PET/CT using ^{68}Ga-DOTA(**L39**)-TATE was superior to [^{18}F]-FDG for imaging well-differentiated neuroendocrine tumors, but [^{18}F]-FDG was more sensitive in detecting high-grade tumors.[442] Additionally, the authors note that the combination use of ^{68}Ga-DOTA(**L39**)-TATE, [^{18}F]-FDG, and PET/CT has the potential for more comprehensive tumor assessment in intermediate and high-grade tumors. Finally, Ugur et al. investigated the potential of ^{66}Ga-DOTA(**L39**)-D-phe^1-Tyr^3-octreotide as a potential PET agent and radiotherapeutic for somatostatin receptor-positive tumors in AR42J rat pancreatic tumors implanted in nude mice.[443] The authors radiolabeled this radiopharmaceutical precursor with ^{66}Ga, ^{67}Ga, and ^{68}Ga. Radiochemical purity of more than 95% was achieved for each radiotracer, and tissue biodistribution demonstrated comparable uptake for the ^{66}Ga, ^{67}Ga, and ^{68}Ga complexes. Small animal PET experiments demonstrated efficient tumor retention, but high radioactivity accumulation in the kidney also was observed, suggesting that effective measures to block renal uptake will be needed before therapeutic and imaging protocols using this radiotracer can be implemented.

Targeted radiopharmaceuticals having high specificity and affinity for individual SST subtypes have also been reported. Recently, Ginj et al. compared somatostatin receptor agonists and antagonists as targeting ligands and their specific affinity for the five different subtypes of the somatostatin receptor.[444] The somatostatin receptor subtype 2 (SSTR(2)) selective antagonist sst$_2$-ANT was determined to have a high affinity for the SSTR(2), which was not decreased by the presence of conjugated DOTA(**L39**) or a conjugated ^{nat}In-DOTA(**L39**) complex. Internalization of the SSTR(2) was not observed using immunofluorescence internalization assays even when the concentration of the antagonist exceeded 9 μM. Biodistribution studies using ^{111}In-DOTA(**L39**)-sst$_2$-ANT revealed high uptake and a slow clearance of the radiopharmaceutical in nude mice bearing tumors comprised of human embryonic kidney (HEK) cells that were stably transfected to only express SSTR(2). Wadas et al. further expanded upon this approach by developing the PET analogue ^{64}Cu-CB-TE2A(**L57**)-sst$_2$-ANT and comparing its properties as a PET radiopharmaceutical to the agonist ^{64}Cu-CB-TE2A(**L57**)-Y^3-TATE.[445] Biodistribution studies revealed that the PET antagonist demonstrated rapid blood clearance but slower clearance from the liver and kidney. Both radiotracers demonstrated substantial uptake in SSTR(+) tissues and AR42J tumors, which was reduced upon the co-injection of blockade indicating that interaction between the radiopharmaceuticals and the tissues are a receptor-mediated process (Figure 68). ^{64}Cu-CB-TE2A(**L57**)-sst$_2$-ANT demonstrated

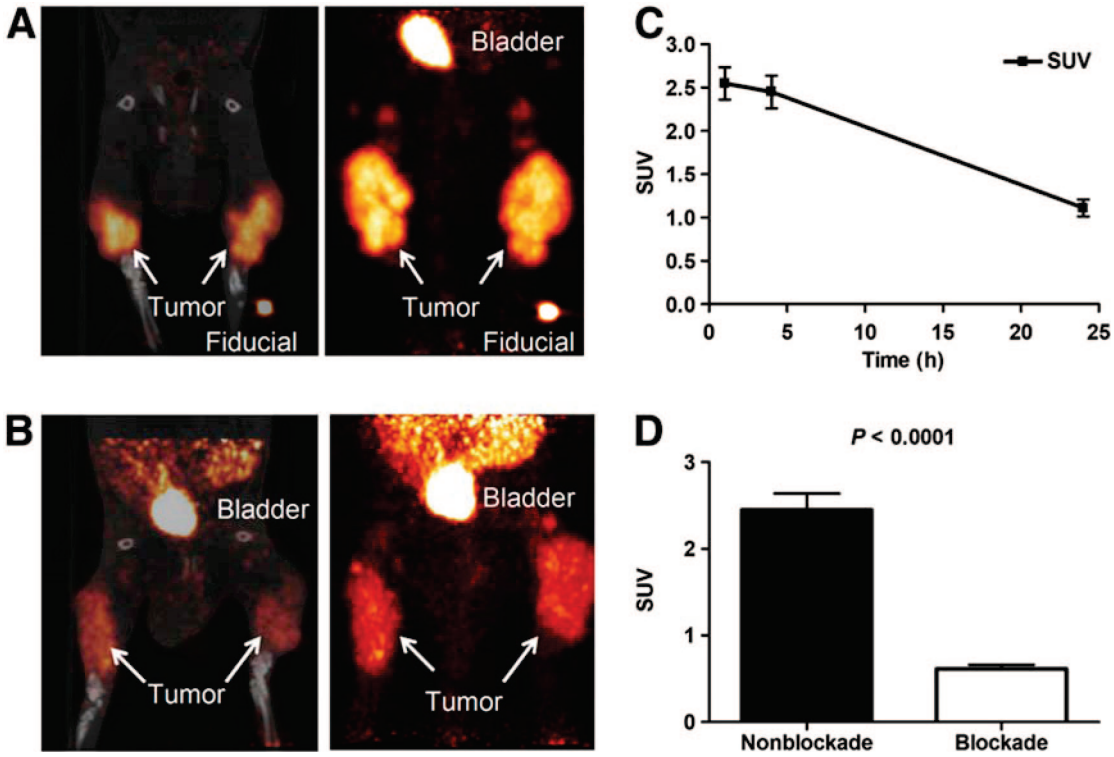

Figure 68. (A) Representative small animal PET image at 4 h of rat injected with ^{64}Cu-CB-TE2A-sst$_2$-ANT. Left image is a representative slice from a small-animal PET/CT fusion image, and right image is a small-animal PET projection view of the same animal. Calculated SUV for the tumor in left hind limb was determined to be 2.7, and SUV for the tumor in right hind limb was determined to be 2.8. (B) Representative small-animal PET image at 4 h of rat injected with ^{64}Cu-CB-TE2A-sst$_2$-ANT and sst$_2$-ANT as blocking agent. Left image is a representative slice from a small-animal PET/CT fusion image, and right image is a small-animal PET projection view of the same animal. In the animal receiving blockade, SUV for tumor in left hind limb was calculated to be 0.74 and SUV for tumor in right hind limb was calculated to be 0.51. (C) Graphical plot of change in average SUV over time. Even after 24 h, SUV remains high, suggesting enhanced binding of ^{64}Cu-CB-TE2A-sst$_2$-ANT for SST2 receptor. (D) Graphical representation that demonstrates change in observed SUV when excess cold sst$_2$-ANT is co-injected with radiopharmaceutical, indicating that binding of radiopharmaceutical to SSTR-positive tumor is receptor-mediated. Reprinted with permission from ref 445. Copyright 2008 Society of Nuclear Medicine.

higher tumor/blood and tumor/muscle ratios at the latest time point of 24 h and excellent tumor visualization during small animal PET imaging experiments, which was believed to reflect the antagonist's increased chemical stability and increased hydrophobicity. Interestingly, the relative tumor uptake observed by Wadas and colleagues was much lower than what was reported by Ginj et al.[444] In the studies by Ginj and co-workers, HEK229 cells that were stably transfected to express SSTR(2) were used, while Wadas and colleagues performed their studies using the SSTR(2) endogenously expressing AR42J rat pancreatic carcinoma cell line. This illustrates the variability in results that can occur when cell lines engineered for receptor expression are used rather than cell lines with a natural phenotype for the receptor of interest.

4.1.3. HER-2/neu Receptor Imaging

HER-2/neu proto-oncogene, which is also called erbB-2 was first identified by transfection studies, when NIH3T3 cells were transformed with DNA from chemically induced rat neuroglioblastomas.[446] It encodes a protein that has extracellular, transmembrane, and intracellular domains and is overexpressed in 25−30% of human breast cancers. Approximately 90−95% of these cases are the result of uncontrolled gene amplification, which produces a malignant phenotype that correlates with shorter disease-free survival and shorter overall survival.[447] Several groups have attempted to image this biomarker by developing SPECT imaging agents such as ^{111}In-labeled trastuzimab[140,448,449] or by developing multimodal imaging agents[450] that will bind tumor cells that overexpress the HER-2/neu receptor. However, the slow elimination of intact monoclonal antibodies from the body yields low tumor/blood and tumor/normal tissue ratios and has forced researchers to investigate smaller targeting systems to improve the biokinetics of these imaging agents without sacrificing specificity. For example, Tang et al. prepared ^{111}In-DTPA(**L12**)-trastuzumab Fab fragments with high radiochemical purity. Although, the measured K_d values for these ligands were 2-fold less than those observed for trastuzumab immunoglobulin gamma (IgG), the maximum number of labeled cell sites was 1.5-fold greater.[451,452] Moreover, biodistribution studies revealed significant tumor to non-target ratios but high kidney uptake after 72 h, and small animal imaging studies revealed the clear visualization of HER-2/neu-positive BT474 human breast cancer xenografts implanted in athymic mice. Similarly, Dennis and colleagues developed ^{111}In-DOTA(**L39**)-AB·Fab4D5, a Fab fragment derived from trastuzumab, which was designed to bind albumin and HER-2/neu simultaneously.[453] Small animal SPECT imaging of MMTV/HER-2 transgenic mice, which develop mammary tumors expressing elevated levels of HER-2, revealed rapid accumulation of ^{111}In-DOTA(**L39**)-AB·Fab4D5 in these tumors, which was comparable with other ^{111}In-DOTA(**L39**)-trastuzumab Fab fragments, but ^{111}In-DOTA(**L39**)-AB·Fab4D5 had better kidney clearance. Finally, Orlova and co-workers described the radiolabeled affibody molecule ^{111}In-DOTA(**L39**)-Z$_{HER2:342-pep2}$.[454] High uptake in SKOV-3 tumor bearing mice at 72 h p.i. was

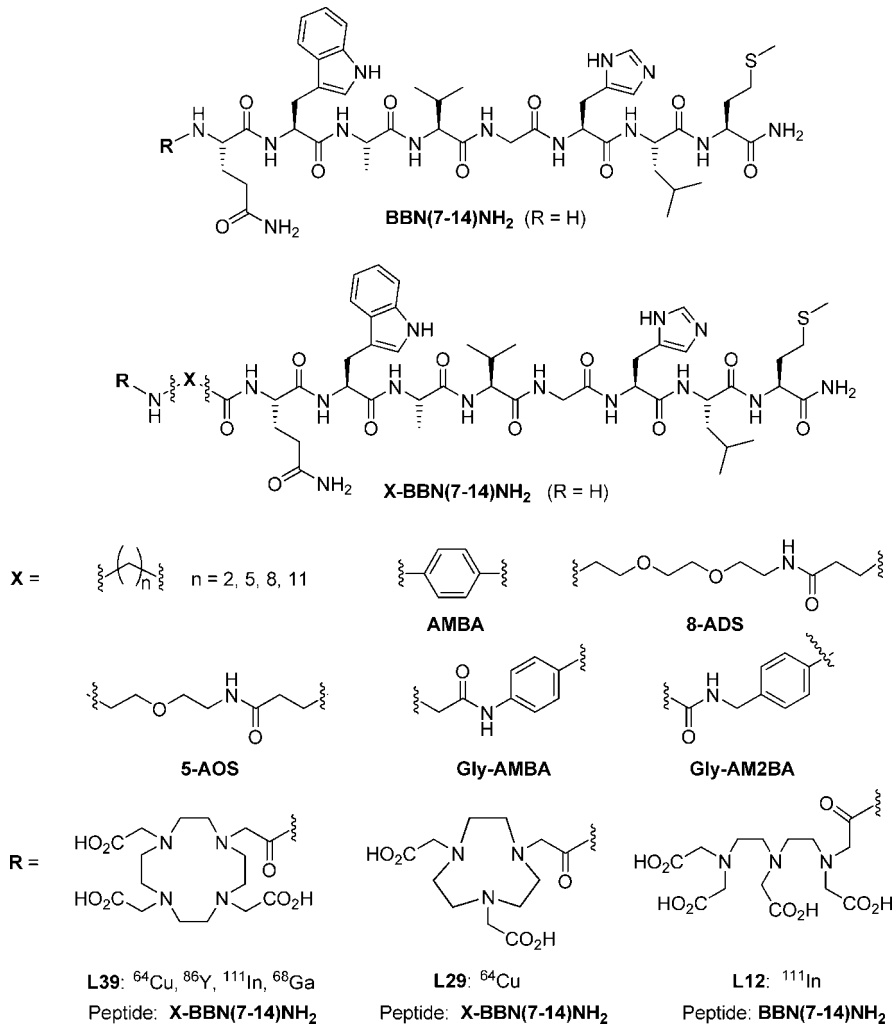

Figure 69. Selected bombesin analogues used in targeting the GRP receptor.

observed but also unusually high kidney retention. Additionally, cell internalization properties of this imaging agent were examined by Wållberg et al., who demonstrated that between 20% and 40% of ^{111}In-DOTA(**L39**)-$Z_{HER2:342-pep2}$ was internalized in several HER-2/neu positive cell lines.[455]

4.1.4. Gastrin Releasing Peptide Receptor Imaging

Bombesin (BBN), a 14 aa peptide present in amphibian tissues, and gastrin releasing peptide (GRP), its human analogue, which consists of 27 amino acids, belong to a family of brain−gut peptides that share very similar activities and occur primarily in the central nervous system.[404] GRP receptors have been observed on a wide variety of human cancers including cancers of the GI tract, lung, prostate and breast and neuroblastomas[404] and represent attractive targets for radiopharmaceutical development. Consequently, numerous bombesin analogues have been developed and labeled with In,[456−458] Ga,[459,460] Y,[461] and Cu[461−466] radiometals in order to evaluate the influence of ligand or chelator structure on the biokinetics of these radiopharmaceuticals (Figure 69). For example, Hoffman et al. examined several DOTA(**L39**)-X-BBN[7−14]-NH_2 peptides where X was a carbon spacer that was either 2, 5, 8, or 11 carbons in length, in order to optimize the pharmacokinetics for specific targeting of human cancers.[457] Once synthesized, these compounds were radiolabeled with ^{111}In and evaluated in cellular assays that utilized the human prostate carcinoma cell line (PC-3). Biodistribution studies on the eight-carbon analogue, which were conducted in SCID mice bearing PC-3 tumors, demonstrated rapid blood clearance with high tumor uptake occurring 15 min p.i. However, washout of the radiotracer was also rapid with only 20% of the injected activity remaining in the tumor by 24 h p.i. Garrison et al. further evaluated the pharmacokinetic changes induced by aliphatic, aromatic, and poly(ethylene glycol) ether functional groups in these analogues.[458] Biodistribution studies and small animal SPECT/CT imaging demonstrated that radiopharmaceuticals containing aromatic groups as linkers exhibited the highest percentage of tumor retention 15 min p.i. but also exhibited higher uptake in the pancreas and in the GI tract, especially at later time points, demonstrating that care needs to be taken when designing radiopharmaceuticals that require chemical linkers between the targeting molecules and the bifunctional chelator.

Recently, Prasanaphich and colleagues explored the bombesin-based radiopharmaceutical ^{64}Cu-NOTA(**L29**)-8-Aoc-BBN(7−14)NH_2 for the PET imaging of GRPR-expressing tissues.[467] This bioconjugate demonstrated high affinity with an IC_{50} of 3.1 nM, while *in vivo* biodistribution studies in PC3 tumor bearing mice demonstrated high uptake in tumor tissue with retention evident at 24 h p.i. Small animal PET/CT corroborated biodistribution studies demonstrating excellent image quality and tumor visualization, especially when compared with the ^{64}Cu-DOTA(**L39**) analogue. Additional

work by the authors has sought to extend this radiopharmaceutical's utility by examining its potential as an imaging agent for breast cancer.[468]

4.1.5. Epidermal Growth Factor Receptor Imaging

The epidermal growth factor receptor (EGFR) family consists of four related transmembrane receptor tyrosine kinases, which can be activated by a variety of ligands including epidermal growth factor (EGF), causing enhanced cellular proliferation, motility, and evasion of apoptosis through downstream pathways.[469] Its overexpression has been observed in up to 60% of human breast cancers with the receptor concentration on these cells being 100 times higher than that on normal epithelial tissues, and several studies have associated this cellular phenotype with poor long-term survival.[470] While some groups have attempted to image other malignancies,[44,471,472] extensive research has been conducted to target EGFR in an attempt to develop imaging agents for breast cancer. For example, Reilly et al. compared the biodistribution properties of ^{111}In-DTPA(**L12**)-hEGF, where hEGF is a 53 aa peptide analogue of human epidermal growth factor, and ^{111}In-DTPA(**L12**) conjugated anti-EGFR monoclonal antibody in cell lines that were known to have low (MCF-7), medium (MDA-MB-231), and high (MDA-MB-468) EGFR expression.[473] As expected, both radiopharmaceuticals bound to MDA-MB-468 cells with high affinity, and the peptide-based radiopharmaceutical cleared more rapidly from the blood of the mice that were implanted with MDA-MB-468, MDA-MB-231, and MCF-7 tumors. However, 72 h after radiopharmaceutical injection, no direct correlation between the level of tumor uptake and EGFR receptor expression on the cell surface could be made, while localization of the peptide radiopharmaceutical was up to 10-fold lower than that observed with the mAb-based radiopharmaceutical. Small animal imaging demonstrated relatively high accumulation of both radiopharmaceuticals in normal tissue such as liver and kidney and sufficient accumulation in MDA-MB-468 human breast cancer xenografts to visualize the tumor at 72 h p.i. Despite the differences in biokinetics, the mAb-based radiopharmaceutical was deemed worthy of future study since its longer circulation time led to high tumor uptake and better tumor visualization at longer time points. Reilly and co-workers have sought to expand upon these interesting results by examining the radiotoxic effect of ^{111}In-DTPA(**L12**)-hEGF on breast cancer cells overexpressing EGFR[474] and comparing the effects of ^{111}In-DTPA(**L12**)-hEGF on normal and malignant tissues in EGFR-positive tumor-bearing mice.[475] Additional reports from this group have evaluated the preclinical pharmacokinetic, toxicologic, and dosimetric properties of ^{111}In-DTPA(**L12**)-hEGF,[476] have correlated the EGFR receptor diversity with nuclear importation,[477] and have described the development of a GMP compliant kit, which allows for the clinical preparation of ^{111}In-DTPA(**L12**)-hEGF.[478]

A ^{68}Ga-labeled analogue, ^{68}Ga-DOTA(**L39**)-hEGF, was also described by Velikyan and colleagues to image EGFR expression in malignant tumors.[479] This radiopharmaceutical demonstrated high affinity for EGFR on A431 cells, and biodistribution results established significant uptake during small animal PET imaging; however, liver and kidney uptake were extremely high and may prevent further investigation of this complex as an imaging agent for hepatic metastases.

Investigations to monitor EGFR expression using ^{64}Cu-DOTA(**L39**)-cetuximab have also been reported.[480] Cai et al. reported the evaluation of ^{64}Cu-DOTA(**L39**)-cetuximab in several tumor-bearing mouse models,[481] and using Western blot analysis, they showed that a positive correlation existed between the expression of EGFR and uptake of ^{64}Cu-DOTA(**L39**)-cetuximab. Li et al. also evaluated ^{64}Cu-DOTA(**L39**)-cetuximab as a PET imaging agent for EGFR-positive tumors.[482] Using A431 cells, they determined that this radiopharmaceutical had a k_d of 0.28 nM, while biodistribution and small animal imaging studies revealed good tumor uptake. More importantly, tumor-to-blood and tumor-to-muscle ratios were comparable to those values reported by Perk et al. using ^{89}Zr-DFO(**L23**)-cetuximab,[44] and ^{64}Cu-DOTA(**L39**)-cetuximab was observed to have a better biodistribution profile than an ^{111}In-DTPA(**L12**)-conjugated cetuximab at 48 h p.i.[483] Eiblmaier and colleagues correlated EGFR expression with ^{64}Cu-DOTA(**L39**)-cetuximab affinity and internalization in cervical cancer using cellular assays and microarray analysis of EGFR gene expression.[484] EGFR mRNA expression was found to correlate with EGFR cell surface populations in five human cancer cell lines, while the amount of internalized radiopharmaceutical correlated with EGFR mRNA expression and observed protein levels. This radiopharmaceutical demonstrated high uptake in Caski cervical cancer tumors 24 h after being injected into nude mice, while small animal imaging revealed excellent image quality comparable to other investigations using ^{64}Cu-labeled cetuximab.[481]

4.1.6. Vascular Endothelial Growth Factor Receptor Imaging

The vascular endothelial growth factor (VEGF) family of growth factors includes VEGF receptors A, B, C, and D, as well as placental growth factor (PlGF). These ligand/receptor pairs are important for the directed proliferation and migration of endothelial cells that occur during embryonic development and other important biological processes such as wound healing and muscle growth.[485] However, they also play a role in the pathological angiogenesis that accompanies the induction and progression of numerous malignancies. More importantly, several VEGF receptors have been shown to play critical roles in tumor progression, metastasis, and angiogenesis and offer scientists a valuable target against which to develop molecular imaging agents.[486,487] For example, Nagengast and co-workers evaluated ^{111}In-DTPA(**L12**)-bevacizumab, a monoclonal antibody that recognizes all VEGF isoforms and blocks tumor angiogenesis, in nude mice bearing human SKOV-3 ovarian tumor xenografts. They demonstrated increasing tumor uptake even after 7 days, with appreciable activity still found in the blood, liver, and kidney.[210] This antibody was also labeled with ^{89}Zr and compared with ^{89}Zr-IGg in ovarian tumor xenografts.[210] Tumors were easily visualized at 24 h p.i., and after 168 h p.i., accumulation of the ^{89}Zr-bevacizumab was still observed to be increasing in the tumor (Figure 70). Based upon PET analysis, significantly more activity had accumulated after several days in the tumors of animals that received ^{89}Zr-bevacizumab than those that received ^{89}Zr-IgG. *Ex vivo* determination of tumor uptake correlated well with the *in vivo* data and demonstrated that quantitative measurement of the tracer in the tumor was possible.

Others have explored the use of radiolabeled recombinant fusion proteins as imaging agents. Chan and co-workers

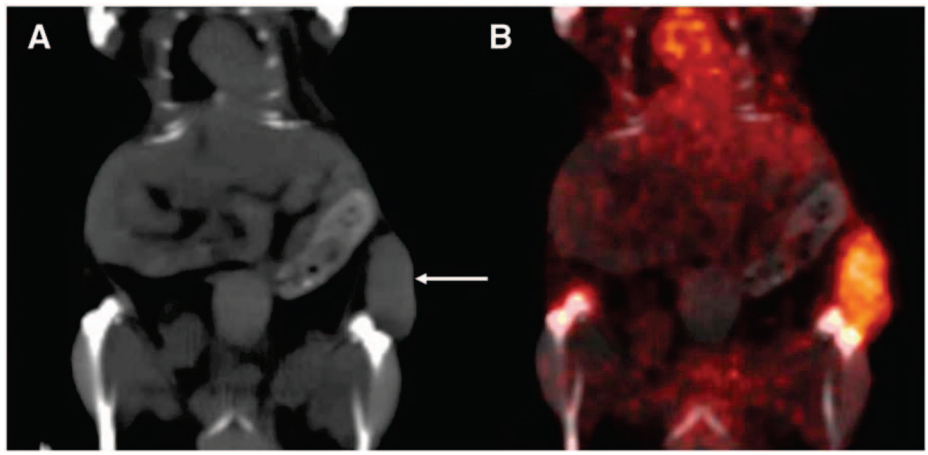

Figure 70. Coronal CT image (A) with clear subcutaneous localization of SKOV-3 tumor (arrow). Fusion of microPET and CT images (B) (168 h after injection) enables adequate quantitative measurement of ^{89}Zr-bevacizumab in the tumor. Reprinted with permission from ref 210. Copyright 2007 Society of Nuclear Medicine.

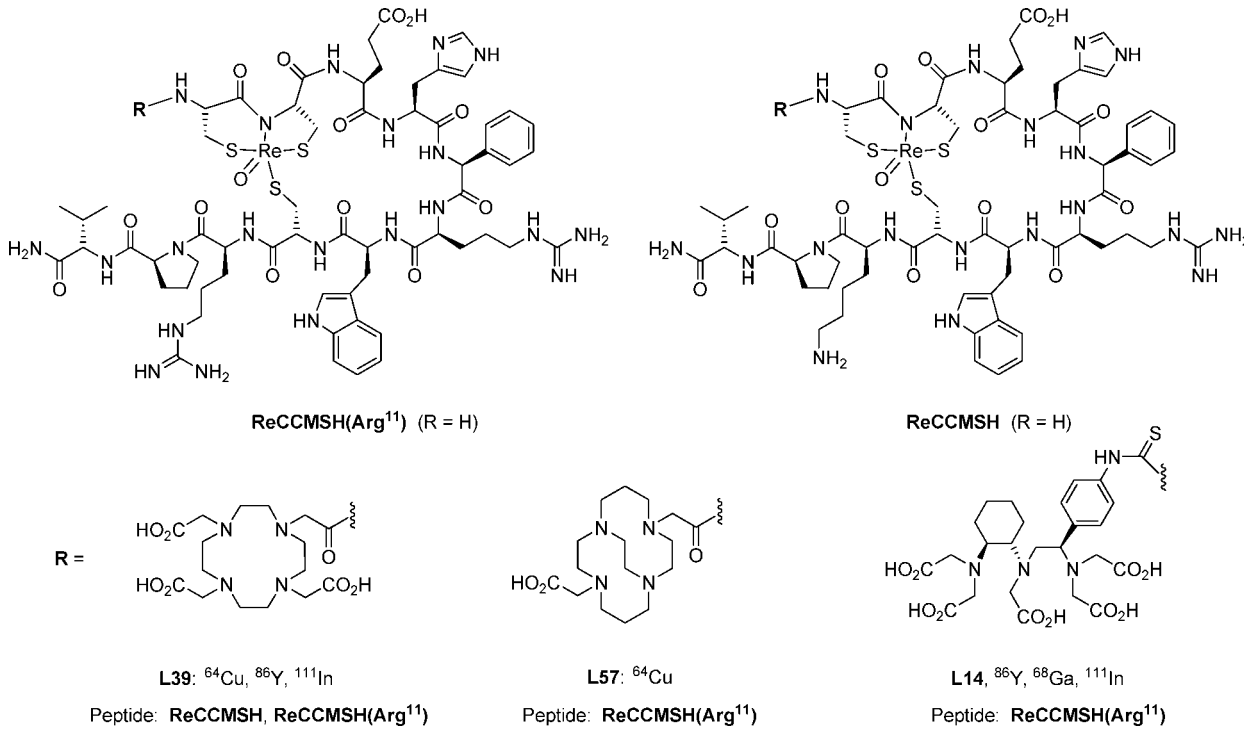

Figure 71. Selected α-MSH analogues that target the melanocortin-1 (MC-1) receptor.

described a novel recombinant fusion protein composed of $VEGF_{165}$ fused to human transferrin (hnTrf), which was used to chelate ^{111}In.[488] This radiopharmaceutical accumulated through receptor-mediated processes in highly vascularized U87MG glioblastoma xenografts allowing imaging as early as 24 h p.i. However, since the ^{111}In was bound to hnTrf without the use of a traditional chelator, approximately 65% of the incorporated activity was observed to be transchelated under physiological conditions after 72 h. Additional work has focused on the preparation of ^{64}Cu-DOTA(**L39**)-$VEGF_{121}$,[489] ^{64}Cu-DOTA(**L39**)-$VEGF_{DEE}$, (which is specific for VEGFR2),[490] and ^{64}Cu-DOTA(**L39**)-QD-VEGF, which was developed as a multimodal imaging agent combining the PET reporter ^{64}Cu-DOTA(**L39**) and the optical properties of quantum dots (QDs).[491,492] Backer et al. developed a single chain, cysteine-tagged VEGF ligand, which is a fusion protein combining two fragments of human $VEGF_{121}$ cloned head to tail.[493] Upon folding, a single cysteine was engineered to be available for chelator conjugation so that the molecule could be radiolabeled with +2 and +3 metal radionuclides. This molecule was also engineered to contain a PEG moiety to increase its blood circulation time. After the chelator DOTA(**L39**) was attached, the molecule was labeled with ^{64}Cu, and biodistribution was determined in female Balb/C mice with 4T1/luc murine mammary carcinoma cells implanted in their mammary fat pads. Data at 2 h p.i. showed prolonged blood circulation due to the addition of the PEG linker and appreciable tumor uptake. Unfortunately, kidney uptake was observed to be extremely high, approaching 60% ID/g at this time point.

4.1.7. Melanoma Imaging

Malignant melanoma is the sixth most commonly diagnosed cancer and the most lethal form of skin cancer.[494] To improve diagnosis and survival rates, the melanoma cortin-1 (MC-1) receptor has been a very promising melanoma-specific target for the development of imaging probes based

upon the alpha melanocyte stimulating hormone (α-MSH), which binds this receptor with nanomolar affinity (Figures 71 and 72).[141,495−503] Chen et al. synthesized several DOTA(**L39**) conjugated α-MSH analogues including DOTA(**L39**)-[Nle^4,D-Phe^7]α-MSH (NDP; Nle = norleucine), DOTA(**L39**)-CCMSH, a linear analogue, DOTA(**L39**)-CMSH, a disulfide-bonded analogue, and DOTA(**L39**)-Re-CCMSH, a rhenium-cyclized analogue in order to optimize the *in vivo* biological properties through structure modification.[496] Of these, ^{111}In-DOTA(**L39**)-ReCCMSH had significantly higher tumor accumulation and displayed lower radioactivity accumulation in the kidney and other normal tissues compared with the linear or disulfide-cyclized analogues. This led Cheng et al. to expand on this work by examining the relationship between the structure of the rhenium metallopeptide and its biological properties.[497−499] One derivative, ^{111}In-DOTA(**L39**)-ReCCMSH(Arg^{11}), which replaced the lysine at position 11 with arginine, demonstrated slightly higher affinity than the ^{111}In-DOTA(**L39**)-ReCCMSH *in vitro* and had significantly higher tumor uptake and lower kidney retention at almost every time point investigated when evaluated in a B16/F1 murine melanoma tumor model.

McQuade, et al. evaluated the analogous PET radiopharmaceuticals ^{86}Y-DOTA(**L39**)-ReCCMSH(Arg^{11}) and ^{64}Cu-DOTA(**L39**)-ReCCMSH(Arg^{11}) using a B16/F1 melanoma model.[500] Biodistribution studies demonstrated that uptake in the tumor peaked at 30 min and remained stable after 4 h, but by 24 h tumor uptake had decreased by 94% and 68%, respectively. Even with significant clearance from the tumor at 24 h, small animal PET experiments revealed good tumor visualization due to low uptake in non-target tissues.

Wei et al. further modified this radiopharmaceutical by replacing DOTA (**L39**) with the ^{64}Cu chelator CB-TE2A (**L57**), whose Cu(II) complex is highly kinetically inert (*vide supra*).[504] While tumor uptake and retention was similar to that observed by McQuade and co-workers, the advantages of the cross-bridged chelator were clearly evident, since it exhibited more rapid renal clearance than either the ^{64}Cu-DOTA(**L39**) or ^{86}Y-DOTA(**L39**) analogues with lower accumulation in non-target tissues. This low level of background radioactivity provided excellent contrast resulting in high-quality PET images, making ^{64}Cu-CB-TE2A(**L57**)-ReCCMSH(Arg^{11}) a promising melanoma imaging agent.

4.2. Imaging Gene Expression

While numerous cell surface molecules have been successfully targeted for imaging, they represent a small fraction of the proteome of a living cell.[505] Since numerous intra- and intercellular regulatory proteins are implicated in cancer initiation and progression, molecular imaging of these biomolecules found within the cytoplasm and nucleus of the cell would provide valuable insight into the phenotype and aggressiveness of cancerous tumors[506] and has become an active area of imaging research.

There are several reports in the literature of the use of ^{86}Y, ^{68}Ga, and ^{64}Cu radiometals to image mRNA expression.[194,507−510] Schlesinger et al. investigated the application of ^{86}Y labeled L-oligonucleotides.[194,509] These mirror-image oligonucleotides have an extended biological half-life due to their high resistance to enzyme degradation. Labeled oligonucleotides had a radiochemical purity that fell within a range of 73−98% depending upon the isomer examined. Biodistribution of these systems in normal Wistar rats revealed that the radiopharmaceuticals are renally excreted

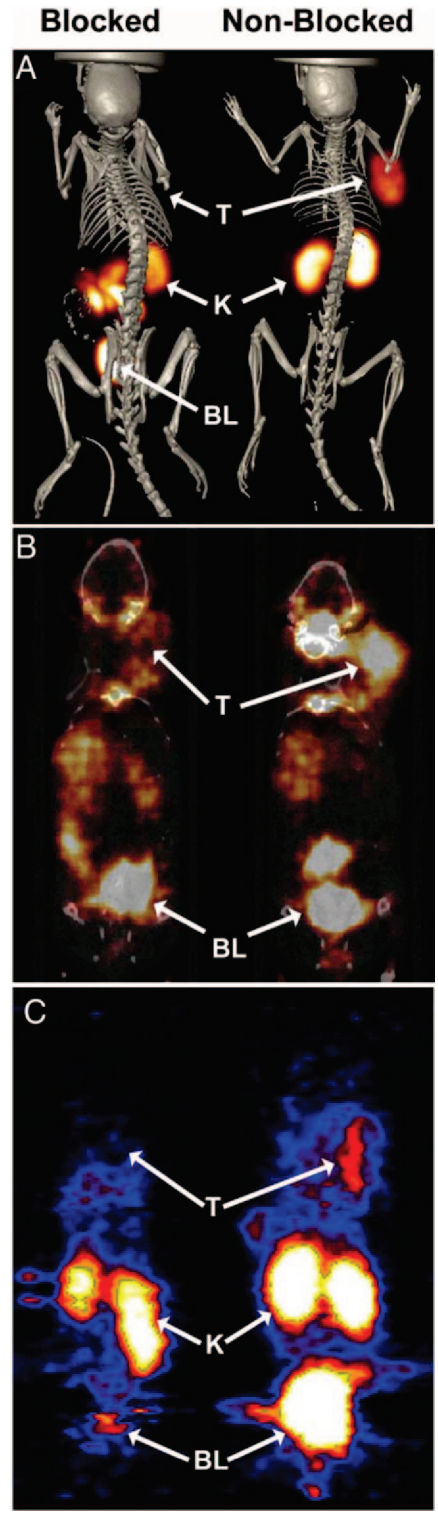

Figure 72. Whole-body SPECT/CT, PET/CT, and PET images of B16 melanoma tumor-bearing C57 mice 2 h post-tail-vein-injection of radiolabeled CHX-A″-Re(Arg^{11})CCMSH. (A) SPECT/CT images of tumor-bearing mice injected intravenously with 12.95 MBq (350 μCi) of ^{111}In-CHX-A″-Re(Arg^{11})CCMSH with (blocked) or without (nonblocked) a 20-μg nonradiolabeled peptide block. PET/CT and PET imaging of melanoma-bearing mice 2 h post-tail-vein-injection of (B) 4.44 MBq (120 μCi) of ^{86}Y-CHX-A″-Re(Arg^{11})CCMSH with a 20-μg NDP block (blocked) and without block (nonblocked) or (C) 3.7 MBq (100 μCi) of ^{68}Ga-CHX-A″-Re(Arg^{11})CCMSH with (blocked) and without (nonblocked) a 60-μg NDP block, respectively. Tumor (T), kidney (K), and (BL) bladder locations are highlighted for each mouse. Reprinted with permission from ref 141. Copyright 2009 Elsevier Limited.

and that they demonstrate appreciable uptake in the adrenal glands, liver, and bone. Additionally, Roivainen et al. labeled DOTA (**L39**)-conjugated antisense oligonucleotides, which were designed to target activated human K-ras oncogene with ^{68}Ga, and these radiopharmaceuticals were evaluated in mice bearing A549 lung carcinoma tumors containing a mutated form of the K-ras oncogene and BxPC3 pancreatic adenocarcinoma cell tumors exhibiting wild-type expression of K-ras.[511] Radiolabeling did not alter the hybridization properties or protein binding of these systems and small animal PET imaging revealed exceptional visualization of tumors bearing WT K-ras expression, while tumors with the K-ras mutations were barely visible above background. Unfortunately, no quantification of the PET data was provided.

Wang et al. developed a DTPA (**L12**)-conjugated 18-mer phosphothioated antisense oligodeoxynucleotide (ODN) that could be labeled with ^{111}In to image p21$^{waf-1/CIP-1}$ gene expression at the RNA level.[510] The p21$^{waf-1/CIP-1}$ gene is a prominent early response gene for DNA damage, which encodes a cyclin-dependent kinase inhibitor that regulates progress through the eukaryotic cell cycle. These oligonucleotide imaging agents were evaluated in athymic mice bearing MDA-MB-468 tumor xenografts where the expression of p21$^{waf-1/CIP-1}$ is induced following the subcutaneous injection of epidermal growth factor (EGF) directly into the tumor. Forty-eight hours after the induced p21$^{waf-1/CIP-1}$ gene expression, biodistribution studies revealed tumor-to-muscle ratios that were approximately 3- and 2-fold greater than that seen in tumors where EGF induction was not performed or where random ODNs were injected, respectively. Moreover, tumors were easily visualized via γ camera scintigraphy.

Developing protein nucleic acid based radiopharmaceuticals has also been investigated. Tian and co-workers developed ^{64}Cu-DOTA(**L39**)-PNA-peptide radiopharmaceuticals to image the overexpression of CCND1 mRNA, which is translated into cyclin D1, a key regulator in cell proliferation.[512] This radiopharmaceutical was designed with dual specificity, containing a peptide sequence that binds to the insulin-like growth factor receptor (IGFR), which allows the radiopharmaceutical to be internalized into the cell, as well as a nucleic acid sequence that can hybridize to the CCND1 mRNA once in the cytosol. These ^{64}Cu-DOTA(**L39**)-PNA-peptide radiopharmaceuticals were observed to be stable to transchelation challenge using 100-fold molar excess of DTPA (**L12**), human serum albumin, or cysteine at 22 °C for 30 min, and once injected *in vivo*, no transchelation to proteins such as superoxide dismutase was observed. Additionally, appreciable tumor uptake was noted that could be blocked with a co-injection of insulin-like growth factor (IGF), and washout was observed to be rapid by 24 h. Moreover, tumor-to-muscle ratios were not significantly different between cohorts that received the radiopharmaceutical and the cohorts that received the PNA or peptide mismatch, respectively. Small animal PET/CT imaging of MCF-7, ER$^+$ breast cancer, xenografts implanted in female SCID mice revealed significantly faster and higher uptake in these tumors than CCND1 scintographic probes previously described.[513] Additional work in this area by this group has also led to the development of ^{111}In-DTPA (**L12**)-conjugated protein nucleic acid (PNA) antisense molecules that could cross the blood−brain barrier (BBB) and tumor cell membrane to image either rat glial fibrillary acidic protein (GFAP) or rat caveolin-1 α (CAV).[514,515] Together these results demonstrate that it is possible to image endogenous gene expression in brain cancer with sequence-specific PNA antisense radiopharmaceuticals conjugated to a drug targeting system.

4.3. Imaging Inflammation and Infection

The imaging of any infection or inflammatory foci, which are characterized by enhanced blood flow, enhanced vascular permeability, and an influx of white blood cells, has become a valuable tool that physicians can utilize to diagnose disease and monitor therapy.[516] There are numerous examples in the literature of nonspecific imaging agents that rely on the differences in vascular dilation between healthy and diseased tissue or targeted radiopharmaceuticals that bind to specific targets present in the inflammation[516−519] or infection[413−417] process. For example, Lazzeri et al. exploited the high affinity between avidin and biotin for inflammation imaging in patients with skeletal lesions that included orthopedic conditions, osteomyelitis of the trunk, infection/inflammation of prosthetic joint replacements, and patients with suspected osteomeylitis of appendicular bones.[520,521] This technique involves an infusion of avidin, which was allowed to localize at the infection site followed 4 h later by an injection of ^{111}In-DTPA(**L12**)-biotin. Imaging was conducted at 30 min and 16−18 h p.i., and to assess its effectiveness, it was compared with ^{99m}Tc-HMPAO-labeled leukocyte scintigraphy. Based upon the results of this study, the ^{111}In-biotin−avidin system was more sensitive at detecting lesions than ^{99m}Tc-leukocyte scintigraphy in patients with prosthetic joint replacement, osteomyelitis of appendicular bones and osteomyelitis of the trunk and was determined to be more practical since these procedures reduce patient burden by 50%.

Receptor-specific radiopharmaceuticals that target the cells involved with immune and inflammatory processes have also been designed. For example, van Erd et al.[522] and Broekema et al.[523] investigated the new imaging agent ^{111}In-DTPA(**L12**)-DPC11870, where DPC11870 is an antagonist of leukotriene B4 (LTB4) receptor, expressed on the surface of neutrophils (Figure 73). This molecule was evaluated in a model of acute colitis, which was induced in New Zealand white rabbits by infusion of trinitrobenzene sulfonic acid in the descending colon, and was compared with [^{18}F]-FDG and ^{99m}Tc-HMPAO granulocytes, which measure metabolic activity and infection response, respectively. Based upon these experiments, all three radiotracers revealed the inflamed colon upon scanning, but ^{111}In-DTPA(**L12**)-DPC11870 was superior to both ^{99m}Tc-HMPAO-granulocytes and [^{18}F]-FDG because it exhibited high uptake in the colonic lesions while generating a low background signal in noninflamed colon. Additionally, Bhargava et al. was able to label leukocytes with ^{64}Cu using a dual chelator method, which demonstrated an equal efficiency to labeling leukocytes with ^{111}In and was superior to labeling leukocytes with ^{18}F-FDG,[524] while Locke and colleagues examined ^{64}Cu-DOTA(**L39**)-PEG-c(FLFLFK). This radiopharmaceutical targets the Formyl peptide receptor (FPR) located on leukocytes, and acts as an antagonist by selectively binding to neutrophils with a k_d of 18 nM, but without inducing neutropenia.[525] Small animal imaging studies were performed on mice that were exposed to *Klebsiella pneumoniae*. Eighteen hours after exposure, small animal PET/CT and SUV analysis revealed a 5-fold increase in radiopharmaceutical uptake in animals exposed to the bacteria when compared with the control cohort, and this was corroborated by an examination of the lung

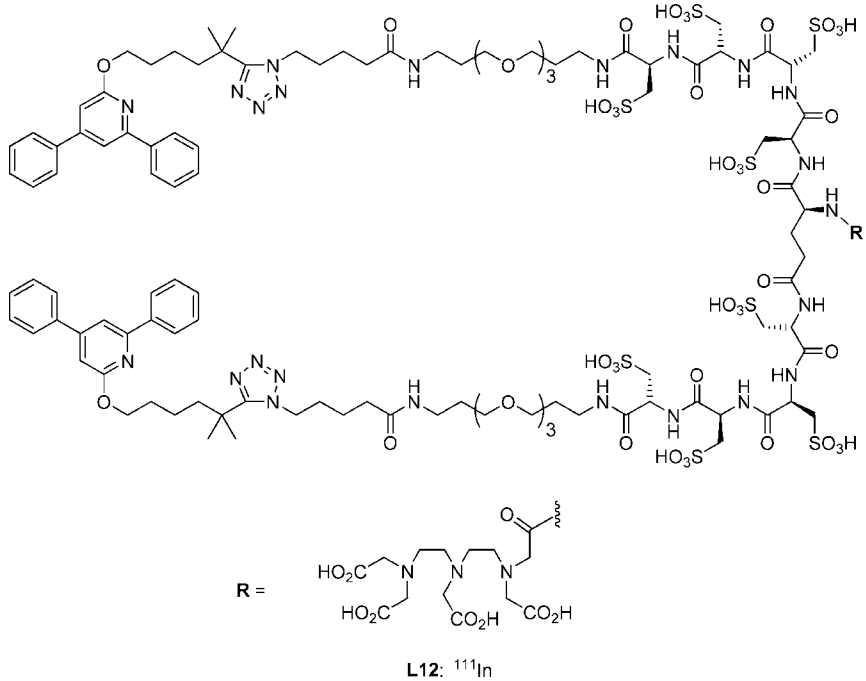

Figure 73. The synthetic antagonist DPC11870 targets the leukotriene B4 (LTB4) receptor.

myeloperoxidase activity, which was determined in both groups of animals.

4.4. Imaging Hypoxia and Perfusion

Perfusion and hypoxia imaging have developed into robust research areas since they allow scientists and clinicians to monitor changes in blood flow and image changes in oxygen demand. Both have important implications in the *in vivo* imaging of myocardial infarction and neurological stroke since changes in perfusion often lead to changes in tissue oxygenation and ischemia.[526,527] Imaging hypoxia also has important implications in cancer since tumor hypoxia is believed to increase a tumor's metastatic potential while reducing its sensitivity to radio- and chemotherapeutic agents.[528] Both perfusion and hypoxia imaging have been exhaustively reviewed.[63,529−531]

Numerous perfusion agents have been developed and evaluated using Ga and Cu radiometals because of their short half-lives.[532−537] Cutler et al. evaluated the small neutral lipophilic complex ^{68}Ga-tris(2-mercaptobenzyl)amine (**L2**) as a potential coronary and neurological perfusion agent.[538] Radiolabeling of this ligand with ^{68}Ga was observed to be facile, and biodistribution studies of this complex in rats demonstrated high uptake in brain and heart after 60 min. PET imaging of canines and non-human primates demonstrated that this imaging agent is taken up in normal myocardium and has the potential to be used as a diagnostic PET agent for cerebral blood flow.

Because of the short half-lives of $^{60/61/62}$Cu, research to develop perfusion agents with these radiometals has also been explored, and the most extensively studied of these perfusion agents is Cu-PTSM (Cu-**L8**). Its popularity is attributed to its higher reduction potential compared with other copper thiosemicarbazone complexes that have been developed to image tumor hypoxia (*vida infra*). This physical property facilitates the reduction of Cu(II) to Cu(I) by the normal electron transport chain found in the mitochondria of both normoxic and hypoxic tissues.[535,536] This reductive process and its low membrane permeability after reduction explain its utility as a perfusion agent of healthy and diseased tissues. For example, Wallhaus and colleagues demonstrated that flow defects identified by ^{62}Cu-PTSM (^{62}Cu-**L8**) correlated well with angiography in patients with significant coronary artery disease, and the results were comparable to those obtained with ^{99m}Tc-sestamibi and ^{82}Ru.[539] Additionally, Flower et al. examined the possibility of using ^{64}Cu-PTSM (^{64}Cu-**L8**) to monitor blood flow changes in patients who presented with colorectal liver metastases and were prescribed vascular manipulation as a component of locoregional chemo- and radiotherapy. Efficacy rates were as high as 78% in patients receiving these treatments.[540] Moreover, Holschenider and colleagues attempted to determine whether ^{64}Cu-PTSM (^{64}Cu-**L8**) could be used to distinguish between active and passive brain function by comparing it with [^{14}C]-iodoantipyrine, a traditional perfusion agent, in Sprague−Dawley rats that were being subjected to a motor skills challenge after being injected with each tracer.[541]

While research had been conducted to develop Ga-based radiopharmaceuticals for hypoxia imaging,[534,542,543] the vast majority has been focused on Cu radiopharmaceuticals, which are based upon the hypoxia-selective imaging agent Cu-ATSM (Cu-**L9**) first reported by Fujibayashi and colleagues.[544] Since then, much research has been published on the nonradioactive chemistry of this complex in order to develop new ATSM (**L9**) derivatives,[545−554] and elucidate the relationships between molecular structure and the hypoxia mechanisms active within the living cell.[34,64,65,81,555−557] Additionally, ATSM (**L9**) has been labeled with several different Cu radiometals,[558−561] studied as a PET radiopharmaceutical for hypoxia imaging in lung cancer[562] and cervical cancer,[563−566] and used to monitor therapy response after laparoscopic surgery.[567] Preclinically, it has been examined as an agent for targeted radiotherapy,[62,568−570] for examining multidrug-resistant tumors,[571] and in conjunction with perfusion imaging.[572,573] Moreover, ^{64}Cu-ATSM (^{64}Cu-**L9**) uptake has been correlated with topoisomerase II expression,[574] fatty acid synthase expression,[575] tissue oxygenation,[576] and uptake of other PET tracers currently used in

the clinic. For example, Dence et al. performed dual tracer experiments that combined autoradiography and small animal PET/CT to correlate the imaging information obtained from ^{64}Cu-ATSM (^{64}Cu-**L9**) imaging with those from ^{18}F-FMISO, ^{18}F-FDG, and ^{18}F-FLT, which are clinically approved tracers for imaging hypoxia, metabolism, and cellular proliferation, respectively.[577] ^{64}Cu-ATSM (^{64}Cu-**L9**) correlated well with the ^{18}F-FMISO and ^{18}F-FLT but not strongly with ^{18}F-FDG. This provides a good example of how dual-tracer imaging can yield more detailed information to the clinician about the physiological processes occurring within the imaged tumor.

5. Conclusion

Metal-based radiopharmaceutical research has progressed rapidly since the first ^{99}Mo/^{99m}Tc generator was produced more than 50 years ago. Since that time great strides have been made in radioisotope production, the coordination chemistry of radiometals, and correlating the chemical structure of metal-based radiopharmaceuticals with their behavior *in vivo*. For example, radiocopper chelate stability is paramount when developing tumor targeting radiopharmaceuticals so that optimum image quality can be achieved. However, the opposite is true when considering radiocopper radiopharmaceuticals for hypoxia and perfusion imaging. As a result, researchers now have the ability to match the physical characteristics of a specific radiometal with the biokinetics of a particular biological targeting molecule leading to the development of diagnostic and therapeutic radiopharmaceuticals that can be tailored to individual disease processes. This impressive achievement has occurred not by chance but by the dedicated and collaborative efforts of physicists, chemists, biologists, engineers, and physicians. Furthermore, as this scientific discipline advances further into the 21st century, this collaboration must continue and is essential if the transition of more of these radiopharmaceuticals from bench to bedside is to occur.

6. Glossary

%ID/g	percent injected dose per gram
aa	amino acid
BBB	blood−brain barrier
BBN	bombesin
BFC	bifunctional chelator
CAV	rat caveolin 1-α
CN	coordination number
CT	computed tomography
DBP	di(*n*-butylphosphate)
DFO	desferrioxamine
DMF	dimethylformamide
EDC	1-ethyl-3-(3-dimethyl-aminopropyl)-carbodiimide
EGF	epidermal growth factor
Fab	fragment, antigen binding region
Fc	fragment crystallizable
FDA	Food and Drug Administration
FDG	[^{18}F]-fluorodeoxy glucose
FLT	[^{18}F]-fluoro-L-thymidine
FMISO	[^{18}F]-fluoromisonidazole
FPR	formyl peptide receptor
Fv	fragment variable
GFAP	rat glial fibrillary acidic protein
GRP	gastrin-releasing peptide
GRPR	gastrin-releasing peptide receptor
HDEHP	bis-(2-ethylhexyl)-phosphate
HEK	human embryonic kidney
HMPAO	hexamethylpropyleneamine oxime
HNSCC	head and neck squamous cell carcinoma
hnTf	human transferrin
HOPO	hydroxypyridinone
HPLC	high-performance liquid chromatography
IGF	insulin-like growth factor
IGFR	insulin-like growth factor receptor
IgG	immunoglobulin gamma
LTB4	leukotriene B4
LTB4R	leukotriene B4 receptor
mAb	monoclonal antibody
MC-1	melanocortin-1
MC-1R	melanocortin-1 receptor
MRI	magnetic resonance imaging
NCA	no carrier added
NET	neuroendocrine tumor
NIR	near-infrared
N-sucDF	*N*-succinyldesferrioxamine B
NTMF	nuclear track microfilters
OC	octreotide
ODNs	oligodeoxynucleotides
p.i.	postinjection
PEG	poly(ethylene glycol)
PET	positron emission tomography
PlGF	placental growth factor
PNA	protein nucleic acid
PTSM	methyl-thio-semicarbazone
QD	quantum dot
RIT	radioimmunotherapy
RP-HPLC	reversed-phase high-performance liquid chromatography
SA	square antiprismatic
SCID	severly combined immunodeficiency
SPECT	single-photon emission computed tomography
SST	somatostatin
SSTR	somatostatin receptor
SUV	standardized uptake value
sulfo-SMCC	sulfosuccinimidyl 4-(*n*-maleimidomethyl)cyclohexane-1-carboxylate
TATE	octreotate
TBP	tributylphosphate
TFP	10-(3-(4-methyl-piperazin-1-yl)-propyl)-2-trifluoromethyl-10*H*-phenothiazine
TOA	trioctyl amine
TSA	twisted square antiprismatic
TTA	4,4,4-trifluoro-1-(2-thienyl)-1,3-butanedione
VEGF	vascular endothelial growth factor
VEGFR	vascular endothelial growth factor receptor
Y^3-OC	tyrosine-3-octreotide
Y^3-TATE	tyrosine-3-octreotate
α-MSH	alpha melanocyte stimulating hormone
β^-	beta − particle
β^+	positron
γ	gamma ray

7. Acknowledgments

The authors gratefully acknowledge Dr. Riccardo Ferdani, Ph.D. for assistance with the creation of Figure 1, the financial support of NIH Grants R01 CA064475 (C.J.A.), CA093375 (E.H.W.), and F32 CA115148 (T.J.W.), and the Gloria G. & Robert E. Lyle Professorship endowment (G.R.W.).

8. References

(1) Society of Nuclear Medicine. http://interactive.snm.org/index.cfm?PageID=5571&RPID=969, 2009.
(2) Welch, M. J.; Redvanly, C. S., Eds.; *Handbook of Radiopharmaceuticals: Radiochemistry and Applications*; John Wiley & Sons Inc.: Hoboken, NJ, 2003.

(3) Blower, P. J.; Lewis, J. S.; Zweit, J. *Nucl. Med. Biol* **1996**, *23* (8), 957.
(4) Wadas, T. J.; Wong, E. H.; Weisman, G. R.; Anderson, C. J. *Curr. Pharm. Des.* **2007**, *13* (1), 3.
(5) Smith, S. V. *IDrugs* **2005**, *8* (10), 827.
(6) Smith, S. V. *J. Inorg. Biochem.* **2004**, *98* (11), 1874.
(7) Shokeen, M.; Anderson, C. J. *Acc. Chem. Res.* **2009**, *42* (7), 832.
(8) Zwanziger, D.; Beck-Sickinger, A. G. *Curr. Pharm. Des.* **2008**, *14* (24), 2385.
(9) de Jong, M.; Breeman, W. A. P.; Kwekkeboom, D. J.; Valkema, R.; Krenning, E. P. *Acc. Chem. Res.* **2009**, *42* (7), 873.
(10) Liu, S. *Adv. Drug Delivery Rev.* **2008**, *60* (12), 1347.
(11) Heeg, M. J.; Jurisson, S. S. *Acc. Chem. Res.* **1999**, *32* (12), 1053.
(12) Anderson, C. J.; Welch, M. J. *Chem. Rev.* **1999**, *99* (9), 2219.
(13) Anderson, C. J.; Wadas, T. J.; Wong, E. H.; Weisman, G. R. Q. J. *Nucl. Med. Mol. Imaging* **2008**, *52* (2), 185.
(14) Rowland, D. J.; Lewis, J. S.; Welch, M. J. *J. Cell. Biochem.* **2002**, (39), 110.
(15) McQuade, P.; Rowland, D. J.; Lewis, J. S.; Welch, M. J. *Curr. Med. Chem.* **2005**, *12* (7), 807.
(16) McQuade, P.; McCarthy, D. W.; Welch, M. J. Metal radionuclides for PET imaging. In *Positron Emission Tomography*; Valk, P. E., Bailey, D. L., Townsend, D. W., Maisey, M. N., Eds.; Springer-Verlag: London, 2003, p 251.
(17) Hoffman, T. J.; Smith, C. J. *Nucl. Med. Biol.* **2009**, *36* (6), 579.
(18) Meares, C. F. Capturing copper for molecular imaging and therapy. In *Recent Advances of Bioconjugation Chemistry in Molecular Imaging*; Chen, X., Ed.; Research Signpost: Kerala, India, 2009; p 227.
(19) Verel, I.; Visser, G. W. M.; Boellaard, R.; Stigter-van Walsum, M.; Snow, G. B.; van Dongen, G. A. M. S. *J. Nucl. Med.* **2003**, *44* (8), 1271.
(20) Bass, L. A.; Wang, M.; Welch, M. J.; Anderson, C. J. *Bioconjugate Chem.* **2000**, *11* (4), 527.
(21) Boswell, C. A.; Sun, X.; Niu, W.; Weisman, G. R.; Wong, E. H.; Rheingold, A. L.; Anderson, C. J. *J. Med. Chem.* **2004**, *47* (6), 1465.
(22) Harrison, A.; Walker, C. A.; Parker, D.; Jankowski, K. J.; Cox, J. P. L.; Craig, A. S.; Sansom, J. M.; Beeley, N. R. A.; Boyce, R. A. *Nucl. Med. Biol.* **1991**, *18* (5), 469.
(23) Camera, L.; Kinuya, S.; Garmestani, K.; Wu, C.; Brechbiel, M. W.; Pai, L. H.; McMurry, T. J.; Gansow, O. A.; Pastan, I.; Paik, C. H. *J. Nucl. Med.* **1994**, *35* (5), 882.
(24) Stimmel, J. B.; Kull, F. C. *Nucl. Med. Biol* **1998**, *25* (2), 117.
(25) Stimmel, J. B.; Stockstill, M. E.; Kull, F. C., Jr. *Bioconjugate Chem.* **1995**, *6* (2), 219.
(26) Byegard, J.; Skarnemark, G.; Skalberg, M. *J. Radioanal. Nucl. Chem.* **1999**, *241* (2), 281.
(27) Kukis, D. L.; DeNardo, S. J.; DeNardo, G. L.; O'Donnell, R. T.; Meares, C. F. *J. Nucl. Med.* **1998**, *39* (12), 2105.
(28) Jang, Y. H.; Blanco, M.; Dasgupta, S.; Keire, D. A.; Shively, J. E.; Goddard, W. A., III *J. Am. Chem. Soc.* **1999**, *121* (26), 6142.
(29) Liu, S.; Edwards, D. S. *Bioconjugate Chem.* **2001**, *12* (1), 7.
(30) Moreau, J.; Guillon, E.; Pierrard, J.-C.; Rimbault, J.; Port, M.; Aplincourt, M. *Chem.—Eur. J.* **2004**, *10* (20), 5218.
(31) Chong, H.-s.; Garmestani, K.; Ma, D.; Milenic, D. E.; Overstreet, T.; Brechbiel, M. W. *J. Med. Chem.* **2002**, *45* (16), 3458.
(32) Li, W. P.; Ma, D. S.; Higginbotham, C.; Hoffman, T.; Ketring, A. R.; Cutler, C. S.; Jurisson, S. S. *Nucl. Med. Biol.* **2001**, *28* (2), 145.
(33) Yoo, J.; Reichert, D. E.; Welch, M. J. *J. Med. Chem.* **2004**, *47* (26), 6625.
(34) Barnard, P. J.; Bayly, S. R.; Holland, J. P.; Dilworth, J. R.; Waghorn, P. A. Q. J. *Nucl. Med. Mol. Imaging* **2008**, *52* (3), 235.
(35) Jurisson, S.; Cutler, C.; Smith, S. V. Q. J. *Nucl. Med. Mol. Imaging* **2008**, *52* (3), 222.
(36) McMurry, T. J.; Pippin, C. G.; Wu, C.; Deal, K. A.; Brechbiel, M. W.; Mirzadeh, S.; Gansow, O. A. *J. Med. Chem.* **1998**, *41* (18), 3546.
(37) Broan, C. J.; Cox, J. P. L.; Craig, A. S.; Kataky, R.; Parker, D.; Harrison, A.; Randall, A.; Ferguson, G. *J. Chem. Soc., Perkin Trans. 2* **1991**, (1), 87.
(38) Achour, B.; Costa, J.; Delgado, R.; Garrigues, E.; Geraldes, C. F. G. C.; Korber, N.; Nepveu, F.; Prata, M. I. *Inorg. Chem.* **1998**, *37* (25), 6552.
(39) Pulukkody, K. P.; Norman, T. J.; Parker, D.; Royle, L.; Broan, C. J. *J. Chem. Soc., Perkin Trans. 2* **1993**, (4), 605.
(40) Rae, T. D.; Schmidt, P. J.; Pufahl, R. A.; Culotta, V. C.; O'Halloran, T. V. *Science* **1999**, *284* (5415), 805.
(41) Kim, B.-E.; Nevitt, T.; Thiele, D. J. *Nat. Chem. Biol.* **2008**, *4* (3), 176.
(42) Arnesano, F.; Banci, L.; Bertini, I.; Ciofi-Baffoni, S. *Eur. J. Inorg. Chem.* **2004**, *8*, 1583.
(43) Rosenzweig, A. C. *Acc. Chem. Res.* **2001**, *34* (2), 119.
(44) Perk, L. R.; Visser, G. W. M.; Vosjan, M. J. W. D.; Stigter-van Walsum, M.; Tijink, B. M.; Leemans, C. R.; van Dongen, G. A. M. S. *J. Nucl. Med.* **2005**, *46* (11), 1898.
(45) Perk, L. R.; Visser, O. J.; Stigter-Van Walsum, M.; Vosjan, M. J. W. D.; Visser, G. W. M.; Zijlstra, J. M.; Huijgens, P. C.; Dongen, G. A. M. S. *Eur. J. Nucl. Med. Mol. Imaging* **2006**, *33* (11), 1337.
(46) Harris, W. R.; Pecoraro, V. L. *Biochemistry* **1983**, *22* (2), 292.
(47) Liu, S.; Pietryka, J.; Ellars, C. E.; Edwards, D. S. *Bioconjugate Chem.* **2002**, *13* (4), 902.
(48) Boswell, C. A.; McQuade, P.; Weisman, G. R.; Wong, E. H.; Anderson, C. J. *Nucl. Med. Biol.* **2005**, *32* (1), 29.
(49) Jalilian, A. R.; Rowshanfarzad, P.; Sabet, M.; Kamalidehlghan, M.; Mirzaii, M.; Rajamand, A. A. *Maj. Ulum va Funun-i Hastah-i* **2005**, *33*, 1.
(50) Cordero, B.; Gomez, V.; Platero-Prats, A. E.; Reves, M.; Echeverria, J.; Cremades, E.; Barragan, F.; Alvarez, S. *Dalton Trans.* **2008**, *21*, 2832.
(51) Pasquarello, A.; Petri, I.; Salmon, P. S.; Parisel, O.; Car, R.; Toth, E.; Powell, D. H.; Fischer, H. E.; Helm, L.; Merbach, A. E. *Science* **2001**, *291* (5505), 856.
(52) Mukherjee, R. Copper. In *Comprehensive Coordination Chemistry II: Transition Metal Groups 7 and 8*; Constable, E. C., Dilworth, J., Eds.; Elsevier Limited: San Diego, CA, 2004; Vol. 6, p 747.
(53) Cabbiness, D. K.; Margerum, D. W. *J. Am. Chem. Soc.* **1969**, *91* (23), 6540.
(54) Bencini, A.; Bianchi, A.; Paoletti, P.; Paoli, P. *Coord. Chem. Rev.* **1992**, *120* (1), 51.
(55) Curtis, N. F. Nitrogen Ligands. In *Comprehensive Coordination Chemistry II: Fundamentals*; Constable, E. C., Dilworth, J., Eds.; Elsevier Limited: San Diego, CA, 2004; Vol. 1, p 447.
(56) Liang, X.; Sadler, P. J. *Chem. Soc. Rev.* **2004**, *33* (4), 246.
(57) Delgado, R.; Felix, V.; Lima, L. M. P.; Price, D. W. *Dalton Trans.* **2007**, *26*, 2734.
(58) Hall, M. D.; Hambley, T. W. *Coord. Chem. Rev.* **2002**, *232* (1−2), 49.
(59) Fry, F. H.; Jacob, C. *Curr. Pharm. Des.* **2006**, *12* (34), 4479.
(60) Hall, M. D.; Failes, T. W.; Yamamoto, N.; Hambley, T. W. *Dalton Trans.* **2007**, *36*, 3983.
(61) Reisner, E.; Arion, V. B.; Keppler, B. K.; Pombeiro, A. J. L. *Inorg. Chim. Acta* **2008**, *361* (6), 1569.
(62) Obata, A.; Yoshimi, E.; Waki, A.; Lewis, J. S.; Oyama, N.; Welch, M. J.; Saji, H.; Yonekura, Y.; Fujibayashi, Y. *Ann. Nucl. Med.* **2001**, *15* (6), 499.
(63) Vavere, A. L.; Lewis, J. S. *Dalton Trans.* **2007**, (43), 4893.
(64) Holland, J. P.; Barnard, P. J.; Collison, D.; Dilworth, J. R.; Edge, R.; Green, J. C.; McInnes, E. J. L. *Chem.—Eur. J.* **2008**, *14* (19), 5890.
(65) Holland, J. P.; Giansiracusa, J. H.; Bell, S. G.; Wong, L.-L.; Dilworth, J. R. *Phys. Med. Biol.* **2009**, *54* (7), 2103.
(66) Holland, J. P.; Hickin, J. A.; Grenville-Mathers, E.; Nguyen, T. N.; Peach, J. M. *J. Chem. Res.* **2008**, *12*, 702.
(67) Heroux, K. J.; Woodin, K. S.; Tranchemontagne, D. J.; Widger, P. C. B.; Southwick, E.; Wong, E. H.; Weisman, G. R.; Tomellini, S. A.; Wadas, T. J.; Anderson, C. J.; Kassel, S.; Golen, J. A.; Rheingold, A. L. *Dalton Trans.* **2007**, (21), 2150.
(68) Dhungana, S.; Taboy, C. H.; Zak, O.; Larvie, M.; Crumbliss, A. L.; Aisen, P. *Biochemistry* **2004**, *43* (1), 205.
(69) Mies, K. A.; Wirgau, J. I.; Crumbliss, A. L. *BioMetals* **2006**, *19* (2), 115.
(70) Bakaj, M.; Zimmer, M. *J. Mol. Struct.* **1999**, *508* (1−3), 59.
(71) Kaden, T. A. Functional tetraazamacrocycles: Ligands with many aspects. In *Advances in Supramolecular Chemistry*; Gokel, G. W., Ed.; Elsevier Limited: San Diego, CA, 1993; Vol. 3, p 65.
(72) Bridger, G. J.; Skerlj, R. T.; Padmanabhan, S.; Thornton, D. *J. Org. Chem.* **1996**, *61* (4), 1519.
(73) Meyer, M.; Dahaoui-Gindrey, V.; Lecomte, C.; Guilard, R. *Coord. Chem. Rev.* **1998**, *178−180* (2), 1313.
(74) Guilard, R.; Bessmertnykh, A. G.; Beletskaya, I. P. *Synlett* **1997**, *10*, 1190.
(75) Konig, B.; Pelka, M.; Klein, M.; Dix, I.; Jones, P. G.; Lex, J. *J. Inclusion Phenom. Macrocyclic Chem.* **2000**, *37* (1−4), 39.
(76) Kaden, T. A. *Chimia* **2000**, *54* (10), 574.
(77) Lewis, E. A.; Allan, C. C.; Boyle, R. W.; Archibald, S. J. *Tetrahedron Lett.* **2004**, *45* (15), 3059.
(78) Massue, J.; Plush, S. E.; Bonnet, C. S.; Moore, D. A.; Gunnlaugsson, T. *Tetrahedron Lett.* **2007**, *48* (45), 8052.
(79) Suchy, M.; Hudson, R. H. E. *Eur. J. Org. Chem.* **2008**, *29*, 4847.
(80) Bharadwaj, P. K.; Potenza, J. A.; Schugar, H. J. *J. Am. Chem. Soc.* **1986**, *108* (6), 1351.
(81) Holland, J. P.; Barnard, P. J.; Collison, D.; Dilworth, J. R.; Edge, R.; Green, J. C.; Heslop, J. M.; McInnes, E. J. L.; Salzmann, C. G.; Thompson, A. L. *Eur. J. Inorg. Chem.* **2008**, *22*, 3549.

(82) Bu, X. H.; Zhang, Z. H.; An, D. L.; Chen, Y. T.; Shionoya, M.; Kimura, E. *Inorg. Chim. Acta* **1996**, *249* (1), 125.
(83) Polyakova, I. N.; Poznyak, A. L.; Sergienko, V. S. *Kristallografiya* **2000**, *45* (1), 41.
(84) Fomenko, V. V.; Polynova, T. N.; Porai-Koshits, M. A.; Varlamova, G. L.; Pechurova, N. I. *Zh. Strukt. Khim.* **1973**, *14* (3), 571.
(85) Borzel, H.; Comba, P.; Hagen, K. S.; Katsichtis, C.; Pritzkow, H. *Chem.—Eur. J.* **2000**, *6* (5), 914.
(86) Juran, S.; Walther, M.; Stephan, H.; Bergmann, R.; Steinbach, J.; Kraus, W.; Emmerling, F.; Comba, P. *Bioconjugate Chem.* **2009**, *20* (2), 347.
(87) Park, G.; Dadachova, E.; Przyborowska, A.; Lai, S.-j.; Ma, D.; Broker, G.; Rogers, R. D.; Planalp, R. P.; Brechbiel, M. W. *Polyhedron* **2001**, *20* (26−27), 3155.
(88) Ma, D.; Lu, F.; Overstreet, T.; Milenic, D. E.; Brechbiel, M. W. *Nucl. Med. Biol.* **2002**, *29* (1), 91.
(89) Siegfried, L.; Kaden, T. A. *Dalton Trans.* **2005**, (6), 1136.
(90) Papini, G.; Alidori, S.; Lewis, J. S.; Reichert, D. E.; Pellei, M.; Gioia Lobbia, G.; Biddlecombe, G. B.; Anderson, C. J.; Santini, C. *Dalton Trans.* **2009**, (1), 177.
(91) Kreher, U.; Hearn, M. T. W.; Moubaraki, B.; Murray, K. S.; Spiccia, L. *Polyhedron* **2007**, *26* (13), 3205.
(92) Wieghardt, K.; Bossek, U.; Chaudhuri, P.; Herrmann, W.; Menke, B. C.; Weiss, J. *Inorg. Chem.* **1982**, *21* (12), 4308.
(93) Pavlishchuk, V.; Birkelbach, F.; Weyhermueller, T.; Wieghardt, K.; Chaudhuri, P. *Inorg. Chem.* **2002**, *41* (17), 4405.
(94) Packard, A. B.; Kronauge, J. F.; Day, P. J.; Treves, S. T. *Nucl. Med. Biol.* **1998**, *25* (6), 531.
(95) Packard, A. B.; Kronauge, J. F.; Barbarics, E.; Kiani, S.; Treves, S. T. *Nucl. Med. Biol.* **2002**, *29* (3), 289.
(96) Kiani, S.; Staples, R. J.; Ted Treves, S.; Packard, A. B. *Polyhedron* **2009**, *28* (4), 775.
(97) Kiani, S.; Staples, R. J.; Packard, A. B. *Acta Crystallogr., Sect. C* **2002**, *C58* (12), m593.
(98) Walker, P. S.; Bergin, P. M.; Grossel, M. C.; Horton, P. N. *Inorg. Chem.* **2004**, *43* (14), 4145.
(99) Motekaitis, R. J.; Sun, Y.; Martell, A. E.; Welch, M. J. *Can. J. Chem.* **1999**, *77* (5−6), 614.
(100) Barnard, P. J.; Holland, J. P.; Bayly, S. R.; Wadas, T. J.; Anderson, C. J.; Dilworth, J. R. *Inorg. Chem.* **2009**, *48* (15), 7117.
(101) Riesen, A.; Zehnder, M.; Kaden, T. A. *Helv. Chim. Acta* **1986**, *69* (8), 2067.
(102) Kumar, K.; Tweedle, M. F.; Malley, M. F.; Gougoutas, J. Z. *Inorg. Chem.* **1995**, *34* (26), 6472.
(103) Sun, X.; Wuest, M.; Kovacs, Z.; Sherry, A. D.; Motekaitis, R.; Wang, Z.; Martell, A. E.; Welch, M. J.; Anderson, C. J. *J. Biol. Inorg. Chem.* **2003**, *8* (1−2), 217.
(104) Kalman, F. K.; Baranyai, Z.; Toth, I.; Banyai, I.; Kiraly, R.; Bruecher, E.; Aime, S.; Sun, X.; Sherry, A. D.; Kovacs, Z. *Inorg. Chem.* **2008**, *47* (9), 3851.
(105) Aneetha, H.; Lai, Y.-H.; Lin, S.-C.; Panneerselvam, K.; Lu, T.-H.; Chung, C.-S. *J. Chem. Soc., Dalton Trans.* **1999**, *16*, 2885.
(106) Tonei, D. M.; Ware, D. C.; Brothers, P. J.; Plieger, P. G.; Clark, G. R. *Dalton Trans.* **2006**, *1*, 152.
(107) Chapman, J.; Ferguson, G.; Gallagher, J. F.; Jennings, M. C.; Parker, D. *J. Chem. Soc., Dalton Trans.* **1992**, *3*, 345.
(108) Silversides, J. D.; Allan, C. C.; Archibald, S. J. *Dalton Trans.* **2007**, *9*, 971.
(109) Moi, M. K.; Yanuck, M.; Deshpande, S. V.; Hope, H.; DeNardo, S. J.; Meares, C. F. *Inorg. Chem.* **1987**, *26* (21), 3458.
(110) Sprague, J. E.; Peng, Y.; Fiamengo, A. L.; Woodin, K. S.; Southwick, E. A.; Weisman, G. R.; Wong, E. H.; Golen, J. A.; Rheingold, A. L.; Anderson, C. J. *J. Med. Chem.* **2007**, *50* (10), 2527.
(111) Wong, E. H.; Weisman, G. R.; Hill, D. C.; Reed, D. P.; Rogers, M. E.; Condon, J. P.; Fagan, M. A.; Calabrese, J. C.; Lam, K.-C.; Guzei, I. A.; Rheingold, A. L. *J. Am. Chem. Soc.* **2000**, *122* (43), 10561.
(112) Woodin, K. S.; Heroux, K. J.; Boswell, C. A.; Wong, E. H.; Weisman, G. R.; Niu, W.; Tomellini, S. A.; Anderson, C. J.; Zakharov, L. N.; Rheingold, A. L. *Eur. J. Inorg. Chem.* **2005**, *23*, 4829.
(113) Lewis, E. A.; Boyle, R. W.; Archibald, S. J. *Chem. Commun.* **2004**, *19*, 2212.
(114) Kotek, J.; Lubal, P.; Hermann, P.; Cisarova, I.; Lukes, I.; Godula, T.; Svobodova, I.; Taborsky, P.; Havel, J. *Chem.—Eur. J.* **2003**, *9* (1), 233.
(115) Boswell, C. A.; Regino, C. A. S.; Baidoo, K. E.; Wong, K. J.; Milenic, D. E.; Kelley, J. A.; Lai, C. C.; Brechbiel, M. W. *Bioorg. Med. Chem.* **2009**, *17* (2), 548.
(116) Sargeson, A. M. *Pure Appl. Chem.* **1986**, *58* (11), 1511.
(117) Bottomley, G. A.; Clark, I. J.; Creaser, I. I.; Engelhardt, L. M.; Geue, R. J.; Hagen, K. S.; Harrowfield, J. M.; Lawrance, G. A.; Lay, P. A. *Aust. J. Chem.* **1994**, *47* (1), 143.
(118) Bernhardt, P. V.; Bramley, R.; Engelhardt, L. M.; Harrowfield, J. M.; Hockless, D. C. R.; Korybut-Daszkiewicz, B. R.; Krausz, E. R.; Morgan, T.; Sargeson, A. M. *Inorg. Chem.* **1995**, *34* (14), 3589.
(119) Di Bartolo, N. M.; Sargeson, A. M.; Donlevy, T. M.; Smith, S. V. *J. Chem. Soc., Dalton Trans.* **2001**, *15*, 2303.
(120) Voss, S. D.; Smith, S. V.; DiBartolo, N.; McIntosh, L. J.; Cyr, E. M.; Bonab, A. A.; Dearling, J. L. J.; Carter, E. A.; Fischman, A. J.; Treves, S. T.; Gillies, S. D.; Sargeson, A. M.; Huston, J. S.; Packard, A. B. *Proc. Natl. Acad. Sci. U. S. A.* **2007**, *104* (44), 17489.
(121) Smith, S. V. Q. J. *Nucl. Med. Mol. Imaging* **2008**, *52* (2), 193.
(122) Cai, W.; Guzman, R.; Hsu, A. R.; Wang, H.; Chen, K.; Sun, G.; Gera, A.; Choi, R.; Bliss, T.; He, L.; Li, Z.-B.; Maag, A.-L. D.; Hori, N.; Zhao, H.; Moseley, M.; Steinberg, G. K.; Chen, X. *Stroke* **2009**, *40* (1), 270.
(123) Cai, H.; Fissekis, J.; Conti, P. S. *Dalton Trans.* **2009**, (27), 5395.
(124) Ma, M. T.; Karas, J. A.; White, J. M.; Scanlon, D.; Donnelly, P. S. *Chem. Commun.* **2009**, *22*, 3237.
(125) Donnelly, P. S.; Harrowfield, J. M.; Skelton, B. W.; White, A. H. *Inorg. Chem.* **2001**, *40* (22), 5645.
(126) Donnelly, P. S.; Harrowfield, J. M.; Skelton, B. W.; White, A. H. *Inorg. Chem.* **2000**, *39* (25), 5817.
(127) Bandoli, G.; Dolmella, A.; Tisato, F.; Porchia, M.; Refosco, F. *Coord. Chem. Rev.* **2009**, *253* (1 + 2), 56.
(128) Harris, W. R.; Chen, Y.; Wein, K. *Inorg. Chem.* **1994**, *33* (22), 4991.
(129) Jarjayes, O.; Mortini, F.; du Moulinet d'Hardemare, A.; Philouze, C.; Serratrice, G. *Eur. J. Inorg. Chem.* **2005**, *21*, 4417.
(130) Motekaitis, R. J.; Martell, A. E.; Koch, S. A.; Hwang, J.; Quarless, D. A., Jr.; Welch, M. J. *Inorg. Chem.* **1998**, *37* (22), 5902.
(131) Francesconi, L. C.; Liu, B. L.; Billings, J. J.; Carroll, P. J.; Graczyk, G.; Kung, H. F. *J. Chem. Soc., Chem. Commun.* **1991**, *2*, 94.
(132) Zheng, Y. Y.; Saluja, S.; Yap, G. P. A.; Blumenstein, M.; Rheingold, A. L.; Francesconi, L. C. *Inorg. Chem.* **1996**, *35* (23), 6656.
(133) Li, Y.; Martell, A. E.; Hancock, R. D.; Reibenspies, J. H.; Anderson, C. J.; Welch, M. J. *Inorg. Chem.* **1996**, *35* (2), 404.
(134) Jung, W.-S.; Chung, Y. K.; Shin, D. M.; Kim, S.-D. *Bull. Chem. Soc. Jpn.* **2002**, *75* (6), 1263.
(135) Ma, R.; Motekaitis, R. J.; Martell, A. E. *Inorg. Chim. Acta* **1994**, *224* (1−2), 151.
(136) Schuhmacher, J.; Kaul, S.; Klivenyi, G.; Junkermann, H.; Magener, A.; Henze, M.; Doll, J.; Haberkorn, U.; Amelung, F.; Bastert, G. *Cancer Res.* **2001**, *61* (9), 3712.
(137) Eder, M.; Waengler, B.; Knackmuss, S.; LeGall, F.; Little, M.; Haberkorn, U.; Mier, W.; Eisenhut, M. *Eur. J. Nucl. Med. Mol. Imaging* **2008**, *35* (10), 1878.
(138) Ma, R.; Murase, I.; Martell, A. E. *Inorg. Chim. Acta* **1994**, *223* (1−2), 109.
(139) Wong, E.; Caravan, P.; Liu, S.; Rettig, S. J.; Orvig, C. *Inorg. Chem.* **1996**, *35* (3), 715.
(140) Blend, M. J.; Stastny, J. J.; Swanson, S. M.; Brechbiel, M. W. *Cancer Biother. Radiopharm.* **2003**, *18* (3), 355.
(141) Wei, L.; Zhang, X.; Gallazzi, F.; Miao, Y.; Jin, X.; Brechbiel, M. W.; Xu, H.; Clifford, T.; Welch, M. J.; Lewis, J. S.; Quinn, T. P. *Nucl. Med. Biol.* **2009**, *36* (4), 345.
(142) Tsang, B. W.; Mathias, C. J.; Fanwick, P. E.; Green, M. A. *J. Med. Chem.* **1994**, *37* (25), 4400.
(143) Sharma, V.; Beatty, A.; Wey, S. P.; Dahlheimer, J.; Pica, C. M.; Crankshaw, C. L.; Bass, L.; Green, M. A.; Welch, M. J.; Piwnica-Worms, D. *Chem. Biol.* **2000**, *7* (5), 335.
(144) Hsiao, Y.-M.; Mathias, C. J.; Wey, S.-P.; Fanwick, P. E.; Green, M. A. *Nucl. Med. Biol.* **2009**, *36* (1), 39.
(145) Martell, A. E.; Motekaitis, R. J.; Clarke, E. T.; Delgado, R.; Sun, Y.; Ma, R. *Supramol. Chem.* **1996**, *6* (3−4), 353.
(146) Moore, D. A.; Fanwick, P. E.; Welch, M. J. *Inorg. Chem.* **1990**, *29* (4), 672.
(147) Clarke, E. T.; Martell, A. E. *Inorg. Chim. Acta* **1991**, *181* (2), 273.
(148) Prata, M. I. M.; Santos, A. C.; Geraldes, C. F. G. C.; Lima, J. J. P. d. *Nucl. Med. Biol.* **1999**, *26* (6), 707.
(149) McMurry, T. J.; Brechbiel, M. W.; Wu, C.; Gansow, O. A. *Bioconjugate Chem.* **1993**, *4* (3), 236.
(150) Cox, J. P. L.; Craig, A. S.; Helps, I. M.; Jankowski, K. J.; Parker, D.; Eaton, M. A. W.; Millican, A. T.; Millar, K.; Beeley, N. R. A.; Boyce, B. A. *J. Chem Soc., Perkin Trans 1* **1999**, 2567.
(151) Studer, M.; Meares, C. F. *Bioconjugate Chem.* **1992**, *34* (4), 3691.
(152) Brechbiel, M. W.; McMurry, T. J.; Gansow, O. A. *Tetrahedron Lett.* **1993**, *34* (23), 3691.
(153) Andre, J. P.; Macke, H. R.; Zehnder, M.; Macko, L.; Acyel, K. G. *Chem. Commun.* **1998**, *12*, 1301.
(154) Eisenwiener, K.-P.; Prata, M. I. M.; Buschmann, I.; Zhang, H.-W.; Santos, A. C.; Wenger, S.; Reubi, J. C.; Maecke, H. R. *Bioconjugate Chem.* **2002**, *13* (3), 530.
(155) Viola, N. A.; Rarig, R. S.; Ouellette, W.; Doyle, R. P. *Polyhedron* **2006**, *25* (18), 3457.

(156) Heppeler, A.; Andre, J. P.; Buschmann, I.; Wang, X.; Reubi, J.-C.; Hennig, M.; Kaden, T. A.; Maecke, H. R. *Chem.—Eur. J.* **2008**, *14* (10), 3026.
(157) Heppeler, A.; Froidevaux, S.; Macke, H. R.; Jermann, E.; Behe, M.; Powell, P.; Hennig, M. *Chem.—Eur. J.* **1999**, *5* (7), 1974.
(158) Yang, C.-T.; Li, Y.; Liu, S. *Inorg. Chem.* **2007**, *46* (21), 8988.
(159) Fani, M.; Andre, J. P.; Maecke, H. R. *Contrast Media Mol. Imaging* **2008**, *3* (2), 67.
(160) Clarke, E. T.; Martell, A. E. *Inorg. Chim. Acta* **1991**, *190* (1), 37.
(161) Decristoforo, C.; Petrik, M.; von Guggenberg, E.; Carlsen, J.; Huisman, M.; Wester, H.-J.; Virgolini, I.; Haubner, R. *J. Lab. Compd. Radiopharm.* **2007**, *50*, S23.
(162) Niu, W.; Wong, E. H.; Weisman, G. R.; Peng, Y.; Anderson, C. J.; Zakharov, L. N.; Golen, J. A.; Rheingold, A. L. *Eur. J. Inorg. Chem.* **2004**, *16*, 3310.
(163) Terova, O. Synthesis, Characterization and Inertness Studies of Gallium(III) and Indium(III) Complexes of Dicarboxymethyl Pendant-armed Cross-bridged Cyclam. MS Thesis, University of New Hampshire, Durham, NH, 2008.
(164) Ward, M. C.; Roberts, K. R.; Babich, J. W.; Bukhari, M. A.; Coghlan, G.; Westwood, J. H.; McCready, V. R.; Ott, R. J. *Int. J. Radiat. Appl. Instrum. B.* **1986**, *13* (5), 505.
(165) Smith-Jones, P. M.; Stolz, B.; Bruns, C.; Albert, R.; Reist, H. W.; Fridrich, R.; Mäcke, H. R. *J. Nucl. Med.* **1994**, *35* (2), 317.
(166) Mathias, C. J.; Lewis, M. R.; Reichert, D. E.; Laforest, R.; Sharp, T. L.; Lewis, J. S.; Yang, Z.-F.; Waters, D. J.; Snyder, P. W.; Low, P. S.; Welch, M. J.; Green, M. A. *Nucl. Med. Biol.* **2003**, *30* (7), 725.
(167) Govindan, S. V.; Michel, R. B.; Griffiths, G. L.; Goldenberg, D. M.; Mattes, M. J. *Nucl. Med. Biol.* **2005**, *32* (5), 513.
(168) Ye, Y.; Liu, M.; Kao, J. L. F.; Marshall, G. R. *Biopolymers* **2006**, *84* (5), 472.
(169) Banin, E.; Lozinski, A.; Brady, K. M.; Berenshtein, E.; Butterfield, P. W.; Moshe, M.; Chevion, M.; Greenberg, E. P.; Banin, E. *Proc. Natl. Acad. Sci. U.S.A.* **2008**, *105* (43), 16761.
(170) Borgias, B.; Hugi, A. D.; Raymond, K. N. *Inorg. Chem.* **1989**, *28* (18), 3538.
(171) Borgias, B. A.; Barclay, S. J.; Raymond, K. N. *J. Coord. Chem.* **1986**, *15* (2), 109.
(172) Motekaitis, R. J.; Sun, Y.; Martell, A. E. *Inorg. Chem.* **1991**, *30* (7), 1554.
(173) Rose, D. J.; Zubieta, J.; Fischman, A. J.; Hillier, S.; Babich, J. W. *Inorg. Chem. Commun.* **1998**, *1* (5), 164.
(174) Ilyukhin, A. B.; Malyarik, M. A.; Petrosyants, S. P.; Davidovich, R. L.; Samsonova, I. N. *Zh. Neorg. Khim.* **1995**, *40* (7), 1125.
(175) Ilyukhin, A. B.; Malyarik, M. A.; Porai-Koshits, M. A.; Davidovich, R. L.; Logvinova, V. B. *Kristallografiya* **1995**, *40* (4), 656.
(176) Maecke, H. R.; Riesen, A.; Ritter, W. *J. Nucl. Med.* **1989**, *30* (7), 1235.
(177) Parker, D.; Pulukkody, K.; Smith, F. C.; Batsanov, A.; Howard, J. A. K. *J. Chem. Soc., Dalton Trans.* **1994**, *5*, 689.
(178) Hsieh, W.-Y.; Liu, S. *Inorg. Chem.* **2004**, *43* (19), 6006.
(179) Craig, A. S.; Helps, I. M.; Parker, D.; Adams, H.; Bailey, N. A.; Williams, M. G.; Smith, J. M. A.; Ferguson, G. *Polyhedron* **1989**, *8* (20), 2481.
(180) Matthews, R. C.; Parker, D.; Ferguson, G.; Kaitner, B.; Harrison, A.; Royle, L. *Polyhedron* **1991**, *10* (16), 1951.
(181) Cole, E.; Copley, R. C. B.; Howard, J. A. K.; Parker, D.; Ferguson, G.; Gallagher, J. F.; Kaitner, B.; Harrison, A.; Royle, L. *J. Chem. Soc., Dalton Trans.* **1994**, *11*, 1619.
(182) Bossek, U.; Hanke, D.; Wieghardt, K.; Nuber, B. *Polyhedron* **1993**, *12* (1), 1.
(183) Clarke, E. T.; Martell, A. E. *Inorg. Chim. Acta* **1991**, *186* (1), 103.
(184) Liu, S.; He, Z.; Hsieh, W.-Y.; Fanwick, P. E. *Inorg. Chem.* **2003**, *42* (26), 8831.
(185) Riesen, A.; Kaden, T. A.; Ritter, W.; Maecke, H. R. *J. Chem. Soc., Chem. Commun.* **1989**, *8*, 460.
(186) Clarke, E. T.; Martell, A. E. *Inorg. Chim. Acta* **1991**, *190* (1), 27.
(187) Moerlein, S. M.; Welch, M. J. *Int. J. Nucl. Med. Biol.* **1981**, *8* (4), 277.
(188) Mistryukov, V. E.; Sergeev, A. V.; Chuklanova, E. B.; Mikhailov, Y. N.; Shchelokov, R. N. *Zh. Neorg. Khim.* **1997**, *42* (6), 969.
(189) Wang, J.; Zhao, J.; Zhang, X.; Gao, J. *Rare Met.* **2000**, *19* (4), 241.
(190) Amin, S.; Marks, C.; Toomey, L. M.; Churchill, M. R.; Morrow, J. R. *Inorg. Chim. Acta* **1996**, *246* (1−2), 99.
(191) Chang, C. A.; Francesconi, L. C.; Malley, M. F.; Kumar, K.; Gougoutas, J. Z.; Tweedle, M. F.; Lee, D. W.; Wilson, L. J. *Inorg. Chem.* **1993**, *32* (16), 3501.
(192) Vojtisek, P.; Cigler, P.; Kotek, J.; Rudovsky, J.; Hermann, P.; Lukes, I. *Inorg. Chem.* **2005**, *44* (16), 5591.
(193) Corneillie, T. M.; Fisher, A. J.; Meares, C. F. *J. Am. Chem. Soc.* **2003**, *125* (49), 15039.
(194) Schlesinger, J.; Koezle, I.; Bergmann, R.; Tamburini, S.; Bolzati, C.; Tisato, F.; Noll, B.; Klussmann, S.; Vonhoff, S.; Wuest, F.; Pietzsch, H.-J.; Steinbach, J. *Bioconjugate Chem.* **2008**, *19* (4), 928.
(195) Kodama, M.; Koike, T.; Mahatma, A. B.; Kimura, E. *Inorg. Chem.* **1991**, *30* (6), 1270.
(196) Cox, J. P. L.; Jankowski, K. J.; Kataky, R.; Parker, D.; Beeley, N. R. A.; Boyce, B. A.; Eaton, M. A. W.; Millar, K.; Millican, A. T. *J. Chem. Soc., Chem. Commun.* **1989**, *12*, 797.
(197) Spirlet, M. R.; Rebizant, J.; Loncin, M. F.; Desreux, J. F. *Inorg. Chem.* **1984**, *23* (25), 4278.
(198) Kang, J.-G.; Na, M.-K.; Yoon, S.-K.; Sohn, Y.; Kim, Y.-D.; Suh, I.-H. *Inorg. Chim. Acta* **2000**, *310* (1), 56.
(199) Maecke, H. R.; Scherer, G.; Heppeler, A.; Henig, M. *Eur. J. Nucl. Med.* **2001**, *28*, 967.
(200) Onthank, D. C.; Liu, S.; Silva, P. J.; Barrett, J. A.; Harris, T. D.; Robinson, S. P.; Edwards, D. S. *Bioconjugate Chem.* **2004**, *15* (2), 235.
(201) Liu, S.; Edwards, D. S. *Bioconjugate Chem.* **2001**, *12* (4), 630.
(202) Singhal, A.; Toth, L. M.; Lin, J. S.; Affholter, K. *J. Am. Chem. Soc.* **1996**, *118* (46), 11529.
(203) Ekberg, C.; Kaellvenius, G.; Albinsson, Y.; Brown, P. L. *J. Solution Chem.* **2004**, *33* (1), 47.
(204) Pozhidaev, A. I.; Porai-Koshits, M. A.; Polynova, T. N. *Zh. Strukt. Khim.* **1974**, *15* (4), 644.
(205) Davidovich, R. L.; Logvinova, V. B.; Teplukhina, L. V. *Koord. Khim.* **1992**, *18* (6), 580.
(206) Meijs, W. E.; Herscheid, J. D. M.; Haisma, H. J.; Pinedo, H. M. *Appl. Radiat. Isot.* **1992**, *43* (12), 1443.
(207) Takahashi, A.; Yamaguchi, H.; Igarashi, S. *Bunseki Kagaku* **1997**, *46* (1), 55.
(208) Verel, I.; Visser, G. W. M.; Boellaard, R.; Boerman, O. C.; van Eerd, J.; Snow, G. B.; Lammertsma, A. A.; van Dongen, G. A. M. S. *J. Nucl. Med.* **2003**, *44* (10), 1663.
(209) Boerjesson, P. K. E.; Jauw, Y. W. S.; Boellaard, R.; de Bree, R.; Comans, E. F. I.; Roos, J. C.; Castelijns, J. A.; Vosjan, M. J. W. D.; Kummer, J. A.; Leemans, C. R.; Lammertsma, A. A.; van Dongen, G. A. M. S. *Clin. Cancer Res.* **2006**, *12* (1), 2133.
(210) Nagengast, W. B.; de Vries, E. G.; Hospers, G. A.; Mulder, N. H.; de Jong, J. R.; Hollema, H.; Brouwers, A. H.; van Dongen, G. A.; Perk, L. R.; Lub-de-Hooge, M. N. *J. Nucl. Med.* **2007**, *48* (8), 1313.
(211) Datta, A.; Raymond, K. N. *Acc. Chem. Res.* **2009**, *42* (7), 938.
(212) Piel, H.; Qaim, S. M.; Stocklin, G. *Radiochim. Acta* **1992**, *57*, 1.
(213) Williams, H. A.; Robinson, S.; Julyan, P.; Zweit, J.; Hastings, D. *Eur. J. Nucl. Med. Mol. Imaging* **2005**, *32* (12), 1473.
(214) Fujibayashi, Y.; Matsumoto, K.; Yonekura, Y.; Konishi, J.; Yokayama, A. *J. Nucl. Med.* **1989**, *30* (11), 1838.
(215) Zweit, J.; Gordall, R.; Cox, M.; Babich, J. W.; Petter, G. A.; Sharma, H. L.; Ott, R. J. *Eur. J. Nucl. Med.* **1992**, *19* (6), 418.
(216) Haynes, N. G.; Lacy, J. L.; Nayak, N.; Martin, C. S.; Dai, D.; Mathias, C. J.; Green, M. A. *J. Nucl. Med.* **2000**, *41* (2), 309.
(217) Fukumura, T.; Okada, K.; Suzuki, H.; Nakao, R.; Mukai, K.; Szelecsenyi, F.; Kovacs, Z.; Suzuki, K. *Nucl. Med. Biol.* **2006**, *33* (6), 821.
(218) Rowshanfarzad, P.; Sabet, M.; Reza Jalilian, A.; Kamalidehghan, M. *Appl. Radiat. Isot.* **2006**, *64* (12), 1563.
(219) McCarthy, D. W.; Bass, L. A.; Cutler, P. D.; Shefer, R. E.; Klinkowstein, R. E.; Herrero, P.; Lewis, J. S.; Cutler, C. S.; Anderson, C. J.; Welch, M. J. *Nucl. Med. Biol.* **1999**, *26* (4), 351.
(220) Szelecsenyi, F.; Kovacs, Z.; Suzuki, K.; Okada, K.; Fukumura, T.; Mukai, K. *Nucl. Instrum. Methods Phys. Res., Sect. B* **2004**, *222* (3−4), 364.
(221) Fukumura, T.; Okada, K.; Szelecsenyi, F.; Kovacs, Z.; Suzuki, K. *Radiochim. Acta* **2004**, *92* (4−6), 209.
(222) Szelecsenyi, F.; Suzuki, K.; Kovacs, Z.; Takei, M.; Okada, K. *Nucl. Instrum. Methods Phys. Res., Sect. B* **2002**, *187* (2), 153.
(223) Novak-Hofer, I.; Schubiger, P. A. *Eur. J. Nucl. Med. Mol.Imaging* **2002**, *29* (6), 821.
(224) Schwarzbach, R.; Zimmermann, K.; Blauenstein, P.; Smith, A.; Schubiger, P. A. *Appl. Radiat. Isot.* **1995**, *46* (5), 329.
(225) Alekseev, I. E.; Darmograi, V. V.; Marchenkov, N. S. *Radiochemistry* **2005**, *47* (5), 502.
(226) Dasgupta, A. K.; Mausner, L. F.; Srivastava, S. C. *Appl. Radiat. Isot.* **1991**, *42*, 371.
(227) Kroger, L. A.; DeNardo, G. L.; Gumerlock, P. H.; Xiong, C. Y.; Winthrop, M. D.; Shi, X. B.; Mack, P. C.; Leshchinsky, T.; DeNardo, S. J. *Cancer Biother. Radiopharm.* **2001**, *16* (3), 213.
(228) Wun, T.; Kwon, D. S.; Tuscano, J. M. *BioDrugs* **2001**, *15* (3), 151.
(229) Zimmermann, K.; Gianollini, S.; Schubiger, P. A.; Novak-Hofer, I. *Nucl. Med. Biol.* **1999**, *26* (8), 943.
(230) Frier, M. *Mini-Rev. Med. Chem.* **2004**, *4* (1), 61.
(231) Zimmermann, K.; Grunberg, J.; Honer, M.; Ametamey, S.; August Schubiger, P.; Novak-Hofer, I. *Nucl. Med. Biol.* **2003**, *30* (4), 417.

(232) DeNardo, G. L.; DeNardo, S. J.; Kukis, D. L.; O'Donnell, R. T.; Shen, S.; Goldstein, D. S.; Kroger, L. A.; Salako, Q.; DeNardo, D. A.; Mirick, G. R.; Mausner, L. F.; Srivastava, S. C.; Meares, C. F. *Anticancer Res.* **1998**, *18*, 2779.
(233) O'Donnell, R. T.; DeNardo, G. L.; Kukis, D. L.; Lamborn, K. R.; Shen, S.; Yuan, A.; Goldstein, D. S.; Mirick, G. R.; DeNardo, S. J. *Clin. Cancer Res.* **1999**, *5* (10), 3330s.
(234) Mirick, G. R.; O'Donnell, R. T.; DeNardo, S. J.; Shen, S.; Meares, C. F.; DeNardo, G. L. *Nucl. Med. Biol.* **1999**, *26* (7), 841.
(235) O'Donnell, R. T.; DeNardo, G. L.; Kukis, D. L.; Lamborn, K. R.; Shen, S.; Yuan, A.; Goldstein, D. S.; Carr, C. E.; Mirick, G. R.; DeNardo, S. J. *J. Nucl. Med.* **1999**, *40* (12), 2014.
(236) Sun, X.; Anderson, C. J. *Methods Enzymol.* **2004**, *386*, 237.
(237) McCarthy, D. W.; Shefer, R. E.; Klinkowstein, R. E.; Bass, L. A.; Margenau, W. H.; Cutler, C. S.; Anderson, C. J.; Welch, M. J. *Nucl. Med. Biol.* **1997**, *24* (1), 35.
(238) McCarthy, D. W.; Shefer, R. F.; Klinkowstein, R. F.; Cutler, C. S.; Anderson, C. J.; Welch, M. J. *J. Labeled Compd. Radiopharm.* **1995**, *37* (9), 830.
(239) Kim, J. Y.; Park, H.; Lee, J. C.; Kim, K. M.; Lee, K. C.; Ha, H. J.; Choi, T. H.; An, G. I.; Cheon, G. J. *Appl. Radiat. Isot.* **2009**, *67* (7−8), 1190.
(240) Le, V. S.; Howse, J.; Zaw, M.; Pellegrini, P.; Katsifis, A.; Greguric, I.; Weiner, R. *Appl. Radiat. Isot.* **2009**, *67* (7−8), 1324.
(241) Hermanne, A.; Tarkanyi, F.; Takacs, S.; Kovalev, S. F.; Ignatyuk, A. *Nucl. Instrum. Methods Phys. Res., Sect. B* **2007**, *258* (2), 308.
(242) Hou, X.; Jacobsen, U.; Jorgensen, J. C. *Appl. Radiat. Isot.* **2002**, *57* (6), 773.
(243) Watanabe, S.; Iida, Y.; Suzui, N.; Katabuchi, T.; Ishii, S.; Kawachi, N.; Hanaoka, H.; Watanabe, S.; Matsuhashi, S.; Endo, K.; Ishioka, N. S. *J. Radioanal. Nucl. Chem.* **2009**, *280* (1), 199.
(244) Obata, A.; Kasamatsu, S.; McCarthy, D. W.; Welch, M. J.; Saji, H.; Yonekura, Y.; Fujibayashi, Y. *Nucl. Med. Biol.* **2003**, *30* (5), 535.
(245) Avila-Rodriguez, M. A.; Nye, J. A.; Nickles, R. J. *Appl. Radiat. Isot.* **2007**, *65* (10), 1115.
(246) Szajek, L. P.; Meyer, W.; Plascjak, P.; Eckleman, W. C. *Radiochim. Acta* **2005**, *93* (4), 239.
(247) Van So, L.; Pellegrini, P.; Katsifis, A.; Howse, J.; Greguric, I. *J. Radioanal. Nucl. Chem.* **2008**, *277* (2), 451.
(248) Spahn, I.; Coenen, H. H.; Qaim, S. M. *Radiochim. Acta* **2004**, *92* (3), 183.
(249) Hilgers, K.; Stoll, T.; Skakun, Y.; Coenen, H. H.; Qaim, S. M. *Appl. Radiat. Isot.* **2003**, *59* (5−6), 343.
(250) Abbas, K.; Kozempel, J.; Bonardi, M.; Groppi, F.; Alfarano, A.; Holzwarth, U.; Simonelli, F.; Hofman, H.; Horstmann, W.; Menapace, E.; Leseticky, L.; Gibson, N. *Appl. Radiat. Isot.* **2006**, *64* (9), 1001.
(251) Kozempel, J.; Abbas, K.; Simonelli, F.; Zampese, M.; Holzwarth, U.; Gibson, N.; Leseticky, L. *Radiochim. Acta* **2007**, *95* (2), 75.
(252) Hassanein, M. A.; El-Said, H.; El-Amir, M. A. *J. Radioanal. Nucl. Chem.* **2006**, *269* (1), 75.
(253) Little, F. E.; Lagunas-Solar, M. C. *Int. J. Appl. Radiat. Isot.* **1983**, *34* (3), 631.
(254) Nagame, Y.; Unno, M.; Nakahara, H.; Murakami, Y. *Int. J. Appl. Radiat. Isot.* **1978**, *29* (11), 615.
(255) Steyn, J.; Meyer, B. R. *Int. J. Appl. Radiat. Isot.* **1973**, *24* (7), 369.
(256) Naidoo, C.; van der Walt, T. N. *Appl. Radiat. Isot.* **2001**, *54* (6), 915.
(257) van der Meulen, N. P.; van der Walt, T. N. *Z. Naturforsch., B: Chem. Sci.* **2007**, *62* (3), 483.
(258) Nayak, D.; Lahiri, S. *Appl. Radiat. Isot.* **2001**, *54* (2), 189.
(259) Nayak, D.; Banerjee, A.; Lahiri, S. *Appl. Radiat. Isot.* **2007**, *65* (8), 891.
(260) Dacosta, A. C. A.; Lelite, S. G. F. *Biotechnol. Lett.* **1991**, *13*, 559.
(261) Yamamoto, F.; Tsukamoto, E.; Nakada, K.; Takei, T.; Zhao, S.; Asaka, M.; Tamaki, N. *Ann. Nucl. Med.* **2004**, *18* (6), 519.
(262) Lambrecht, R.; Sajjad, M. *Radiochim. Acta.* **1988**, *43* (1), 171.
(263) Mirzadeh, S.; Lambrecht, R. *J. Radioanal. Nucl. Chem.* **1996**, *202* (1−2), 7.
(264) Zhernosekov, K. P.; Filosofov, D. V.; Baum, R. P.; Aschoff, P.; Bihl, H.; Razbash, A. A.; Jahn, M.; Jennewein, M.; Rosch, F. *J. Nucl. Med.* **2007**, *48* (10), 1741.
(265) Velikyan, I.; Beyer, G. J.; Langstrom, B. *Bioconjugate Chem.* **2004**, *15* (3), 554.
(266) Breeman, W. A.; de Jong, M.; de Blois, E.; Bernard, B. F.; Konijnenberg, M.; Krenning, E. P. *Eur. J. Nucl. Med. Mol. Imaging* **2005**, *32* (4), 478.
(267) Azhdarinia, A.; Yang, D. J.; Chao, C.; Mourtada, F. *Nucl. Med. Biol.* **2007**, *34* (1), 121.
(268) Lewis, M. R.; Reichert, D. E.; Laforest, R.; Margenau, W. H.; Shefer, R. E.; Klinkowstein, R. E.; Hughey, B. J.; Welch, M. J. *Nucl. Med. Biol.* **2002**, *29* (6), 701.
(269) Lundqvist, H.; Tolmachev, V.; Bruskin, A.; Einarsson, L.; Malmborg, P. *Appl. Radiat. Isot.* **1995**, *46* (9), 859.
(270) Schlyer, D. J. Production of radionuclides in accelerators. In *Handbook of Radiopharmaceuticals: Radiochemistry and Applications*; Welch, M. J., Redvanly, C. S., Eds.; John Wiley & Sons Inc.: Hoboken, NJ, 2003; p 1.
(271) Lubberink, M.; Tolmachev, V.; Widstroem, C.; Bruskin, A.; Lundqvist, H.; Westlin, J.-E. *J. Nucl. Med.* **2002**, *43* (10), 1391.
(272) Tolmachev, V.; Bernhardt, P.; Forssell-Aronsson, E.; Lundqvist, H. *Nucl. Med. Biol.* **2000**, *27* (2), 183.
(273) Nortier, F. M.; Mills, S. J.; Steyn, G. F. *Appl. Radiat. Isot.* **1990**, *41* (12), 1201.
(274) Thakare, S. V.; Nair, G. C.; Chakrabarty, S.; Tomar, B. S. *J. Radioanal. Nucl. Chem.* **1999**, *242* (2), 537.
(275) Mukhopadhyay, B.; Lahiri, S.; Mukhopadhyay, K.; Ramaswami, A. *J. Radioanal. Nucl. Chem.* **2003**, *256* (2), 307.
(276) Shikano, K.; Katoh, M.; Shigematsu, T.; Yonezawa, H. *J. Radioanal. Nucl. Chem.* **1987**, *119* (6), 433.
(277) Lewis, J. S.; Laforest, R.; Lewis, M. R.; Anderson, C. J. *Cancer Biother. Radiopharm.* **2000**, *15* (6), 593.
(278) Casella, V. R.; Grant, P. M.; O'Brien, H. A., Jr. *Radiochim. Acta.* **1975**, *22* (1−2), 31.
(279) Claessens, R. A. M. J.; Janssen, A. G. M.; Van den Bosch, R. L. P.; De Goeij, J. J. M. *Dev. Nucl. Med.* **1986**, *10*, 46.
(280) Janssen, A. G. M.; Claessens, R. A. M. J.; Van den Bosch, R. L. P.; De Goeij, J. J. M. *Appl. Radiat. Isot.* **1986**, *37* (4), 297.
(281) Abbasi, I. A.; Zaidi, J. H.; Arif, M.; Waheed, S.; Subhani, M. S. *Radiochim. Acta.* **2006**, *94* (8), 381.
(282) Bray, L. A.; Wheelwright, E. J.; Wester, D. W.; Carson, K. J.; Elovich, R. J.; Shade, E. H.; Alexander, D. L.; Culley, G. E.; Atkin, S. D. *Radioact. Radiochem.* **1992**, *3* (4), 22.
(283) Hsieh, B. T.; Ting, G.; Hsieh, H. T.; Shen, L. H. *Radioact. Radiochem.* **1992**, *3* (4), 26.
(284) Happel, S.; Streng, R.; Vater, P.; Ensinger, W. *Radiat. Meas.* **2003**, *36* (1−6), 761.
(285) Rane, A. T.; Bhatki, K. S. *Anal. Chem.* **1966**, *38*, 1598.
(286) Kawashima, T. *Int. J. Appl. Radiat. Isot.* **1969**, *20* (11), 806.
(287) Suzuki, Y. *Int. J. Appl. Radiat. Isot.* **1964**, *15* (10), 599.
(288) Doering, R. F.; Tucker, W. D.; Stang, L. G. J. *J. Nucl. Med.* **1963**, *4*, 54.
(289) Chinol, M.; Hnatowich, D. J. *J. Nucl. Med.* **1987**, *28* (9), 1465.
(290) Skraba, W. J.; Arino, H.; Kramer, H. H. *Int. J. Appl. Radiat. Isot.* **1978**, *29* (2), 91.
(291) Chakravarty, R.; Pandey, U.; Manolkar, R. B.; Dash, A.; Venkatesh, M.; Pillai, M. R. A. *Nucl. Med. Biol.* **2008**, *35* (2), 245.
(292) Pal, S.; Chattopadhyay, S.; Das, M. K.; Sudersanan, M. *Appl. Radiat. Isot.* **2006**, *64* (12), 1521.
(293) Roesch, F.; Qaim, S. M.; Stoecklin, G. *Appl. Radiat. Isot.* **1993**, *44* (4), 677.
(294) Sadeghi, M.; Aboudzadeh, M.; Zali, A.; Mirzaii, M.; Bolourinovin, F. *Appl. Radiat. Isot.* **2009**, *67* (1), 7.
(295) Sadeghi, M.; Aboudzadeh, M.; Zali, A.; Mirzaii, M.; Bolourinovin, F. *Appl. Radiat. Isot.* **2008**, *67* (1), 7.
(296) Garmestani, K.; Milenic, D. E.; Plascjak, P. S.; Brechbiel, M. W. *Nucl. Med. Biol.* **2002**, *29* (5), 599.
(297) Park, L. S.; Szajek, L. P.; Wong, K. J.; Pascjak, P. S.; Garmestani, K.; Googins, S.; Eckelman, W. C.; Carrasquillo, J. A.; Paik, C. H. *Nucl. Med. Biol.* **2004**, *31* (2), 297.
(298) Reischl, G.; Rosch, F.; Machulla, H. J. *Radiochim. Acta* **2002**, *90* (4), 225.
(299) Yoo, J.; Tang, L.; Perkins Todd, A.; Rowland Douglas, J.; Laforest, R.; Lewis Jason, S.; Welch Michael, J. *Nucl. Med. Biol.* **2005**, *32* (8), 891.
(300) Lukic, D.; Tamburella, C.; Buchegger, F.; Beyer, G.-J.; Comor Jozef, J.; Seimbille, Y. *Appl. Radiat. Isot.* **2009**, *67* (4), 523.
(301) Saha, G. B.; Porile, N. T.; Yaffe, L. *Phys. Rev.* **1966**, *144* (3), 962.
(302) Link, J. M.; Krohn, K. A.; Eary, J. F.; Kishore, R.; Lewellen, T. K.; Johnson, M. W.; Badger, C. C.; Richter, K. Y.; Nelp, W. B. *J. Labeled Compd. Radiopharm.* **1986**, *23* (10−12), 1297.
(303) DeJesus, O. T.; Nickles, R. J. *Appl. Radiat. Isot.* **1990**, *41* (8), 789.
(304) Zweit, J.; Downey, S.; Sharma, H. L. *Appl. Radiat. Isot.* **1991**, *42* (2), 199.
(305) Hohn, A.; Zimmermann, K.; Schaub, E.; Hirzel, W.; Schubiger, P. A.; Schibli, R. Q. J. *Nucl. Med. Mol. Imaging* **2008**, *52* (2), 145.
(306) Meijs, W. E.; Herscheid, J. D. M.; Haisma, H. J.; van Leuffen, P. J.; Mooy, R.; Pinedo, H. M. *Appl. Radiat. Isot.* **1994**, *45*, 1143.
(307) Sharma, V.; Prior, J. L.; Belinsky, M. G.; Kruh, G. D.; Piwnica-Worms, D. *J. Nucl. Med.* **2005**, *46* (2), 354.
(308) Sharma, V. *Bioconjugate Chem.* **2004**, *15* (6), 1464.
(309) Jacob, R.; Smith, T.; Prakasha, B.; Joannides, T. *Rheumatol. Int.* **2003**, *23* (5), 216.
(310) Turkmen, C.; Ozturk, S.; Unal, S. N.; Zulfikar, B.; Taser, O.; Sanli, Y.; Cefle, K.; Kilicoglu, O.; Palanduz, S. *Cancer Biother. Radiopharm.* **2007**, *22* (3), 393.

(311) Cancer Research UK Home Page. http://info.cancerresearchuk.org (accessed August 2009).
(312) Gonsalves, C. F.; Brown, D. B.; Carr, B. I. *Exp. Rev. Gastroenterol. Hepatol.* **2008**, *2* (4), 453.
(313) Nelson, K.; Vause, P. E., Jr.; Koropova, P. *Health Phys.* **2008**, *95* (5), S156.
(314) Khodjibekova, M.; Szyszko, T.; Khan, S.; Nijran, K.; Tait, P.; Al-Nahhas, A. *Rev. Recent Clin. Trials* **2007**, *2* (3), 212.
(315) Dijkgraaf, I.; Boerman, O. C.; Oyen, W. J. G.; Corstens, F. H. M.; Gotthardt, M. *Anti-Cancer Agents Med. Chem.* **2007**, *7* (5), 543.
(316) Vente, M. A. D.; Hobbelink, M. G. G.; van het Schip, A. D.; Zonnenberg, B. A.; Nijsen, J. F. W. *Anti-Cancer Agents Med. Chem.* **2007**, *7* (4), 441.
(317) Mier, W.; Haberkorn, U.; Eisenhut, M. *Signaling Mol. Targets Cancer Ther.* **2007**, 215.
(318) Gates, V. L.; Atassi, B.; Lewandowski, R. J.; Ryu, R. K.; Sato, K. T.; Nemcek, A. A.; Omary, R.; Salem, R. *Future Oncol.* **2007**, *3* (1), 73.
(319) Salem, R.; Hunter, R. D. *Int. J. Radiat. Oncol., Biol., Phys.* **2006**, *66* (2), S83.
(320) Welsh, J. S.; Kennedy, A. S.; Thomadsen, B. *Int. J. Radiat. Oncol., Biol., Phys.* **2006**, *66* (2), S62.
(321) Pohlman, B.; Sweetenham, J.; Macklis, R. M. *Expert Rev. Anticancer Ther.* **2006**, *6* (3), 445.
(322) Rao, A. V.; Akabani, G.; Rizzieri, D. A. *Clin. Med. Res.* **2005**, *3* (3), 157.
(323) Stolz, B. Expanding Role of Octreotide I, Presented at the 1st Advances in Oncology Symposium, Noordwijk, Netherlands, 2002, 203.
(324) de Herder, W. W.; Lamberts, S. W. J. *Endocrine* **2003**, *20* (3), 285.
(325) Behr, T. M.; Behe, M.; Sgouros, G. *Cancer Biother. Radiopharm.* **2002**, *17* (4), 445.
(326) Podoloff, D. A. *Curr. Pharm. Des.* **2002**, *8* (20), 1809.
(327) Virgolini, I.; Traub, T.; Novotny, C.; Leimer, M.; Fuger, B.; Li, S. R.; Patri, P.; Pangerl, T.; Angelberger, P.; Raderer, M.; Burggasser, G.; Andreae, F.; Kurtaran, A.; Dudczak, R. *Curr. Pharm. Des.* **2002**, *8* (20), 1781.
(328) Nijsen, J. F. W.; Van het Schip, A. D.; Hennink, W. E.; Rook, D. W.; Van Rijk, P. P.; De Klerk, J. M. H. *Curr. Med. Chem.* **2002**, *9* (1), 73.
(329) Vriesendorp, H. M.; Quadri, S. M. *Cancer Biother. Radiopharm.* **2000**, *15* (5), 431.
(330) Bal, C. S.; Kumar, A. *Trop. Gastroenterol.* **2008**, *29* (2), 62.
(331) Price, T. J.; Townsend, A. *Arch. Surg.* **2008**, *143* (3), 313.
(332) Shimoni, A.; Nagler, A. *Leuk. Lymphoma* **2007**, *48* (11), 2110.
(333) Salem, R.; Thurston, K. G. *J. Vasc. Interventional Radiol.* **2006**, *17* (10), 1571.
(334) Salem, R.; Thurston Kenneth, G. *J. Vasc. Interventional Radiol.* **2006**, *17* (9), 1425.
(335) Salem, R.; Thurston Kenneth, G. *J. Vasc. Interventional Radiol.* **2006**, *17* (8), 1251.
(336) Murthy, R.; Nunez, R.; Szklaruk, J.; Erwin, W.; Madoff David, C.; Gupta, S.; Ahrar, K.; Wallace Michael, J.; Cohen, A.; Coldwell Douglas, M.; Kennedy Andrew, S.; Hicks Marshall, E. *Radiographics* **2005**, *25* (1), S41.
(337) Stipsanelli, E.; Valsamaki, P. *Hell. J. Nucl. Med.* **2005**, *8* (2), 103.
(338) Mulcahy, M. F. *Curr. Treat. Opt. Oncol.* **2005**, *6* (5), 423.
(339) Hagenbeek, A.; Lewington, V. *Ann. Oncol.* **2005**, *16* (5), 786.
(340) Hernandez, M. C.; Knox, S. J. *Semin. Oncol.* **2003**, *30* (6, Suppl 17), 6.
(341) Mahmoud-Ahmed, A. S.; Suh, J. H. *Pituitary* **2002**, *5* (3), 175.
(342) Salem, R.; Thurston Kenneth, G.; Carr Brian, I.; Goin James, E.; Geschwind Jean-Francois, H. *J. Vasc. Interventional Radiol.* **2002**, *13* (9, Part 2), S223.
(343) Pharmacother, E. O.; Illidge, T. M.; Bayne, M. C. *Expert Opin. Pharm.* **2001**, *2* (6), 953.
(344) Riva, P.; Franceschi, G.; Riva, N.; Casi, M.; Santimaria, M.; Adamo, M. *Eur. J. Nucl. Med.* **2000**, *27* (5), 601.
(345) Sims, E.; Doughty, D.; Macaulay, E.; Royle, N.; Wraith, C.; Darlison, R.; Plowman, P. N. *Clin. Oncol.* **1999**, *11* (5), 303.
(346) Muller, C.; Schibli, R.; Krenning Eric, P.; de Jong, M. *J. Nucl. Med.* **2008**, *49* (4), 623.
(347) Mathias, C. J.; Wang, S.; Low, P. S.; Waters, D. J.; Green, M. A. *Nucl. Med. Biol.* **1998**, *26* (1), 23.
(348) de Visser, M.; Janssen, P. J.; Srinivasan, A.; Reubi, J. C.; Waser, B.; Erion, J. L.; Schmidt, M. A.; Krenning, E. P.; de Jong, M. *Eur. J. Nucl. Med. Mol. Imaging* **2003**, *30* (8), 1134.
(349) Hillairet de Boisferon, M.; Raguin, O.; Thiercelin, C.; Dussaillant, M.; Rostene, W.; Barbet, J.; Pelegrin, A.; Gruaz-Guyon, A. *Bioconjugate Chem.* **2002**, *13* (3), 654.
(350) Bussolati, G.; Chinol, M.; Chini, B.; Nacca, A.; Cassoni, P.; Paganelli, G. *Cancer Res.* **2001**, *61* (11), 4393.
(351) Schoenberger, J.; Bauer, J.; Moosbauer, J.; Eilles, C.; Grimm, D. *Curr. Med. Chem.* **2008**, *15* (2), 187.
(352) Sarda-Mantel, L.; Hervatin, F.; Michel, J.-B.; Louedec, L.; Martet, G.; Rouzet, F.; Lebtahi, R.; Merlet, P.; Khaw, B.-A.; Le Guludec, D. *Eur. J. Nucl. Med. Mol. Imaging* **2008**, *35* (1), 158.
(353) Sarda-Mantel, L.; Michel, J.-B.; Rouzet, F.; Martet, G.; Louedec, L.; Vanderheyden, J.-L.; Hervatin, F.; Raguin, O.; Vrigneaud, J.-M.; Khaw, B. A.; Guludec, D. *Eur. J. Nucl. Med. Mol. Imaging* **2006**, *33* (3), 239.
(354) Ke, S.; Wen, X.; Wu, Q.-P.; Wallace, S.; Charnsangavej, C.; Stachowiak, A. M.; Stephens, C. L.; Abbruzzese, J. L.; Podoloff, D. A.; Li, C. *J. Nucl. Med.* **2004**, *45* (1), 108.
(355) Wen, X.; Wu, Q.-P.; Ke, S.; Wallace, S.; Charnsangavej, C.; Huang, P.; Liang, D.; Chow, D.; Li, C. *Cancer Biother. Radiopharm.* **2003**, *18* (5), 819.
(356) Liu, D.; Overbey, D.; Watkinson, L.; Giblin, M. F. *Bioconjugate Chem.* **2009**, *20* (5), 888.
(357) Hanaoka, H.; Mukai, T.; Habashita, S.; Asano, D.; Ogawa, K.; Kuroda, Y.; Akizawa, H.; Iida, Y.; Endo, K.; Saga, T.; Saji, H. *Nucl. Med. Biol.* **2007**, *34* (5), 503.
(358) Giersing, B. K.; Rae, M. T.; Carballido, B. M.; Williamson, R. A.; Blower, P. J. *Bioconjugate Chem.* **2001**, *12*, 964.
(359) Perk, L. R.; Stigter-van Walsum, M.; Visser, G. W. M.; Kloet, R. W.; Vosjan, M. J. W. D.; Leemans, C. R.; Giaccone, G.; Albano, R.; Comoglio, P. M.; van Dongen, G. A. M. S. *Eur. J. Nucl. Med. Mol. Imaging* **2008**, *35* (10), 1857.
(360) Borjesson, P. K. E.; Jauw, Y. W. S.; Boellaard, R.; de Bree, R.; Comans, E. F. I.; Roos, J. C.; Castelijns, J. A.; Vosjan, M. J. W. D.; Kummer, J. A.; Leemans, C. R.; Lammertsma, A. A.; van Dongen, G. A. M. S. *Clin. Cancer Res.* **2006**, *12* (7), 2133.
(361) Murata, Y.; Ishida, R.; Umehara, I.; Ishikawa, N.; Komatsuzaki, A.; Kurabayashi, T.; Ishii, Y.; Ogura, I.; Ishii, J.; Okada, N.; Shibuya, H. *Nucl. Med. Commun.* **1999**, *20* (7), 599.
(362) Kotani, J.; Kawabe, J.; Higashiyama, S.; Kawamura, E.; Oe, A.; Hayashi, T.; Kurooka, H.; Tsumoto, C.; Kusuki, M.; Yamane, H.; Shiomi, S. *Ann. Nucl. Med.* **2008**, *22* (4), 297.
(363) Van Den Bossche, B.; Lambert, B.; De Winter, F.; Kolindou, A.; Dierckx, R. A.; Noens, L.; Van De Wiele, C. *Nucl. Med. Commun.* **2002**, *23* (11), 1079.
(364) Ballani, N. S.; Khan, H. A.; Al-Mohannadi, S. H.; Abu Al-Huda, F.; Usmani, S.; Tuli, M. M.; Al-Shemmari, S. H.; Al-Sawagh, H. F.; Al-Enezi, F. H. *Nucl. Med. Commun.* **2008**, *29* (6), 527.
(365) Kita, T.; Watanabe, S.; Yano, F.; Hayashi, K.; Yamamoto, M.; Iwasaki, Y.; Kosuda, S. *Ann. Nucl. Med.* **2007**, *21* (9), 499.
(366) Even-Sapir, E.; Israel, O. *Eur. J. Nucl. Med. Mol. Imaging* **2003**, *30* (1), S65.
(367) Nejmeddine, F.; Raphael, M.; Martin, A.; Le Roux, G.; Moretti, J.-L.; Caillat-Vigneron, N. *J. Nucl. Med.* **1999**, *40* (1), 40.
(368) Herman, M.; Paucek, B.; Raida, L.; Myslivecek, M.; Zapletalova, J. *Eur. J. Radiol.* **2007**, *64* (3), 432.
(369) Sun, S.-S.; Lin, C.-Y.; Chuang, F.-J.; Kao, C.-H. *Clin. Nucl. Med.* **2003**, *28* (10), 869.
(370) Israel, O.; Mekel, M.; Bar-Shalom, R.; Epelbaum, R.; Hermony, N.; Haim, N.; Dann, E. J.; Frenkel, A.; Ben-Arush, M.; Gaitini, D. *J. Nucl. Med.* **2002**, *43* (10), 1295.
(371) Rehm, P. K. *Cancer Biother. Radiopharm.* **1999**, *14* (4), 251.
(372) Watanabe, R.; Iizuka, H.; Kaira, K.; Mori, T.; Takise, A.; Ito, J.; Motegi, A.; Onozato, Y.; Ishihara, H. *Radiat. Med.* **2006**, *24* (6), 456.
(373) Nakahara, T.; Togawa, T.; Nagata, M.; Kikuchi, K.; Hatano, K.; Yui, N.; Kubo, A. *Eur. J. Nucl. Med. Mol. Imaging* **2002**, *29* (8), 1072.
(374) Horton, M. A. *Int. J. Biochem. Cell Biol.* **1997**, *29* (5), 721.
(375) Albelda, S. M.; Buck, C. A. *FASEB J.* **1990**, *4* (11), 2868.
(376) Hausner, S. H.; Kukis, D. L.; Gagnon, M. K. J.; Stanecki, C. E.; Ferdani, R.; Marshall, J. F.; Anderson, C. J.; Sutcliffe, J. L. *Mol. Imaging* **2009**, *8* (2), 111.
(377) Sutcliffe, J. L.; Liu, R.; Peng, L.; DeNardo, S. J.; Cherry, S. R.; Kukis, D. L.; Hausner, S. H.; Lam, K. S. *J. Nucl. Med.* **2007**, *48* (1), 69P.
(378) Denardo, S. J.; Liu, R.; Albrecht, H.; Natarajan, A.; Sutcliffe, J. L.; Anderson, C.; Peng, L.; Ferdani, R.; Cherry, S. R.; Lam, K. S. *J. Nucl. Med.* **2009**, *50* (4), 625.
(379) Clezardin, P. *Cell. Mol. Life Sci.* **1998**, *54* (6), 541.
(380) Jin, H.; Varner, J. *Br. J. Cancer.* **2004**, *90* (3), 561.
(381) Kimura, R. H.; Cheng, Z.; Gambhir, S.; Cochran, J. R. *Cancer Res.* **2009**, *69* (6), 2435.
(382) McQuade, P.; Knight, L. C.; Welch, M. J. *Bioconjugate Chem.* **2004**, *15* (5), 988.
(383) Harris, T. D.; Cheesman, E.; Harris, A. R.; Sachleben, R.; Edwards, D. S.; Liu, S.; Bartis, J.; Ellars, C.; Onthank, D.; Yalamanchili, P.; Heminway, S.; Silva, P.; Robinson, S.; Lazewatsky, J.; Rajopadhye, M.; Barrett, J. *Bioconjugate Chem.* **2007**, *18* (4), 1266.

(384) Harris, T. D.; Kalogeropoulos, S.; Nguyen, T.; Dwyer, G.; Edwards, D. S.; Liu, S.; Bartis, J.; Ellars, C.; Onthank, D.; Yalamanchili, P.; Heminway, S.; Robinson, S.; Lazewatsky, J.; Barrett, J. *Bioconjugate Chem.* **2006**, *17* (5), 1294.
(385) Harris, T. D.; Kalogeropoulos, S.; Nguyen, T.; Liu, S.; Bartis, J.; Ellars, C.; Edwards, S.; Onthank, D.; Silva, P.; Yalamanchili, P.; Robinson, S.; Lazewatsky, J.; Barrett, J.; Bozarth, J. *Cancer Biother. Radiopharm.* **2003**, *18* (4), 627.
(386) Jang, B.-S.; Lim, E.; Park, S. H.; Shin, I. S.; Danthi, S. N.; Hwang, I. S.; Le, N.; Yu, S.; Xie, J.; Li, K. C. P.; Carrasquillo, J. A.; Paik, C. H. *Nucl. Med. Biol.* **2007**, *34* (4), 363.
(387) Shin, I. S.; Jang, B.-S.; Danthi, S. N.; Xie, J.; Yu, S.; Le, N.; Maeng, J.-S.; Hwang, I. S.; Li, K. C. P.; Carrasquillo, J. A.; Paik, C. H. *Bioconjugate Chem.* **2007**, *18* (3), 821.
(388) Yoshimoto, M.; Ogawa, K.; Washiyama, K.; Shikano, N.; Mori, H.; Amano, R.; Kawai, K. *Int. J. Cancer.* **2008**, *123* (3), 709.
(389) van Hagen, P. M.; Breeman, W. A. P.; Bernard, H. F.; Schaar, M.; Mooij, C. M.; Srinivasan, A.; Schmidt, M. A.; Krenning, E. P.; de Jong, M. *Int. J. Cancer.* **2000**, *90* (4), 186.
(390) Dumont, R. A.; Hildebrandt, I.; Su, H.; Haubner, R.; Reischl, G.; Czernin, J. G.; Mischel, P. S.; Weber, W. A. *Cancer Res.* **2009**, *69* (7), 3173.
(391) Wu, Y.; Zhang, X.; Xiong, Z.; Cheng, Z.; Fisher, D. R.; Liu, S.; Gambhir, S. S.; Chen, X. *J. Nucl. Med.* **2005**, *46* (10), 1707.
(392) Cao, Q.; Cai, W.; Li, Z.-B.; Chen, K.; He, L.; Li, H.-C.; Hui, M.; Chen, X. *Eur. J. Nucl. Med. Mol. Imaging* **2007**, *34* (11), 1832.
(393) Chen, X.; Sievers, E.; Hou, Y.; Park, R.; Tohme, M.; Bart, R.; Bremner, R.; Bading, J. R.; Conti, P. S. *Neoplasia* **2005**, *7* (3), 271.
(394) Cao, F.; Li, Z.; Lee, A.; Liu, Z.; Chen, K.; Wang, H.; Cai, W.; Chen, X.; Wu, J. C. *Cancer Res.* **2009**, *69* (7), 2709.
(395) Li, Z.-B.; Cai, W.; Cao, Q.; Chen, K.; Wu, Z.; He, L.; Chen, X. *J. Nucl. Med.* **2007**, *48* (7), 1162.
(396) Shi, J.; Kim, Y.-S.; Zhai, S.; Liu, Z.; Chen, X.; Liu, S. *Bioconjugate Chem.* **2009**, *20* (4), 750.
(397) Lee, H.-Y.; Li, Z.; Chen, K.; Hsu Andrew, R.; Xu, C.; Xie, J.; Sun, S.; Chen, X. *J. Nucl. Med.* **2008**, *49* (8), 1371.
(398) Cai, W.; Chen, K.; Li, Z.-B.; Gambhir, S. S.; Chen, X. *J. Nucl. Med.* **2007**, *48* (11), 1862.
(399) Wei, L.; Ye, Y.; Wadas, T. J.; Lewis, J. S.; Welch, M. J.; Achilefu, S.; Anderson, C. J. *Nucl. Med. Biol.* **2009**, *36* (3), 277.
(400) Sprague, J. E.; Kitaura, H.; Zou, W.; Ye, Y.; Achilefu, S.; Weilbaecher, K. N.; Teitelbaum, S. L.; Anderson, C. J. *J. Nucl. Med.* **2007**, *48* (2), 311.
(401) Jeong Jae, M.; Hong Mee, K.; Chang Young, S.; Lee, Y.-S.; Kim Young, J.; Cheon Gi, J.; Lee Dong, S.; Chung, J.-K.; Lee Myung, C. *J. Nucl. Med.* **2008**, *49* (5), 830.
(402) Li, Z.-B.; Chen, K.; Chen, X. *Eur. J. Nucl. Med. Mol. Imaging* **2008**, *35* (6), 1100.
(403) Liu, Z.; Niu, G.; Shi, J.; Liu, S.; Wang, F.; Liu, S.; Chen, X. *Eur. J. Nucl. Med. Mol. Imaging* **2009**, *36* (6), 947.
(404) Reubi, J. C. *Endocr. Rev.* **2003**, *24* (4), 389.
(405) Reubi, J. C.; Waser, B.; Schaer, J.-C.; Laissue, J. A. *Eur. J. Nucl. Med.* **2001**, *28* (7), 836.
(406) Rogers, B. E.; Zinn, K. R.; Buchsbaum, D. J. *Q. J. Nucl. Med.* **2000**, *44* (3), 208.
(407) Kwekkeboom, D. J.; Kooij, P. P.; Bakker, W. H.; Maecke, H. R.; Krenning, E. P. *J. Nucl. Med.* **1999**, *40* (5), 762.
(408) Kwekkeboom, D. J.; Bakker, W. H.; Kooij, P. P. M.; Konijnenberg, M. W.; Srinivasan, A.; Erion, J. L.; Schmidt, M. A.; Bugaj, J. E.; de Jong, M.; Krenning, E. P. *Eur. J. Nucl. Med.* **2001**, *28* (9), 1319.
(409) Lebtahi, R.; Moreau, S.; Marchand-Adam, S.; Debray, M.-P.; Brauner, M.; Soler, P.; Marchal, J.; Raguin, O.; Gruaz-Guyon, A.; Reubi, J.-C.; Le Guludec, D.; Crestani, B. *J. Nucl. Med.* **2006**, *47* (8), 1281.
(410) Lebtahi, R.; Le Cloirec, J.; Houzard, C.; Daou, D.; Sobhani, I.; Sassolas, G.; Mignon, M.; Bourguet, P.; Le Guludec, D. *J. Nucl. Med.* **2002**, *43* (7), 889.
(411) Traub, T.; Petkov, V.; Ofluoglu, S.; Pangerl, T.; Raderer, M.; Fueger, B. J.; Schima, W.; Kurtaran, A.; Dudczak, R.; Virgolini, I. *J. Nucl. Med.* **2001**, *42* (9), 1309.
(412) Cremonesi, M.; Ferrari, M.; Zoboli, S.; Chinol, M.; Stabin, M. G.; Orsi, F.; Maecke, H. R.; Jermann, E.; Robertson, C.; Fiorenza, M.; Tosi, G.; Paganelli, G. *Eur. J. Nucl. Med.* **1999**, *26* (8), 877.
(413) Forrer, F.; Uusijarvi, H.; Waldherr, C.; Cremonesi, M.; Bernhardt, P.; Mueller-Brand, J.; Maecke, H. R. *Eur. J. Nucl. Med. Mol. Imaging* **2004**, *31* (9), 1257.
(414) Rodrigues, M.; Gabriel, M.; Heute, D.; Putzer, D.; Griesmacher, A.; Virgolini, I. *Eur. J. Nucl. Med. Mol. Imaging* **2008**, *35* (10), 1796.
(415) Rodrigues, M.; Traub-Weidinger, T.; Leimer, M.; Li, S.; Andreae, F.; Angelberger, P.; Dudczak, R.; Virgolini, I. *Eur. J. Nucl. Med. Mol. Imaging* **2005**, *32* (10), 1144.
(416) Becherer, A.; Szabo, M.; Karanikas, G.; Wunderbaldinger, P.; Angelberger, P.; Raderer, M.; Kurtaran, A.; Dudczak, R.; Kletter, K. *J. Nucl. Med.* **2004**, *45* (7), 1161.
(417) Decristoforo, C.; Mather, S. J.; Cholewinski, W.; Donnemiller, E.; Riccabona, G.; Moncayo, R. *Eur. J. Nucl. Med.* **2000**, *27* (9), 1318.
(418) Meisetschlager, G.; Poethko, T.; Stahl, A.; Wolf, I.; Scheidhauer, K.; Schottelius, M.; Herz, M.; Wester Hans, J.; Schwaiger, M. *J. Nucl. Med.* **2006**, *47* (4), 566.
(419) Gabriel, M.; Decristoforo, C.; Donnemiller, E.; Ulmer, H.; Rychlinski, C. W.; Mather, S. J.; Moncayo, R. *J. Nucl. Med.* **2003**, *44* (5), 708.
(420) Anderson, C. J.; Dehdashti, F.; Cutler, P. D.; Schwarz, S. W.; Laforest, R.; Bass, L. A.; Lewis, J. S.; McCarthy, D. W. *J. Nucl. Med.* **2001**, *42* (2), 213.
(421) Parry, J. J.; Eiblmaier, M.; Andrews, R.; Meyer, L. A.; Higashikubo, R.; Anderson, C. J.; Rogers, B. E. *Mol. Imaging* **2007**, *6* (1), 56.
(422) Wang, M.; Caruano, A. L.; Lewis, M. R.; Ballard, L.; Kelly, K.; Vanderwaal, R. P.; Anderson, C. J. *Q. J. Nucl. Med.* **2001**, *45* (2), S12.
(423) Wang, M.; Caruano, A. L.; Lewis, M. R.; Meyer, L. M.; VanderWaal, R. P.; Anderson, C. J. *Cancer Res.* **2003**, *63* (20), 6864.
(424) Li, W. P.; Lewis, J. S.; Kim, J.; Bugaj, J. E.; Johnson, M. A.; Erion, J. L.; Anderson, C. J. *Bioconjugate Chem.* **2002**, *13* (4), 721.
(425) Edwards, W. B.; Xu, B.; Akers, W.; Cheney, P. P.; Liang, K.; Rogers, B. E.; Anderson, C. J.; Achilefu, S. *Bioconjugate Chem.* **2008**, *19* (1), 192.
(426) de Jong, M.; Breeman, W. A. P.; Bernard, B. F.; van Gameren, A.; de Bruin, E.; Bakker, W. H.; van der Pluijm, M. E.; Visser, T. J.; Macke, H. R.; Krenning, E. P. *Eur. J. Nucl. Med.* **1999**, *26* (7), 693.
(427) Lewis, J. S.; Lewis, M. R.; Cutler, P. D.; Srinivasan, A.; Schmidt, M. A.; Schwarz, S. W.; Morris, M. M.; Miller, J. P.; Anderson, C. J. *Clin. Cancer Res.* **1999**, *5* (10), 3608.
(428) Lewis, J. S.; Srinivasan, A.; Schmidt, M. A.; Anderson, C. J. *Nucl. Med. Biol.* **1999**, *26* (3), 267.
(429) Weisman, G. R.; Rogers, M. E.; Wong, E. H.; Jasinski, J. P.; Paight, E. S. *J. Am. Chem. Soc.* **1990**, *112* (23), 8604.
(430) Sprague, J. E.; Peng, Y.; Sun, X.; Weisman, G. R.; Wong, E. H.; Achilefu, S.; Anderson, C. J. *Clin. Cancer Res.* **2004**, *10* (24), 8674.
(431) Eiblmaier, M.; Andrews, R.; Laforest, R.; Rogers, B. E.; Anderson, C. J. *J. Nucl. Med.* **2007**, *48* (8), 1390.
(432) Milenic, D. E.; Brady, E. D.; Brechbiel, M. W. *Nat. Rev. Drug Discovery* **2004**, *3* (6), 488.
(433) Clifford, T.; Boswell, C. A.; Biddlecombe, G. B.; Lewis, J. S.; Brechbiel, M. W. *J. Med. Chem.* **2006**, *49* (14), 4297.
(434) Lincke, T.; Singer, J.; Kluge, R.; Sabri, O.; Paschke, R. *Thyroid* **2009**, *19* (4), 381.
(435) Fanti, S.; Ambrosini, V.; Tomassetti, P.; Castellucci, P.; Montini, G.; Allegri, V.; Grassetto, G.; Rubello, D.; Nanni, C.; Franchi, R. *Biomed. Pharmacother.* **2008**, *62* (10), 667.
(436) Koukouraki, S.; Strauss, L. G.; Georgoulias, V.; Eisenhut, M.; Haberkorn, U.; Dimitrakopoulou-Strauss, A. *Eur. J. Nucl. Med. Mol. Imaging* **2006**, *33* (10), 1115.
(437) Wild, D.; Schmitt, J. S.; Ginj, M.; Maecke, H. R.; Bernard, B. F.; Krenning, E.; de Jong, M.; Wenger, S.; Reubi, J.-C. *Eur. J. Nucl. Med. Mol. Imaging* **2003**, *30* (10), 1338.
(438) Froidevaux, S.; Eberle, A. N.; Christe, M.; Sumanovski, L.; Heppeler, A.; Schmiti, J. S.; Eisenwiener, K.; Beglinger, C.; Macke, H. R. *Int. J. Cancer* **2002**, *98* (6), 930.
(439) Hofmann, M.; Maecke, H.; Boerner, A. R.; Weckesser, E.; Schoeffski, P.; Oei, M. L.; Schumacher, J.; Henze, M.; Heppeler, A.; Meyer, G. J.; Knapp, W. H. *Eur. J. Nucl. Med.* **2001**, *28* (12), 1751.
(440) Gabriel, M.; Decristoforo, C.; Kendler, D.; Dobrozemsky, G.; Heute, D.; Uprimny, C.; Kovacs, P.; Von Guggenberg, E.; Bale, R.; Virgolini, I. J. *J. Nucl. Med.* **2007**, *48* (4), 508.
(441) Henze, M.; Schuhmacher, J.; Hipp, P.; Kowalski, J.; Becker, D. W.; Doll, J.; Macke, H. R.; Hofmann, M.; Debus, J.; Haberkorn, U. *J. Nucl. Med.* **2001**, *42* (7), 1053.
(442) Kayani, I.; Bomanji, J. B.; Groves, A.; Conway, G.; Gacinovic, S.; Win, T.; Dickson, J.; Caplin, M.; Ell, P. J. *Cancer* **2008**, *112* (11), 2447.
(443) Ugur, O.; Kothari, P. J.; Finn, R. D.; Zanzonico, P.; Ruan, S.; Guenther, I.; Maecke, H. R.; Larson, S. M. *Nucl. Med. Biol.* **2002**, *29* (2), 147.
(444) Ginj, M.; Zhang, H.; Waser, B.; Cescato, R.; Wild, D.; Wang, X.; Erchegyi, J.; Rivier, J.; Macke, H. R.; Reubi, J. C. *Proc. Natl. Acad. Sci. U.S.A.* **2006**, *103* (44), 16436.
(445) Wadas, T. J.; Eiblmaier, M.; Zheleznyak, A.; Sherman, C. D.; Ferdani, R.; Liang, K.; Achilefu, S.; Anderson, C. J. *J. Nucl. Med.* **2008**, *49* (11), 1819.
(446) Slamon, D. J.; Godolphin, W.; Jones, L. A.; Holt, J. A.; Wong, S. G.; Keith, D. E.; Levin, W. J.; Stuart, S. G.; Udove, J.; Ullrich, A. *Science* **1989**, *244* (4905), 707.
(447) Pauletti, G.; Dandekar, S.; Rong, H.; Ramos, L.; Peng, H.; Seshadri, R.; Slamon, D. J. *J. Clin. Oncol.* **2000**, *18* (21), 3651.
(448) Perik, P. J.; Lub-De Hooge, M. N.; Gietema, J. A.; van der Graaf, W. T. A.; de Korte, M. A.; Jonkman, S.; Kosterink, J. G. W.; van

Veldhuisen, D. J.; Sleijfer, D. T.; Jager, P. L.; de Vries, E. G. E. *J. Clin. Oncol.* **2006**, *24* (15), 2276.
(449) Lub-de Hooge, M. N.; Kosterink, J. G. W.; Perik, P. J.; Nijnuis, H.; Tran, L.; Bart, J.; Suurmeijer, A. J. H.; de Jong, S.; Jager, P. L.; de Vries, E. G. E. *Br. J. Pharmacol.* **2004**, *143* (1), 99.
(450) Sampath, L.; Kwon, S.; Ke, S.; Wang, W.; Schiff, R.; Mawad, M. E.; Sevick-Muraca, E. M. *J. Nucl. Med.* **2007**, *48* (9), 1501.
(451) Tang, Y.; Scollard, D.; Chen, P.; Wang, J.; Holloway, C.; Reilly, R. M. *Nucl. Med. Commun.* **2005**, *26* (5), 427.
(452) Tang, Y.; Wang, J.; Scollard, D. A.; Mondal, H.; Holloway, C.; Kahn, H. J.; Reilly, R. M. *Nucl. Med. Biol.* **2005**, *32* (1), 51.
(453) Dennis, M. S.; Jin, H.; Dugger, D.; Yang, R.; McFarland, L.; Ogasawara, A.; Williams, S.; Cole, M. J.; Ross, S.; Schwall, R. *Cancer Res.* **2006**, *67* (1), 254.
(454) Orlova, A.; Tolmachev, V.; Pehrson, R.; Lindborg, M.; Tran, T.; Sandstroem, M.; Nilsson, F. Y.; Wennborg, A.; Abrahmsen, L.; Feldwisch, J. *Cancer Res.* **2007**, *67* (5), 2178.
(455) Wallberg, H.; Orlova, A. *Cancer Biother. Radiopharm.* **2008**, *23* (4), 435.
(456) Breeman, W. A. P.; De Jong, M.; Bernard, B. F.; Kwekkeboom, D. J.; Srinivasan, A.; Van Der Pluijm, M. E.; Hofland, L. J.; Visser, T. J.; Krenning, E. P. *Int. J. Cancer.* **1999**, *83* (5), 657.
(457) Hoffman, T. J.; Gali, H.; Smith, C. J.; Sieckman, G. L.; Hayes, D. L.; Owen, N. K.; Volkert, W. A. *J. Nucl. Med.* **2003**, *44* (5), 823.
(458) Garrison, J. C.; Rold, T. L.; Sieckman, G. L.; Naz, F.; Sublett, S. V.; Figueroa, S. D.; Volkert, W. A.; Hoffman, T. J. *Bioconjugate Chem.* **2008**, *19* (9), 1803.
(459) Schuhmacher, J.; Zhang, H.; Doll, J.; Maecke, H. R.; Matys, R.; Hauser, H.; Henze, M.; Haberkorn, U.; Eisenhut, M. *J. Nucl. Med.* **2005**, *46* (4), 691.
(460) Dimitrakopoulou-Strauss, A.; Hohenberger, P.; Eisenhut, M.; Maecke, H. R.; Haberkorn, U.; Strauss, L. *J. Nucl. Med.* **2006**, *47* (S1), 102P.
(461) Biddlecombe, G. B.; Rogers, B. E.; de Visser, M.; Parry, J. J.; de Jong, M.; Erion, J. L.; Lewis, J. S. *Bioconjugate Chem.* **2007**, *18* (3), 724.
(462) Gasser, G.; Tjioe, L.; Graham, B.; Belousoff, M. J.; Juran, S.; Walther, M.; Kuenstler, J.-U.; Bergmann, R.; Stephan, H.; Spiccia, L. *Bioconjugate Chem.* **2008**, *19* (3), 719.
(463) Rogers, B. E.; Bigott, H. M.; McCarthy, D. W.; Della Manna, D.; Kim, J.; Sharp, T. L.; Welch, M. J. *Bioconjugate Chem.* **2003**, *14* (4), 756.
(464) Parry, J. J.; Andrews, R.; Rogers, B. E. *Breast Cancer Res. Treat.* **2007**, *101* (2), 175.
(465) Parry, J. J.; Kelly, T. S.; Andrews, R.; Rogers, B. E. *Bioconjugate Chem.* **2007**, *18* (4), 1110.
(466) Chen, X.; Park, R.; Hou, Y.; Tohme, M.; Shahinian, A. H.; Bading, J. R.; Conti, P. S. *J. Nucl. Med.* **2004**, *45* (8), 1390.
(467) Prasanphanich, A. F.; Nanda, P. K.; Rold, T. L.; Ma, L.; Lewis, M. R.; Garrison, J. C.; Hoffman, T. J.; Sieckman, G. L.; Figueroa, S. D.; Smith, C. J. *Proc. Natl. Acad. Sci. U.S.A.* **2007**, *104* (30), 12462.
(468) Prasanphanich, A. F.; Retzloff, L.; Lane, S. R.; Nanda, P. K.; Sieckman, G. L.; Rold, T. L.; Ma, L.; Figueroa, S. D.; Sublett, S. V.; Hoffman, T. J.; Smith, C. J. *Nucl. Med. Biol.* **2009**, *36* (2), 171.
(469) Klein, S.; Levitzki, A. *Curr. Opin. Cell Biol.* **2009**, *21* (2), 185.
(470) Klijn, J. G. M.; Berns, P. M. J. J.; Schmitz, P. I. M.; Foekens, J. A. *Endocr. Rev.* **1992**, *13* (1), 3.
(471) Kurihara, A.; Pardridge, W. M. *Cancer Res.* **1999**, *59* (24), 6159.
(472) Kurihara, A.; Deguchi, Y.; Pardridge, W. M. *Bioconjugate Chem.* **1999**, *10* (3), 502.
(473) Reilly, R. M.; Kiarash, R.; Sandhu, J.; Lee, Y. W.; Cameron, R. G.; Hendler, A.; Vallis, K.; Gariepy, J. *J. Nucl. Med.* **2000**, *41* (5), 903.
(474) Reilly, R. M.; Kiarash, R.; Cameron, R. G.; Porlier, N.; Sandhu, J.; Hill, R. P.; Vallis, K.; Hendler, A.; Gariepy, J. *J. Nucl. Med.* **2000**, *41* (3), 429.
(475) Chen, P.; Cameron, R.; Wang, J.; Vallis, K. A.; Reilly, R. M. *J. Nucl. Med.* **2003**, *44* (9), 1469.
(476) Reilly, R. M.; Chen, P.; Wang, J.; Scollard, D.; Cameron, R.; Vallis, K. A. *J. Nucl. Med.* **2006**, *47* (6), 1023.
(477) Hu, M.; Scollard, D.; Chan, C.; Chen, P.; Vallis, K.; Reilly, R. M. *Nucl. Med. Biol.* **2007**, *34* (8), 887.
(478) Reilly, R. M.; Scollard, D. A.; Wang, J.; Mondal, H.; Chen, P.; Henderson, L. A.; Bowen, B. M.; Vallis, K. A. *J. Nucl. Med.* **2004**, *45* (4), 701.
(479) Velikyan, I.; Sundberg, A. L.; Lindhe, O.; Hoeglund, A. U.; Eriksson, O.; Werner, E.; Carlsson, J.; Bergstroem, M.; Laangstroem, B.; Tolmachev, V. *J. Nucl. Med.* **2005**, *46* (11), 1881.
(480) Niu, G.; Cai, W.; Chen, K.; Chen, X. *Mol. Imaging Biol.* **2008**, *10* (2), 99.
(481) Cai, W.; Chen, K.; He, L.; Cao, Q.; Koong, A.; Chen, X. *Eur. J. Nucl. Med. Mol. Imaging* **2007**, *34* (6), 850.
(482) Li, W. P.; Meyer, L. A.; Capretto, D. A.; Sherman, C. D.; Anderson, C. J. *Cancer Biother. Radiopharm.* **2008**, *23* (2), 158.
(483) Wen, X.; Wu, Q. P.; Ke, S.; Ellis, L.; Charnsangavej, C.; Delpassand, A. S.; Wallace, S.; Li, C. *J. Nucl. Med.* **2001**, *42* (10), 1530.
(484) Eiblmaier, M.; Meyer, L. A.; Watson, M. A.; Fracasso, P. M.; Pike, L. J.; Anderson, C. J. *J. Nucl. Med.* **2008**, *49* (9), 1472.
(485) Lohela, M.; Bry, M.; Tammela, T.; Alitalo, K. *Curr. Opin. Cell Biol.* **2009**, *21* (2), 154.
(486) Kaplan, R. N.; Rafii, S.; Lyden, D. *Cancer Res.* **2006**, *66* (23), 11089.
(487) Kaplan, R. N.; Riba, R. D.; Zacharoulis, S.; Bramley, A. H.; Vincent, L.; Costa, C.; MacDonald, D. D.; Jin, D. K.; Shido, K.; Kerns, S. A.; Zhu, Z.; Hicklin, D.; Wu, Y.; Port, J. L.; Altorki, N.; Port, E. R.; Ruggero, D.; Shmelkov, S. V.; Jensen, K. K.; Rafii, S.; Lyden, D. *Nature* **2005**, *438* (7069), 820.
(488) Chan, C.; Sandhu, J.; Guha, A.; Scollard, D. A.; Wang, J.; Chen, P.; Bai, K.; Lee, L.; Reilly, R. M. *J. Nucl. Med.* **2005**, *46* (10), 1745.
(489) Cai, W.; Chen, K.; Mohamedali, K. A.; Cao, Q.; Gambhir, S. S.; Rosenblum, M. G.; Chen, X. *J. Nucl. Med.* **2006**, *47* (12), 2048.
(490) Wang, H.; Cai, W.; Chen, K.; Li, Z.-B.; Kashefi, A.; He, L.; Chen, X. *Eur. J. Nucl. Med. Mol. Imaging* **2007**, *34* (12), 2001.
(491) Chen, K.; Li, Z.-B.; Wang, H.; Cai, W.; Chen, X. *Eur. J. Nucl. Med. Mol. Imaging* **2008**, *35* (12), 2235.
(492) Hsu, A. R.; Cai, W.; Veeravagu, A.; Mohamedali, K. A.; Chen, K.; Kim, S.; Vogel, H.; Hou, L. C.; Tse, V.; Rosenblum, M. G.; Chen, X. *J. Nucl. Med.* **2007**, *48* (3), 445.
(493) Backer, M. V.; Levashova, Z.; Patel, V.; Jehning, B. T.; Claffey, K.; Blankenberg, F. G.; Backer, J. M. *Nat. Med.* **2007**, *13* (4), 504.
(494) Jemal, A.; Siegel, R.; Ward, R.; Murray, T.; Xu, J.; Thun, M. J. *Cancer J. Clin.* **2007**, *57*, 43.
(495) Miao, Y.; Quinn, T. P. *Front. Biosci.* **2007**, *12* (12), 4514.
(496) Chen, J.; Cheng, Z.; Owen, N. K.; Hoffman, T. J.; Miao, Y.; Jurisson, S. S.; Quinn, T. P. *J. Nucl. Med.* **2001**, *42* (12), 1847.
(497) Cheng, Z.; Chen, J.; Miao, Y.; Owen, N. K.; Quinn, T. P.; Jurisson, S. S. *J. Med. Chem.* **2002**, *45* (14), 3048.
(498) Chen, J.; Cheng, Z.; Miao, Y.; Jurisson, S. S.; Quinn, T. P. *Cancer* **2002**, *94* (4), 1196.
(499) Bapst, J.-P.; Calame, M.; Tanner, H.; Eberle, A. N. *Bioconjugate Chem.* **2009**, *20* (5), 984.
(500) McQuade, P.; Miao, Y.; Yoo, J.; Quinn, T. P.; Welch, M. J.; Lewis, J. S. *J. Med. Chem.* **2005**, *48* (8), 2985.
(501) Cheng, Z.; Xiong, Z.; Subbarayan, M.; Chen, X.; Gambhir, S. S. *Bioconjugate Chem.* **2007**, *18* (3), 765.
(502) Froidevaux, S.; Calame-Christe, M.; Schuhmacher, J.; Tanner, H.; Saffrich, R.; Henze, M.; Eberle, A. N. *J. Nucl. Med.* **2004**, *45* (1), 116.
(503) Wei, L.; Miao, Y.; Gallazzi, F.; Quinn, T. P.; Welch, M. J.; Vavere, A. L.; Lewis, J. S. *Nucl. Med. Biol.* **2007**, *34* (8), 945.
(504) Wei, L.; Butcher, C.; Miao, Y.; Gallazzi, F.; Quinn, T. P.; Welch, M. J.; Lewis, J. S. *J. Nucl. Med.* **2007**, *48* (1), 64.
(505) Misek, D. E.; Imafuku, Y.; Hanash, S. M. *Pharmacogenomics J.* **2004**, *5* (8), 1129.
(506) Giannios, J.; Ioannidou-Mouzaka, L. *Eur. J. Gynecol. Oncol.* **1997**, *18* (5), 387.
(507) Lendvai, G.; Velikyan, I.; Estrada, S.; Eriksson, B.; Laangstroem, B.; Bergstroem, M. *Oligonucleotides* **2008**, *18* (1), 33.
(508) Lendvai, G.; Velikyan, I.; Bergstroem, M.; Estrada, S.; Laryea, D.; Vaelilae, M.; Salomaeki, S.; Langstroem, B.; Roivainen, A. *Eur. J. Pharm. Sci.* **2005**, *26* (1), 26.
(509) Schlesinger, J.; Bergmann, R.; Klussmann, S.; Wuest, F. *Lett. Drug Discovery* **2006**, *3* (5), 330.
(510) Wang, J.; Chen, P.; Mrkobrada, M.; Hu, M.; Vallis, K. A.; Reilly, R. M. *Eur. J. Nucl. Med. Mol. Imaging* **2003**, *30* (9), 1273.
(511) Roivainen, A.; Tolvanen, T.; Salomaki, S.; Lendvai, G.; Velikyan, I.; Numminen, P.; Valila, M.; Sipila, H.; Bergstrom, M.; Harkonen, P.; Lonnberg, H.; Langstrom, B. *J. Nucl. Med.* **2004**, *45* (2), 347.
(512) Tian, X.; Aruva, M. R.; Zhang, K.; Shanthly, N.; Cardi, C. A.; Thakur, M. L.; Wickstrom, E. *J. Nucl. Med.* **2007**, *48* (10), 1699.
(513) Tian, X.; Aruva, M. R.; Qin, W.; Zhu, W.; Duffy, K. T.; Sauter, E. R.; Thakur, M. L.; Wickstrom, E. *J. Nucl. Med.* **2004**, *45* (12), 2070.
(514) Suzuki, T.; Zhang, Y.; Zhang, Y.-f.; Schlachetzki, F.; Pardridge, W. M. *Mol. Imaging* **2004**, *3* (4), 356.
(515) Suzuki, T.; Wu, D.; Schlachetzki, F.; Li, J. Y.; Boado, R. J.; Pardridge, W. M. *J. Nucl. Med.* **2004**, *45* (10), 1766.
(516) Boerman, O. C.; Dams, E. T. M.; Oyen, W. J. G.; Corstens, F. H. M.; Storm, G. *Inflammation Res.* **2001**, *50* (2), 55.
(517) Hughes, D. K. *J. Nucl. Med. Technol.* **2003**, *31* (4), 196.
(518) Liu, S.-F.; Liu, J.-W.; Lin, M.-C.; Lee, C.-H.; Huang, H.-H.; Lai, Y.-F. *Am. J. Roentgenol.* **2007**, *188* (5), W403.
(519) Hang, L. W.; Hsu, W. H.; Tsai, J. J. P.; Jim, Y. F.; Lin, C. C.; Kao, A. *Rheumatol. Int.* **2004**, *24* (3), 153.
(520) Lazzeri, E.; Pauwels, E. K. J.; Erba, P. A.; Volterrani, D.; Manca, M.; Bodei, L.; Trippi, D.; Bottoni, A.; Cristofani, R.; Consoli, V.; Palestro, C. J.; Mariani, G. *Eur. J. Nucl. Med. Mol. Imaging* **2004**, *31* (11), 1505.

(521) Lazzeri, E.; Manca, M.; Molea, N.; Marchetti, S.; Consoli, V.; Bodei, L.; Bianchi, R.; Chinol, M.; Paganelli, G.; Mariani, G. *Eur. J. Nucl. Med.* **1999**, *26* (6), 606.
(522) van Eerd, J. E. M.; Oyen, W. J. G.; Harris, T. D.; Rennen, H. J. J. M.; Edwards, D. S.; Liu, S.; Ellars, C. E.; Corstens, F. H. M.; Boerman, O. C. *J. Nucl. Med.* **2003**, *44* (7), 1087.
(523) Broekema, M.; Van Eerd, J. E. M.; Oyen, W. J. G.; Corstens, F. H. M.; Liskamp, R. M. J.; Boerman, O. C.; Harris, T. D. *J. Med. Chem.* **2005**, *48* (20), 6442.
(524) Bhargava, K. K.; Gupta, R. K.; Nichols, K. J.; Palestro, C. J. *Nucl. Med. Biol.* **2009**, *36* (5), 545.
(525) Locke, L. W.; Chordia, M. D.; Zhang, Y.; Kundu, B.; Kennedy, D.; Landseadel, J.; Xiao, L.; Fairchild, K. D.; Berr, S. S.; Linden, J.; Pan, D. *J. Nucl. Med.* **2009**, *50* (5), 790.
(526) Heusch, G. *Br. J. Pharmacol.* **2008**, *153* (8), 1589.
(527) Moustafa, R. R.; Baron, J. C. *Br. J. Pharmacol.* **2008**, *153* (1), S44.
(528) Hardee, M. E.; Dewhirst, M. W.; Agarwal, N.; Sorg, B. S. *Curr. Mol. Med.* **2009**, *9* (4), 435.
(529) Hwang, D.-R.; Bergmann, S. R. Radiopharmaceuticals for studying the heart. In *Handbook of Radiopharmaceuticals: Radiochemistry and Applications*; Welch, M. J., Redvanly, C. S., Eds.; John Wiley & Sons Inc.: Hoboken, NJ, 2003; p 529.
(530) Keng, F. Y. J. *Ann. Acad. Med. Singapore* **2004**, *33* (2), 175.
(531) Yetkin, F. Z.; Mendelsohn, D. *Neuroimaging Clin. North Am.* **2002**, *12* (4), 537.
(532) Hoffend, J.; Mier, W.; Schuhmacher, J.; Schmidt, K.; Dimitrakopoulou-Strauss, A.; Strauss, L. G.; Eisenhut, M.; Kinscherf, R.; Haberkorn, U. *Nucl. Med. Biol.* **2005**, *32* (3), 287.
(533) Kiratli, P. O.; Tuncel, M.; Ozkutlu, S.; Caglar, M. *Nucl. Med. Commun.* **2008**, *29* (10), 907.
(534) Kinuya, S.; Li, X. F.; Yokoyama, K.; Mori, H.; Shiba, K.; Watanabe, N.; Shuke, N.; Bunko, H.; Michigishi, T.; Tonami, N. *Nucl. Med. Commun.* **2004**, *25* (1), 49.
(535) Takahashi, N.; Fujibayashi, Y.; Yonekura, Y.; Welch, M. J.; Waki, A.; Tsuchida, T.; Sadato, N.; Sugimoto, K.; Nakano, A.; Lee, J. D.; Itoh, H. *Ann. Nucl. Med.* **2001**, *15* (3), 293.
(536) Fujibayashi, Y.; Cutler, C. S.; Anderson, C. J.; McCarthy, D. W.; Jones, L. A.; Sharp, T.; Yonekura, Y.; Welch, M. J. *Nucl. Med. Biol.* **1999**, *26* (1), 117.
(537) Plossl, K.; Chandra, R.; Qu, W.; Lieberman Brian, P.; Kung, M.-P.; Zhou, R.; Huang, B.; Kung Hank, F. *Nucl. Med. Biol.* **2008**, *35* (1), 83.
(538) Cutler, C. S.; Giron, M. C.; Reichert, D. E.; Snyder, A. Z.; Herrero, P.; Anderson, C. J.; Quarless, D. A.; Koch, S. A.; Welch, M. J. *Nucl. Med. Biol.* **1999**, *26* (3), 305.
(539) Wallhaus, T. R.; Lacy, J.; Stewart, R.; Bianco, J.; Green, M. A.; Nayak, N.; Stone, C. K. *J. Nucl. Cardiol.* **2001**, *8* (1), 67.
(540) Flower, M. A.; Zweit, J.; Hall, A. D.; Burke, D.; Davies, M. M.; Dworkin, M. J.; Young, H. E.; Mundy, J.; Ott, R. J.; McCready, V. R.; Carnochan, P.; Allen-Mersh, T. G. *Eur. J. Nucl. Med.* **2001**, *28* (1), 99.
(541) Holschneider, D. P.; Yang, J.; Sadler, T. R.; Galifianakis, N. B.; Bozorgzadeh, M. H.; Bading, J. R.; Conti, P. S.; Maarek, J. M. I. *Brain Res.* **2008**, *1234* (9), 32.
(542) Yang, D. J.; Ilgan, S.; Higuchi, T.; Zareneyrizi, F.; Oh, C. S.; Liu, C. W.; Kim, E. E.; Podoloff, D. A. *Pharm. Res.* **1999**, *16* (5), 743.
(543) Ito, M.; Yang David, J.; Mawlawi, O.; Mendez, R.; Oh, C.-S.; Azhdarinia, A.; Greenwell, A. C.; Yu, D.-F.; Kim, E. E. *Acad. Radiol.* **2006**, *13* (5), 598.
(544) Fujibayashi, Y.; Taniuchi, H.; Yonekura, Y.; Ohtani, H.; Konishi, J.; Yokoyama, A. *J. Nucl. Med.* **1997**, *38* (7), 1155.
(545) Holland, J. P.; Aigbirhio, F. I.; Betts, H. M.; Bonnitcha, P. D.; Burke, P.; Christlieb, M.; Churchill, G. C.; Cowley, A. R.; Dilworth, J. R.; Donnelly, P. S.; Green, J. C.; Peach, J. M.; Vasudevan, S. R.; Warren, J. E. *Inorg. Chem.* **2007**, *46* (2), 465.
(546) Bonnitcha, P. D.; Vavere, A. L.; Lewis, J. S.; Dilworth, J. R. *J. Med. Chem.* **2008**, *51* (10), 2985.
(547) Barnard, P.; Bayly, S.; Betts, H.; Bonnitcha, P.; Christlieb, M.; Dilworth, J.; Holland, J.; Pascu, S. Q. J. *Nucl. Med. Mol. Imaging* **2008**, *52* (2), 174.
(548) Ackerman, L. J.; West, D. X.; Mathias, C. J.; Green, M. A. *Nucl. Med. Biol.* **1999**, *26* (5), 551.
(549) McQuade, P.; Martin, K. E.; Castle, T. C.; Went, M. J.; Blower, P. J.; Welch, M. J.; Lewis, J. S. *Nucl. Med. Biol.* **2005**, *32* (2), 147.
(550) Cowley, A. R.; Dilworth, J. R.; Donnelly, P. S.; Heslop, J. M.; Ratcliffe, S. J. *Dalton Trans.* **2007**, (2), 209.
(551) Cowley, A. R.; Dilworth, J. R.; Donnelly, P. S.; White, J. M. *Inorg. Chem.* **2006**, *45* (2), 496.
(552) Cowley, A. R.; Dilworth, J. R.; Donnelly, P. S.; Gee, A. D.; Heslop, J. M. *Dalton Trans.* **2004**, (16), 2404.
(553) Blower, P. J.; Castle, T. C.; Cowley, A. R.; Dilworth, J. R.; Donnelly, P. S.; Labisbal, E.; Sowrey, F. E.; Teat, S. J.; Went, M. J. *Dalton Trans.* **2003**, (23), 4416.
(554) Castle, T. C.; Maurer, R. I.; Sowrey, F. E.; Went, M. J.; Reynolds, C. A.; McInnes, E. J. L.; Blower, P. J. *J. Am. Chem. Soc.* **2003**, *125* (33), 10040.
(555) Maurer, R. I.; Blower, P. J.; Dilworth, J. R.; Reynolds, C. A.; Zheng, Y.; Mullen, G. E. D. *J. Med. Chem.* **2002**, *45* (7), 1420.
(556) Dearling, J. L. J.; Lewis, J. S.; Mullen, G. E. D.; Welch, M. J.; Blower, P. J. *J. Biol. Inorg. Chem.* **2002**, *7* (3), 249.
(557) Burgman, P.; O'Donoghue, J. A.; Lewis, J. S.; Welch, M. J.; Humm, J. L.; Ling, C. C. *Nucl. Med. Biol.* **2005**, *32* (6), 623.
(558) Laforest, R.; Dehdashti, F.; Lewis, J. S.; Schwarz, S. W. *Eur. J. Nucl. Med. Mol. Imaging* **2005**, *32* (7), 764.
(559) Lewis, J. S.; McCarthy, D. W.; McCarthy, T. J.; Fujibayashi, Y.; Welch, M. J. *J. Nucl. Med.* **1999**, *40* (1), 177.
(560) Yuan, H.; Schroeder, T.; Bowsher, J. E.; Hedlund, L. W.; Wong, T.; Dewhirst, M. W. *J. Nucl. Med.* **2006**, *47* (6), 989.
(561) Obata, A.; Yoshimoto, M.; Kasamatsu, S.; Naiki, H.; Takamatsu, S.; Kashikura, K.; Furukawa, T.; Lewis, J. S.; Welch, M. J.; Saji, H.; Yonekura, Y.; Fujibayashi, Y. *Nucl. Med. Biol.* **2003**, *30* (5), 529.
(562) Dehdashti, F.; Mintun, M. A.; Lewis, J. S.; Bradley, J.; Govindan, R.; Laforest, R.; Welch, M. J.; Siegel, B. A. *Eur. J. Nucl. Med. Mol. Imaging* **2003**, *30* (6), 844.
(563) Dehdashti, F.; Grigsby, P. W.; Mintun, M. A.; Lewis, J. S.; Siegel, B. A.; Welch, M. J. *Int. J. Radiat. Oncol. Biol. Phys.* **2003**, *55* (5), 1233.
(564) Dehdashti, F.; Grigsby, P. W.; Lewis, J. S.; Laforest, R.; Siegel, B. A.; Welch, M. J. *J. Nucl. Med.* **2008**, *49* (2), 201.
(565) Grigsby, P. W.; Malyapa, R. S.; Higashikubo, R.; Schwarz, J. K.; Welch, M. J.; Huettner, P. C.; Dehdashti, F. *Mol. Imaging Biol.* **2007**, *9* (5), 278.
(566) Lewis, J. S.; Laforest, R.; Dehdashti, F.; Grigsby, P. W.; Welch, M. J.; Siegel, B. A. *J. Nucl. Med.* **2008**, *49* (7), 1177.
(567) Lewis, J. S.; Connett, J. M.; Garbow, J. R.; Buettner, T. L.; Fujibayashi, Y.; Fleshman, J. W.; Welch, M. J. *Cancer Res.* **2002**, *62* (2), 445.
(568) Aft, R. L.; Lewis, J. S.; Zhang, F.; Kim, J.; Welch, M. J. *Cancer Res.* **2003**, *63* (17), 5496.
(569) Lewis, J. S.; Laforest, R.; Buettner, T. L.; Song, S. K.; Fujibayashi, Y.; Connett, J. M.; Welch, M. J. *Proc. Natl. Acad. Sci. U.S.A.* **2001**, *98* (3), 1206.
(570) Obata, A.; Kasamatsu, S.; Lewis, J. S.; Furukawa, T.; Takamatsu, S.; Toyohara, J.; Asai, T.; Welch, M. J.; Adams, S. G.; Saji, H. *Nucl. Med. Biol.* **2005**, *32* (1), 21.
(571) Lewis, J. S.; Dearling, J. L. J.; Sosabowski, J. K.; Zweit, J.; Carnochan, P.; Kelland, L. R.; Coley, H. M.; Blower, P. J. *Eur. J. Nucl. Med.* **2000**, *27* (6), 638.
(572) Black, N. F.; McJames, S.; Rust, T. C.; Kadrmas, D. J. *Phys. Med. Biol.* **2008**, *53* (1), 217.
(573) Green, M. A.; Mathias, C. J.; Willis, L. R.; Handa, R. K.; Lacy, J. L.; Miller, M. A.; Hutchins, G. D. *Nucl. Med. Biol.* **2007**, *34* (3), 247.
(574) Wei, L.; Easmon, J.; Nagi, R. K.; Muegge, B. D.; Meyer, L. A.; Lewis, J. S. *J. Nucl. Med.* **2006**, *47* (12), 2034.
(575) Vavere, A. L.; Lewis, J. S. *Nucl. Med. Biol.* **2008**, *35* (3), 273.
(576) Lewis, J. S.; Sharp, T. L.; Laforest, R.; Fujibayashi, Y.; Welch, M. J. *J. Nucl. Med.* **2001**, *42* (4), 655.
(577) Dence, C. S.; Ponde, D. E.; Welch, M. J.; Lewis, J. S. *Nucl. Med. Biol.* **2008**, *35* (6), 713.
(578) *Table of Isotopes*, 7th ed.; Lederer, C. M., Shirley, V. S., Eds.; John Wiley & Sons: New York, 1978.
(579) Shannon, R. D. *Acta Crystallogr., Sect. A* **1976**, *A32* (5), 751.
(580) Baes, C. F., Jr.; Mesmer, R. E. *The Hydrolysis of Cations*; Wiley-Interscience: New York, 1976.
(581) Martell, A. E.; Smith, R. M. *Critical Stability Constants, Vol. 3: Other Organic Ligands*; Plenum Press: New York, 1977.
(582) Wulfsberg, G. *Inorganic Chemistry*; University Science Books: Sausalito, CA, 2000.
(583) Douglas, B.; McDaniel, D.; Alexander, J. *Concepts and Models of Inorganic Chemistry*, 3rd ed.; John Wiley & Sons: New York, 1994.
(584) Hancock, R. D.; McDougall, G. J. *J. Am. Chem. Soc.* **1980**, *102* (21), 6551.
(585) Hancock, R. D.; McDougall, G. J. *Adv. Mol. Relax. Interact. Processes* **1980**, *18* (2), 99.
(586) Martell, A. E.; Hancock, R. D. *Metal Complexes in Aqueous Solutions*; Plenum Press: New York, 1996.
(587) Martell, A. E., Smith, R. M., Eds.; *Critical Stability Constants, Vol. 1: Amino Acids*; Plenum Press: New York, 1974.
(588) Delgado, R.; De Carmo, F. M.; Quintino, S. *Talanta* **1997**, *45* (2), 451.
(589) Martell, A. E.; Smith, R. M. *Critical Stability Constants*; Plenum Press: New York, 1982.
(590) Bleiholder, C.; Boerzel, H.; Comba, P.; Ferrari, R.; Heydt, M.; Kerscher, M.; Kuwata, S.; Laurenczy, G.; Lawrance, G. A.; Lienke,

A.; Martin, B.; Merz, M.; Nuber, B.; Pritzkow, H. *Inorg. Chem.* **2005**, *44* (22), 8145.
(591) Bevilacqua, A.; Gelb, R. I.; Hebard, W. B.; Zompa, L. J. *Inorg. Chem.* **1987**, *26* (16), 2699.
(592) Garcia, E. Synthesis of TACN-derived Chelators and Studies of their Metal Complexes. University of New Hampshire, Durham, NH. Unpublished work, 2009.
(593) Smith, R. M.; Martell, A. E. *Critical Stability Contants*; Plenum Press: New York, 1989.
(594) Delgado, R.; Frausto da Silva, J. J. R. *Talanta* **1982**, *29* (10), 815.
(595) Chaves, S.; Delgado, R.; Dasilva, J. J. R. F. *Talanta* **1992**, *39* (3), 249.
(596) Sun, X.; Wuest, M.; Weisman, G. R.; Wong, E. H.; Reed, D. P.; Boswell, C. A.; Motekaitis, R.; Martell, A. E.; Welch, M. J.; Anderson, C. J. *J. Med. Chem.* **2002**, *45* (2), 469.
(597) Delgado, R.; Sun, Y.; Motekaitis, R. J.; Martell, A. E. *Inorg. Chem.* **1993**, *32* (15), 3320.
(598) Motekaitis, R. J.; Sun, Y.; Martell, A. E.; Welch, M. J. *Inorg. Chem.* **1991**, *30* (13), 2737.
(599) Evers, A.; Hancock, R. D.; Martell, A. E.; Motekaitis, R. J. *Inorg. Chem.* **1989**, *28* (11), 2189.
(600) Bottari, E.; Anderegg, G. *Helv. Chim. Acta* **1967**, *50* (8), 2349.
(601) Kumar, K.; Chang, C. A.; Francesconi, L. C.; Dischino, D. D.; Malley, M. F.; Gougoutas, J. Z.; Tweedle, M. F. *Inorg. Chem.* **1994**, *33* (16), 3567.
(602) Koudelkova, M.; Vinsova, H.; Jedinakova-Krizova, V. *Czech. J. Phys.* **2003**, *53* (2), A769.
(603) Lovqvist, A.; Humm, J. L.; Sheikh, A.; Finn, R. D.; Koziorowski, J.; Ruan, S.; Pentlow, K. S.; Jungbluth, A.; Welt, S.; Lee, F. T.; Brechbiel, M. W.; Larson, S. M. *J. Nucl. Med.* **2001**, *42* (8), 1281.
(604) Dimitrakopoulou-Strauss, A.; Hohenberger, P.; Haberkorn, U.; Macke, H. R.; Eisenhut, M.; Strauss, L. G. *J. Nucl. Med.* **2007**, *48* (8), 1245.
(605) Asti, M.; De Pietri, G.; Fraternali, A.; Grassi, E.; Sghedoni, R.; Fioroni, F.; Roesch, F.; Versari, A.; Salvo, D. *Nucl. Med. Biol.* **2008**, *35* (6), 721.
(606) Hofmann, M.; Weitzel, T.; Krause, T. *Nucl. Instrum. Methods Phys. Res., Sect. A* **2006**, *569* (2), 522.
(607) van Eerd, J. E. M.; Oyen, W. J. G.; Harris, T. D.; Rennen, H. J. J. M.; Edwards, D. S.; Corstens, F. H. M.; Boerman, O. C. *J. Nucl. Med.* **2005**, *46* (5), 786.
(608) Xu, H.; Baidoo, K.; Gunn, A. J.; Boswell, C. A.; Milenic, D. E.; Choyke, P. L.; Brechbiel, M. W. *J. Med. Chem.* **2007**, *50* (19), 4759.
(609) Li, W. P.; Lewis, J. S.; Srinivasan, A.; Schmidt, M. A.; Anderson, C. J. *J. Labeled Compd. Radiopharm.* **2001**, *44* (1), S948.
(610) Lewis, J. S.; Lewis, M. R.; Srinivasan, A.; Schmidt, M. A.; Wang, J.; Anderson, C. J. *J. Med. Chem.* **1999**, *42* (8), 1341.
(611) Wadas, T. J.; Anderson, C. J. *Nat. Protoc.* **2006**, *1* (6), 3062.
(612) Liu, Z.; Yan, Y.; Liu, S.; Wang, F.; Chen, X. *Bioconjugate Chem.* **2009**, *20* (5), 1016.

CR900325H